Remote Sensing Series 62

Daniel Odermatt

Spaceborne Inland Water Quality Monitoring

Remote Sensing Laboratories
Department of Geography
University of Zurich, 2011

Front page: “The Stargazer I”, Robert Llimós, Barcelona.

Author:

Daniel Odermatt
Remote Sensing Laboratories RSL
Department of Geography, University of Zurich
Winterthurerstrasse 190, CH-8057 Zurich, Switzerland

www.geo.uzh.ch/rsl

Odermatt, Daniel

Spaceborne Inland Water Quality Monitoring

Remote Sensing Series, Vol. 62, Remote Sensing Laboratories, Department of Geography, University of Zurich, Switzerland, 2011

ISBN: 13 978-3-03703-028-8

This work was approved as a PhD thesis by the Faculty of Science of the University of Zurich in the autumn semester of 2011. Doctorate committee: Prof. Dr. Michael E. Schaepman (chair), Dr. Mathias Kneubühler.

TABLE OF CONTENTS

LIST OF FIGURES

LIST OF TABLES

Remote Sensing Series 62

Daniel Odermatt

Spaceborne Inland Water Quality Monitoring

Remote Sensing Laboratories
Department of Geography
University of Zurich, 2011

Front page: “The Stargazer I”, Robert Llimós, Barcelona.

Author:

Daniel Odermatt
Remote Sensing Laboratories RSL
Department of Geography, University of Zurich
Winterthurerstrasse 190, CH-8057 Zurich, Switzerland

www.geo.uzh.ch/rsl

Odermatt, Daniel

Spaceborne Inland Water Quality Monitoring

Remote Sensing Series, Vol. 62, Remote Sensing Laboratories, Department of Geography, University of Zurich, Switzerland, 2011

ISBN: 13 978-3-03703-028-8

This work was approved as a PhD thesis by the Faculty of Science of the University of Zurich in the autumn semester of 2011. Doctorate committee: Prof. Dr. Michael E. Schaepman (chair), Dr. Mathias Kneubühler.

It is only the superficial qualities that last.
Man's deeper nature is soon found out.

Oscar Wilde, The Importance of Being Earnest (1894)

SUMMARY

Aquatic remote sensing conduces to the quantification of biogeochemical parameters of surface waters from spectroradiometric measurements with ground based, airborne or spaceborne instruments. In the past three decades instruments and methods have been improved, enabling corresponding applications that deal with an increasing optical complexity. The current generation of spaceborne oceanographic imaging spectrometers and corresponding water constituent algorithms provide already operational products for case 1, i.e. open ocean water. This thesis aims at the development of comparable products for case 2, i.e. optically complex water.

The first part of the present thesis is on the validation of two eligible inversion algorithms for measuring chlorophyll-a in perialpine lakes by means of data from the Medium Resolution Imaging Spectrometer (MERIS). The first algorithm is based on a relatively simple downhill-simplex inversion for a semi-analytical reflectance model. It is adjustable to variable acquatic and atmospheric optical properties and applicable to data from any sensor. Its main limitations lie in the a priori assumption of the water's backscattering at near-infrared wavelengths and the neglect of adjacency effects. Both issues are addressed in the second validation experiment, with a neural network for inversion and a corresponding adjacency effect correction algorithm. Numerically modeled reflectances and a more flexible atmospheric model are further improvements.

In the second part, the validated neural network algorithm is applied according to the European Water Framework Directive. Chlorophyll-a concentrations in the largest perialpine lakes are thereby statistically analyzed regarding their spatio-temporal variations. Concentrations in most lakes follow a typical seasonal cycle with maxima around the turn of the year. Lake Garda is the only example with a perennial trend towards reoligotrophication during 2003-2009. Measured Spatio-temporal variations furthermore indicate that common in situ monitoring programs on their own may not be sufficiently representative for

the Water Framework Directive. A synoptic approach with in situ and remote measurements is thus recommended.

Part three consists of a review of further case 2 algorithm validation experiments. Quantitative validity ranges describe thereby the suitability of each algorithm for the investigation of specific water types. Band ratio algorithms provide relatively accurate results for suspended matter and moderate to high chlorophyll-a concentrations, whereas the retrieval of colored dissolved organic matter achieves significantly lower correlations with in situ reference measurements. Spectral inversion algorithms have a fair potential to fill in such gaps, but lack a comparable abundance of independent validation experiments. Finally, a classification scheme is derived that allows for a further division of optical water types beyond the two commonly separated cases.

This thesis demonstrates the feasibility of spaceborne chlorophyll-a concentration monitoring in perialpine lakes, and gives an outlook on other sufficiently validated applications. Most of these methods achieve accuracies in the range of probe measurements by means of entirely automatic image processing. They therefore indicate an essential progress towards operational use.

ZUSAMMENFASSUNG

Mittels aquatischer Fernerkundung werden biogeochemische Parameter in Oberflächengewässern quantifiziert, indem spektroradiometrische Messungen am Boden, aus der Luft oder dem Weltraum erhoben werden. In den letzten drei Jahrzehnten sind Instrumente und Methoden verbessert worden, um entsprechende Anwendungen von zunehmender optischer Komplexität zu ermöglichen. Die aktuelle Generation satellitengestützter Bildspektrometer für die Ozeanographie und entsprechende Algorithmen zur Bestimmung von Wasserinhaltsstoffen liefern bereits operationelle Produkte für ‚case 1', den offenen Ozean. Diese Arbeit zielt auf die Entwicklung vergleichbarer Produkte für ‚case 2', optisch komplexe Gewässer, ab.

Der erste Teil der vorliegenden Arbeit behandelt die Validierung zweier geeigneter Inversionsalgorithmen zur Messung von Chlorophyll-a in voralpinen Seen mittels Daten des Medium Resolution Imaging Spectrometer (MERIS). Der erste Algorithms basiert auf einer relativ einfachen Downhill-Simplex inversion für ein semi-analytisches Reflektanzmodell. Er kann an unterschiedliche aquatische und atmosphärische optische Eigenschaften angepasst und mit Daten von beliebigen Sensoren verwendet werden. Die grössten Einschränkungen liegen in der a priori Annahme der Rückstreuung aus dem Wasserkörper im nahinfraroten Wellenlängenbereich sowie in der Vernachlässigung von Nachbarschaftseffekten. Beide Sachverhalte werden im zweiten Validierungsexperiment behandelt, mittels eines Neuronalen Netzes für die Inversion und eines zugehörigen Algorithmus' zur Korrektur der Nachbarschaftseffekte. Numerisch modellierte Reflektanzen sowie ein flexibleres Atmosphärenmodell stellen weitere Verbesserungen dar.

Im zweiten Teil wird der validierte, auf einem Neuronalen Netz basierende Algorithmus gemäss der Europäischen Wasserrahmenrichtlinien angewendet. Die Chlorophyll-a-Konzentrationen der grössten voralpinen Seen werden dabei statistisch auf räumliche und zeitliche Variationen untersucht. In den meisten Seen folgen die Konzentrationen einem typischen saisonalen Verlauf mit Maxima um den Jahreswechsel. Der Gardasee ist das einzige Beispiel mit mehr-

jährigem Trend zur Reoligotrophierung in den Jahren 2003-2009. Gemessene raum-zeitliche Variationen deuten ferner darauf hin, dass herkömmliche in situ Monitoringprogramme alleine möglicherweise für die Europäischen Wasserrahmenrichtlinien nicht representativ genug sind. Eine synoptische Herangehensweise mit Messungen vor Ort und Fernerkundungsdaten wird deshalb empfohlen.

Teil drei enthält eine Rezension weiterer Validierungsexperimente für ‚case 2'-Algorithmen. Quantitative Gültigkeitsbereiche beschreiben dabei die Eignung zur Untersuchung bestimmter Gewässertypen. Bandquotient-Algorithmen liefern relativ genaue Abschätzungen für Schwebstoffe und mittlere bis hohe Chlorophyll-Konzentrationen, während die Ableitung von Gelbstoffen erheblich tiefere Korrelationen mit in situ Messungen erzielt. Spektrale Inversionsalgorithmen verfügen über ein grosses Potential um solche Lücken auszufüllen, es mangelt jedoch an einer vergleichbaren Anzahl unabhängiger Validationsexperimente. Schlussendlich wird ein Klassifikationsschema abgeleitet, das eine weitere Unterteilung von optischen Gewässertypen über die beiden gemeinhin unterschiedenen Fälle hinaus ermöglicht.

Dieser wissenschaftliche Beitrag demonstriert die Machbarkeit eines satellitengestützen Monitorings von Chlorophyll-a-Konzentrationen in voralpinen Seen und gibt einen Ausblick auf weitere ausreichend validierte Anwendungen. Die meisten dieser Methoden erzielen Genauigkeiten im Bereich von in situ Sondenmessungen bei vollkommen automatischer Bildverarbeitung. Sie stellen somit einen entscheidenden Fortschritt in Richtung operationeller Anwendung dar.

TABLE OF CONTENTS

LIST OF FIGURES

LIST OF TABLES

PREFACE

Operational environmental earth observation services have first been established in climatology and oceanography. Land surface related products have only recently emerged from regional to global datasets acquired by wide swath imaging spectrometers such as MERIS and MODIS. In this context, research on the retrieval of environmental parameters of inland waters is a promising field that connects the advanced knowledge from optical oceanography with limnology and new image analysis methods. The belief and prospect of having a stake in the progress of this interdisciplinary field towards the establishment of operational services is prerequisite and motivation for the present thesis.

1 INTRODUCTION

1.1 Water quality monitoring

Water is an essential resource and at the same time a frightening natural hazard. Its availability and quality delimit anthropogenic activities as well as habitable environments for all kinds of life. About 97% of the Earth's water is saline, 2% are bound in ice caps and glaciers, and 0.9% are groundwater, leaving 0.01% or 190'000 km^3 fresh surface water in storages such as lakes, swamps and rivers (Gleick, 1996). Altogether, 304 million Lakes larger than 0.1 hectares cover 2.8% of the Earth's land surface, equaling half the size of the contiguous United States (Downing et al., 2006).

According to the UNEP (1994), toxic contamination, eutrophication and acidification are the three major environmental problems that may degrade water quality in lakes and reservoirs. Water quality in turn affects fishery, freshwater supply, biodiversity and sanitation, whereas safeguard or recovery of the latter three are addressed by the UN Millennium Development Goals (UN Secretary General, 2000; WHO/UNICEF, 2004). Monitoring of water quality is thus a principal task in water quality management. The United Nation's Global Environment Monitoring System (GEMS) Water Program maintains therefore a global information system where water quality data from more than 100 countries is collected and analyzed (UNEP GEMS, 2008). At a regional level, water quality monitoring remains however a matter of political initiatives, such as the Water Framework Directive (WFD) in the European Union (European Parliament, 2000) or the Clean Water (US Congress, 1977) and Water Quality Act (US Congress, 1987) in the United States. Water quality regulations in Switzerland fulfill a similar purpose with regard to monitoring and protection of natural waters, although they lack mandatory measures as specified in the WFD (Rey and Müller, 2007). The anthropogenic eutrophication of most Swiss lakes in the second half of the 20th century (Figure 1-1) has accordingly been reversed in most cases, with only a few surface waters in areas with intensive livestock farming remaining in critical states (BAG/BAFU, 2010; BWG, 2005).

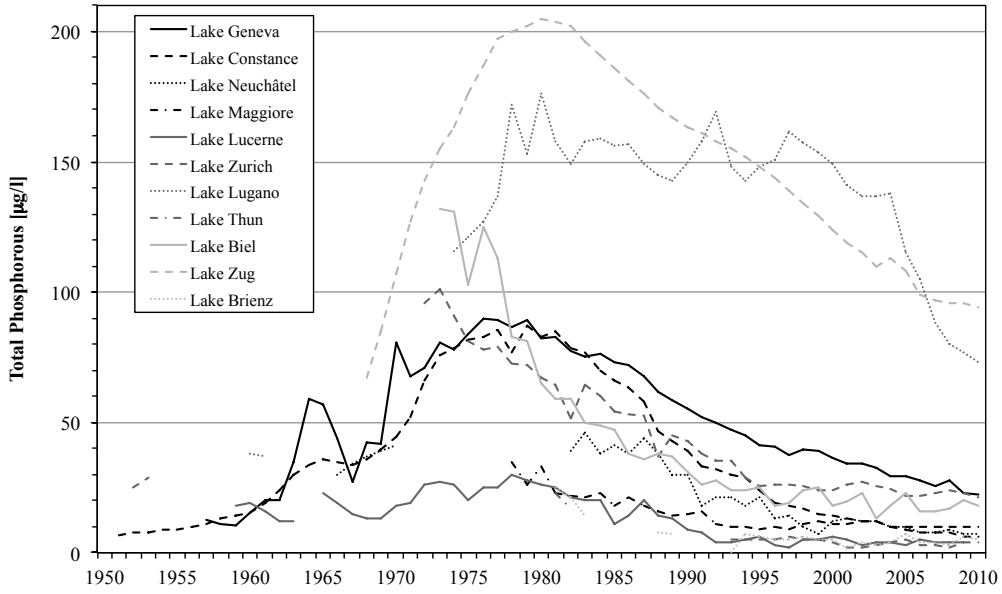

Figure 1-1: Phosphorus concentrations measured in the largest 11 lakes in Switzerland since 1950 or the beginning of monitoring activities. Data collected by cantonal environmental agencies, provided by the Federal Office for the Environment (BAFU, 2011).

1.2 Aquatic remote sensing

Optical remote sensing enables spatiotemporally comprehensive assessment of water quality parameters at unparalleled efficiency. Absorption, scattering and attenuation properties of a water body are thereby retrieved from air- or space-borne measured datasets of the visible domain of the solar reflective spectrum. Such optical properties allow for the estimation of primary production, turbidity, eutrophication, particulate and dissolved carbon contents, or the assessment of currents and algae blooms (IOCCG, 2008).

Since the early days of aquatic remote sensing, water targets have been classified in a bipartite scheme. Originally, two idealistic classes referred to phytoplankton (case 1) and inorganic particle (case 2) dominated waters (Morel and Prieur, 1977). With time and frequent practical use, this definition evolved into a convenient partitioning of two methodologically diverging fields of application (Gordon and Morel, 1983; IOCCG, 2000; Morel, 1988). Case 1 now refers to open ocean water, whose optical properties are dominated by phytoplankton

and associated organic substances. These substances are to some degree quantitatively correlated (Morel et al., 2007; Siegel et al., 2005). Case 2 waters on the other hand may consist of a variety of independently mixed, auto- and allochthonous constituents (Figure 1-2), and are therefore alternatively addressed as 'optically complex'. For remote sensing purposes, the generic water constituent types in Figure 1-2 are replaced by the three optically functional types chlorophyll-*a* (*chl-a*), total suspended matter (*tsm*) and coloured dissolved organic matter (*cdom*). *Chl-a* as the dominant light harvesting pigment is thereby used as an integrative bioindicator for photosynthetic pigments. It is also used for indirect estimates of primary production since it is universally present in all green and red algae and cyanobacteria (Schalles, 2006).

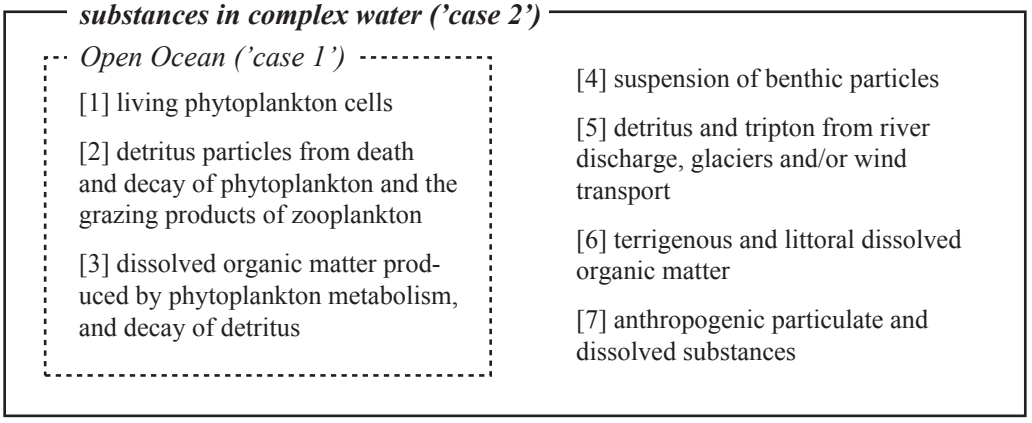

Figure 1-2: Optically active water constituents in phytoplankton dominated case 1 water (substances [1]-[3]) and materials from outside the water column that only occur in case 2 water(substances [4]-[7]). According to Schalles (2006).

As far as case 1 is concerned, biological oceanography has been revolutionized in the past three decades by global observations from so-called ocean color satellite sensors, and important contributions were made to biogeochemistry, physical oceanography and fishery and coastal management (IOCCG, 2008). This line of sensors includes chronologically: the Coastal Zone Color Scanner CZCS (Hovis et al., 1980), the Modular Optoelectronic Scanner MOS (Zimmermann et al., 1993), the Sea-viewing Wide Field-Of-View Sensor SeaWiFS (Hooker et al., 1992), and for present observations the Medium Resolution Imaging Spectrometer MERIS (Rast and Bezy, 1999) and the Moderate Resolution Imaging Spectrometers MODIS (Guenther et al., 2002). Corre-

sponding global ocean color products are usually derived by means of band ratio algorithms that make use of the green to blue portion of the reflected solar spectrum. Such algorithms have been in operational use for more than 10 years (O'Reilly et al., 1998).

Case 2, i.e. inland and coastal waters, are however affected by aquatic and atmospheric variations that exceed in many ways those over open ocean (c.f. Figure 1-2 and Chapter 1.4.4). Corresponding technological and methodological challenges complicate the remote measurement of water quality parameters (IOCCG, 2000). Remote sensing applications of optically complex case 2 waters therefore lag behind the operational stage reached with case 1. The earliest spaceborne remote sensing experiments with inland waters are summarized by Dekker (1995) and exclusively on North American and European waters. Perialpine lakes have first been investigated with empirical classifications of lake types and sub-basins using Landsat TM (Jaquet and Zand, 1989; Zilioli and Brivio, 1997). Empirical relationships found in Landsat data are also applied to the first quantitative investigation of Secchi depth and chlorophyll by Giardino et al. (2001). Quantitative water constituent retrieval based on bio-optical models is first examined using the Compact Airborne Spectrographic Imager CASI (Keller, 2001) and Daedalus data (Heege and Fischer, 2004), followed by spaceborne Hyperion data (Brando and Dekker, 2003; Giardino et al., 2007).

1.3 Optical properties of water

Preisendorfer (1961) defines two fundamental types of optical properties of natural water, inherent (IOP) and apparent (AOP). IOPs are instantaneously invariant and depend only on the type and concentration of water constituents. AOPs depend on illumination conditions and geometry. IOPs are the link between remotely measured AOPs and water constituent concentrations (Dekker et al., 1995).

1.3.1 Inherent optical properties

The two most essential IOPs are the absorption coefficient *a* and scattering coefficient *b*. They are the sum of absorption and scattering by each individual constituent (IOCCG, 2006). In case of Chapter 2, *a* includes absorption by pure water (a_w), chlorophyll pigments ($a_{chl\text{-}a}$) and coloured dissolved organic matter

(a_{cdom}) (Equation [1-1]). b is accordingly the sum of molecular scattering by water (b_w) and scattering by total suspended matter (b_{tsm}) as in Equation [1-2] (Odermatt et al., 2008a). Spectral absorption variations of the three substances depicted in Figure 1-3.

$$a = a_w + a_{chl} + a_{cdom} \quad [1\text{-}1]$$

$$b = b_w + b_{tsm} \quad [1\text{-}2]$$

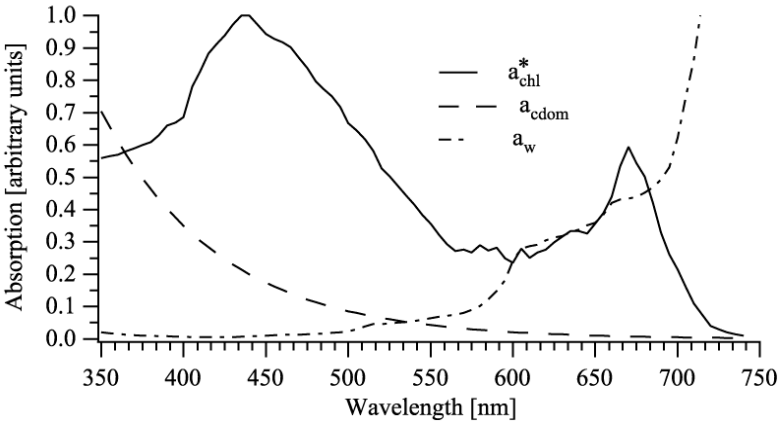

Figure 1-3: A comparison of the spectral absorption by pure water (Kou et al., 1993; Pope and Fry, 1997; Sogandares and Fry, 1997; Van Zee et al., 2002) chlorophyll (Prieur and Sathyendranath, 1981) and cdom (Morel and Maritorena, 2001). Figure from Pegau et al. (2003).

a_w increases with wavelength, which causes clear water's intrinsic, blue color (Braun and Smirnov, 1993). $a_{chl\text{-}a}$ has a primary and secondary maximum at 440 (blue) and 665 nm (red), respectively, shifting the water's colour towards a green reflectance peak as known from other photosynthetically active targets. *cdom* absorbs predominantly at blue wavelengths, and is accordingly also addressed as gelbstoff, gilvin or yellow substance.

b is the spherical integral of the volume scattering function β (Equation [1-3]). The scattering contribution towards remote sensors is alternatively represented by the hemispherical integral over the backward directions of scattering angle

ψ, known as backscattering coefficient b_b according to Equation [1-4]. b_b however refers to the direction opposing incidence rather than the direction of observation. A more appropriate but also more complex formulation of scattering towards a nadir centred hemisphere is given in (Sathyendranath and Platt, 1991).

$$b = 2\pi \int_0^{\pi} \beta \sin\psi \, d\psi \qquad [1\text{-}3]$$

$$b_b = 2\pi \int_{\pi/2}^{\pi} \beta \sin\psi \, d\psi \qquad [1\text{-}4]$$

The phase functions by Petzold (Mobley et al., 1993; Petzold, 1972) and Fournier-Forand (Fournier and Forand, 1994; Fournier and Jonasz, 1999) are widely used since measurements of β are complicated and have only recently become more numerous (Chami et al., 2006; Freda et al., 2007; Sokolov et al., 2010; Sullivan and Twardowski, 2009). Therefore, exact model inputs of β are rare and b_b is usually approximated by the backscattering ratio $b:b_b$, which is 0.0183 for the Petzold phase function (Mobley et al., 2002), but may vary considerably for other water types (Boss et al., 2004; Zhang et al., 2010). A comparison of volume scattering in pure water and the Petzold example is given in Figure 1-4, whereas the depicted scattering phase function $\tilde{\beta}$ is a normalized β according to Equation [1-5] (Lee and Lewis, 2003).

$$\tilde{\beta}(\psi) = \frac{\beta(\psi)}{b} \qquad [1\text{-}5]$$

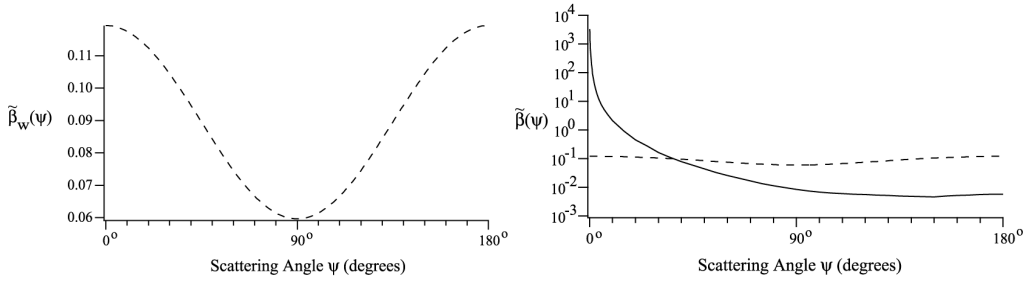

Figure 1-4: A comparison of the molecular scattering phase function for pure water (dashed lines, Mueller et al., 2003) and particle scattering dominated phase function for measurements in the San Diego Harbor (Petzold, 1972). Figures from Pegau et al. (2003).

The spectral shape of b in clear natural waters is almost flat but shows a weak exponential decrease with wavelength. An increase in *tsm* and accordintly b_{tsm} intensifies this decrease (Babin et al., 2003; Gould Jr et al., 1999).

A direct derivative of the IOPs, the ratios of a, b and b_b constitute the single scattering albedo ω_0 in Equation [1-6] (Gordon and Brown, 1973) and the single backscattering albedo ω_b in Equation [1-7] (Park and Ruddick, 2005).

$$\omega_0 = \frac{b}{a+b} \qquad [1\text{-}6]$$

$$\omega_b = \frac{b_b}{a+b_b} \qquad [1\text{-}7]$$

1.3.2 Apparent optical properties

AOPs are defined with hemispherical, conical or directional reference, whereas the latter is a mere concept for an infinitely small cone (Schaepman-Strub et al., 2006). Hemispherical integrals of a radiant flux Φ per surface area A are referred to as irradiance E, conical integrals as radiance L. Φ, E and L are related according to Equation [1-8]. All quantities are superscript with + and - if referring to above and below the air-water interface, respectively. Subscript u and d indicate up- and downwelling direction, respectively.

$$E(\theta,\phi) = \frac{d\Phi(\theta,\phi)}{dA} = \int_0^{2\pi}\int_0^{\pi/2} L(\theta,\phi)\cos\theta\sin\theta\, d\theta\, d\phi \qquad [1\text{-}8]$$

where θ and ϕ are zenith and azimuth angles, respectively. Early studies on optical properties of natural waters focus predominantly on E, which is easier to measure but has limited directional expressiveness. Equation [1-9] defines the dimensionless subsurface irradiance reflectance R^- as the ratio of up- and downwelling irradiances below the surface, E_u^- and E_d^-, respectively. R^- varies with illumination zenith angle θ_s^-.

$$R^-(\theta_s^-) = \frac{E_u^-}{E_d^-(\theta_s^-)} \qquad [1\text{-}9]$$

The remote sensing reflectance R_{rs} (Equation [1-10]) is a hemispherical-conical reflectance of unit [sr^{-1}]. It is defined as sub- or above surface term, which dif-

fer by the internally reflected upwelling radiance. Constributions by the surface reflected downwelling irradiance must in both cases be considered separately. R_{rs} implies the directional properties of the water-leaving, i. e. upwelling, interface transmitted radiance L_w, which are not accounted for by R^-. The water leaving reflectance R_w is the analogous bihemispherical reflectance assuming a Lambertian L_w according to Equation [1-11] (Voss, 1989).

$$R_{rs}(\theta_s^+,\theta_v^+,\phi) = \frac{L_w(\theta_v^+,\phi)}{E_d^+(\theta_s^+,\phi)} \qquad [1\text{-}10]$$

$$R_w(\theta_s^+,\theta_v^+,\phi) = \frac{\pi L_w(\theta_v^+,\phi)}{E_d^+(\theta_s^+,\phi)} \qquad [1\text{-}11]$$

1.3.3 Optical properties of a flat air-water interface

Snell's law describes the interaction of a collimated, downwelling beam from incidence zenith direction θ_i with the flat air-water interface. The reflected portion remains in air and is mirrored towards direction ($\theta_r^+ = \theta_i^+$, $\phi_r^+ = \phi_i^+ + 180°$). The refracted portion penetrates into the water but is redirected towards transmission direction θ_t^- according to Equation [1-12]. Analogous processes occur for an upwelling beam in water (Equation [1-13]).

$$\theta_t^- = \sin^{-1}\left(\frac{1}{n_w}\sin\theta_i^+\right) \qquad [1\text{-}12]$$

$$\theta_t^+ = \sin^{-1}\left(n_w \sin\theta_i^-\right) \qquad [1\text{-}13]$$

where $n_w \approx 1.34$ (Hale and Querry, 1973) is the refraction index of water. The Fresnel interface reflectance $r_f(\theta_i)$ and transmittance $t_f(\theta_i) = 1 - r_f(\theta_i)$ for incidence angle θ_i are quantified by Equation [1-14] for skew incidence, and by Equation [1-15] for nadir incidence (Austin, 1974). Variations of air and water incident $r_f(\theta_i)$ with zenith angle are given in Figure 1-5. It displays complete internal reflectance for upwelling, i.e. water-incident rays at about $\theta_i > 48°$, and a decrease in downwelling transmittance with θ_i. A more detailed description of interface effects as well as the representation of rough surfaces is given in (Mobley, 1994, 1999).

$$r_f(\theta_i) = \frac{1}{2}\left\{\left[\frac{\sin(\theta_i - \theta_t)}{\sin(\theta_i + \theta_t)}\right]^2 + \left[\frac{\tan(\theta_i - \theta_t)}{\tan(\theta_i + \theta_t)}\right]^2\right\} \quad [1\text{-}14]$$

$$r_f(0) = \left(\frac{n_w - 1}{n_w + 1}\right)^2 \quad [1\text{-}15]$$

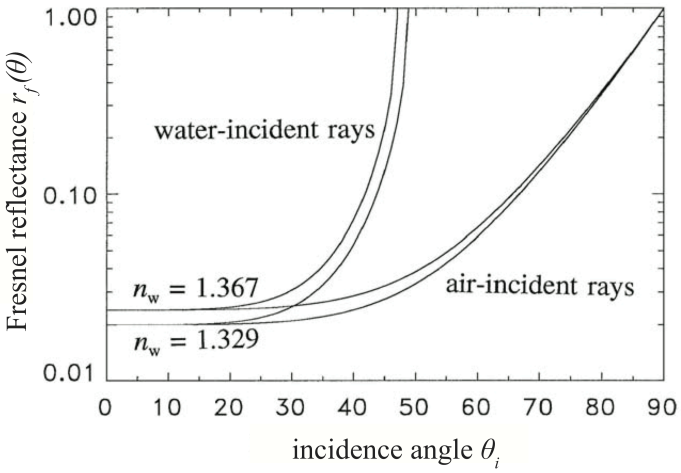

Figure 1-5: Directional Fresnel reflectance for an assumed maximum variability of n_w in natural waters. Figure from Mobley (1994).

1.4 Radiative transfer in water and atmosphere

Forward models predict the color of water from its composition, i.e. AOPs from IOPs and concentrations (Mobley, 1994). Semi-analytical models are the most convenient way to establish this relationship for water reflectance. This simplicity is a major asset when it comes to inversion, but requires adequate coupling with an atmospheric model. On the other hand, numerical models are the most accurate representation of radiative transfer in air, water and combined, layered systems. They are however also more laborious in terms of implementation, computing and inversion (IOCCG, 2000).

1.4.1 Semi-analytical reflectance models

Semi-analytical reflectance models describe continuous spectral reflectance from IOPs and concentrations, by means of a single equation. Parameterizing such equations requires the empirical quantification of coefficients (Carder et al., 1999; Gordon et al., 1988; Morel and Prieur, 1977), which are the reason for the epithet "semi". In this approach, R^- is found proportional to a and b_b (Gordon et al., 1975; Morel and Prieur, 1977). This relation is usually expressed with ω_b (Equation [1-6]) or ω_0 (Equation [1-7]) (Morel and Gentili, 1996). The experiment described in Chapter 2 makes use of the former.

$$R^-(\theta_s^-,\theta_v^-) \approx f(\theta_s^-)\,\omega_b \qquad [1\text{-}16]$$

The magnitude of R^- varies among others with the angle of surface transmitted incidence θ_s^- (Gordon, 1989). This dependence can be integrated in the coefficient $f(\theta_s^-)$ as described in Equation [1-17]. The nadir illuminated $f(0°)$ is estimated to be about 0.29 to 0.33 for a choice of different water types (Kirk, 1991).

$$f(\theta_s^-) = M(1-\cos\theta_s^-) + f(0°) \qquad [1\text{-}17]$$

where M is an empirical coefficient between 0.36 and 0.77. Several other approximations for f are described. Sathyendranath and Platt (1997) derive f by means of an upward instead of the backward scattering coefficient. Morel and Gentili (1991, 1993) account for variations of f with the water's scattering properties, since variations in f are different for predominantly absorbing, isotropically or aniosotropically scattering water.

Semi-analytical models for R_{rs} apply the anisotropy factor Q along with f. Q is defined as the ratio of diffuse and directional upwelling radiance in water (Equation [1-18]) (Gordon et al., 1988).

$$R_{rs}^-(\theta_s^-,\theta_v^-,\phi) \approx \frac{f(\theta_s^-,\phi)}{Q(\theta_s^-,\theta_v^-,\phi)} \cdot \omega_b \text{ with } Q(\theta_s^-,\theta_v^-,\phi) = \frac{E_u^-(\theta_s^-,\phi)}{L_u^-(\theta_s^-,\theta_v^-,\phi)} \qquad [1\text{-}18]$$

Variations of Q are described by Morel and Gentili (1993). Its spectral variations are barely accounted for in practice. $Q(\theta_v^- = 90°)$ would equal π sr^{-1} at Lambertian conditions, but is usually around 4.5 in natural waters. The full di-

rectional variations are in the range of 0.3 to 6.5 for different water types. The directional variation of Q is inversely proportional to the one of L_u^- and partly compensates the directional variation of f (Morel and Gentili, 1993). Therefore, f and Q are merged into other coefficients such as l_1 and l_2 in Equation [1-19] (Gordon et al., 1988) or g_0-g_2 in Equation [1-20] (Lee et al., 1998).

$$R_{rs}^-(\theta_s^-,\theta_v^-,\phi) \approx \sum_{i=1}^{2} l_i\, \omega_b^i \qquad [1\text{-}19]$$

$$R_{rs}^-(\theta_t^-,\theta_i^-,\phi) = (g_0 + g_1\, \omega_b^{g_2})\, \omega_b \qquad [1\text{-}20]$$

The most recent semi-analytical reflectance models relate reflectance to polynomials of 3rd and 4th degree similar to Equation [1-19]. The polynomial regression approach by Albert and Mobley (2003) describes R^- and R_{rs} in dependence of ω_b, wind speed u and θ_s^-, according to Equation [1-21], and R_{rs} additionally with θ_v^- as in Equation [1-22].

$$R^- = p_1(1 + p_2\omega_b + p_3\omega_b^2 + p_4\omega_b^3)\left(1 + p_5 \frac{1}{\cos\theta_s^-}\right)(1 + p_6 u)\omega_b \qquad [1\text{-}21]$$

$$R_{rs} = p_1(1 + p_2\omega_b + p_3\omega_b^2 + p_4\omega_b^3)\left(1 + p_5 \frac{1}{\cos\theta_s^-}\right)\left(1 + p_7 \frac{1}{\cos\theta_s^-}\right)(1 + p_6 u)\omega_b \qquad [1\text{-}22]$$

Specific p_1-p_7 for Lake Constance are quantified by Albert and Mobley (2003) for both Equations, derived from Hydrolight simulations (Mobley, 1994). Unfortunately, no analogous regressions for other water types are reported that would allow estimating the magnitude of variations in p_1-p_7 for different IOPs. With the zenith angles already accounted for in the regression by Albert and Mobley (2003), further progress is achieved by considering also the relative azimuth angle $\Delta\phi$ as by the reflectance model in Equation [1-23] (Park and Ruddick, 2005).

$$R_{rs} = \sum_{i=1}^{4} h_i(\theta_s^+,\theta_v^+,\Delta\phi,\gamma_b)\omega_b^i \qquad [1\text{-}23]$$

whereas h_i are bidirectional coefficients that depend on the particle fraction of total backscattering $\gamma_b = b_{bp}/b_b$. Such h_i are calculated and tabulated for more

than 4 Million Hydrolight simulations consisting of 7 variations in θ_s^+, 10 in θ_v^+, 13 in $\Delta\phi$, and further variations of λ, *chl-a*, detritus and *cdom* absorption, particle scattering, wind speed and cloud coverage. The look-up-tables are available online for public use.

1.4.2 Numerical reflectance models

Numerical models are based e.g. on the Monte Carlo, discrete-ordinate, adding and doubling, invariant imbedding, matrix operator or successive orders of scattering (SOS) methods (Zhai et al., 2009). These methods allow the accurate solution of radiative transfer in turbid media. Air-water interface and atmosphere are integral parts of most numerical models for the ocean-atmosphere system (Bulgarelli et al., 1999; Jin and Stamnes, 1994; Zhai et al., 2009). They allow a precise treatment of anisotropic light fields and a rough air-water interface (Jin et al., 2006; Kisselev and Bulgarelli, 2004; Zhai et al., 2010).

Due to their demanding constitution, numerical models are predominantly used in the exploration of bidirectional reflectance variations and in the training and validation of empirical and semi-analytical models (Mobley, 1994; Morel and Gentili, 1996). However, the recently emerging neural network (NN) inversion of remote sensing imagery afford an opportunity to apply numerical models in image processing (Doerffer and Schiller, 2007; Schiller and Doerffer, 1999).

1.4.3 Atmospheric correction

Remote measurements are affected by atmospheric effects. These effects need to be compensated for before the reflectance of the surface beneath can be interpreted. The strong absorption of water bodies and thus generally low water-leaving signals at near-infrared (NIR) wavelengths provide a good spectral domain to estimate these effects (Gordon, 1978). The constitution of the sensor measured signal according to Equation [1-24] and Equation [1-25] is therefore calculated (IOCCG, 2010).

$$L_{TOA}(\lambda) = L_r(\lambda) + L_a(\lambda) + L_{ra}(\lambda) + T_u(\lambda)L_{wc} + T_u(\lambda)L_g + T_u(\lambda)T_d(\lambda)\cos\theta_s^+[L_w(\lambda)]_N \quad [1\text{-}24]$$

$$L_{path}(\lambda) = L_r(\lambda) + L_a(\lambda) + L_{ra}(\lambda) \quad [1\text{-}25]$$

where L_{TOA} is top-of-atmosphere (TOA) radiance, L_r is molecular (Rayleigh) scattered radiance, L_a is aerosol scattered radiance, L_{ra} is combined molecular aerosol scattered radiance, L_{wc} is white cap and L_g water surface reflected radiance, respectively. T_d and T_u are the diffuse atmospheric transmittances from TOA to the target and vice versa. $[L_w]_N$ is L_w normalized to nadir direction. The contribution of L_{path} over clear water is generally around 90% in green and blue bands, and even larger at larger wavelengths. The before mentioned applications are therefore relatively similar in estimating L_{path} at NIR wavelengths, while they differ more significantly in transferring this estimate to the visible wavelength portion (IOCCG, 2010).

Concerning sensors CZCS lacked a band in the NIR portion of the spectrum, and the 670 nm band was used as replacement (Gordon, 1980). Subsequent ocean color sensors remove this shortcoming. Bands at wavelengths >700 nm are thus applied for the retrieval of atmospheric properties by case 1 atmospheric corrections for SeaWiFS and MODIS (Gordon and Wang, 1994), MERIS (Antoine and Morel, 1999), Ocean Color and Temperature Scanner (OCTS) and Global Land Imager (GLI) (Fukushima et al., 1998) and the POLarization and Directionality of the Earth's Reflectances sensor (POLDER) (Nicolas et al., 2005).

Both L_{path} estimation and the spectral extrapolation of atmospheric properties to visible wavelengths are more complex for case 2 water. On one hand, larger variations in *tsm* cause further variations in the water-leaving NIR signal. On the other hand, variable *cdom* will affect the transfer of L_w to short wavelengths. Therefore, the standard case 1 atmospheric corrections are unsuitable for case 2 waters, and special case 2 algorithms for SeaWiFS (Ruddick et al., 2000; Stumpf et al., 2003) and MERIS (Moore et al., 1999; Vidot and Santer, 2003) are used instead. One challenge is thereby the separability of atmospheric and aquatic NIR signals.

1.4.4 Adjacency effects

Natural water bodies are often remarkably darker than surrounding surfaces (e.g. terrestrial vegetation). Atmospheric scattering blurs this difference in the upwelling signal, leaving the at-sensor signal of near-shore waters considerably increased at NIR wavelengths (Tanré et al., 1987), as in Figure 1-6 (solid lines). Figure 1-6 and subsequent considerations of the application of the Im-

proved Contrast between Ocean and Land algorithm (ICOL) to MERIS images of Lake Constance are summarized from Odermatt et al. (2008b).

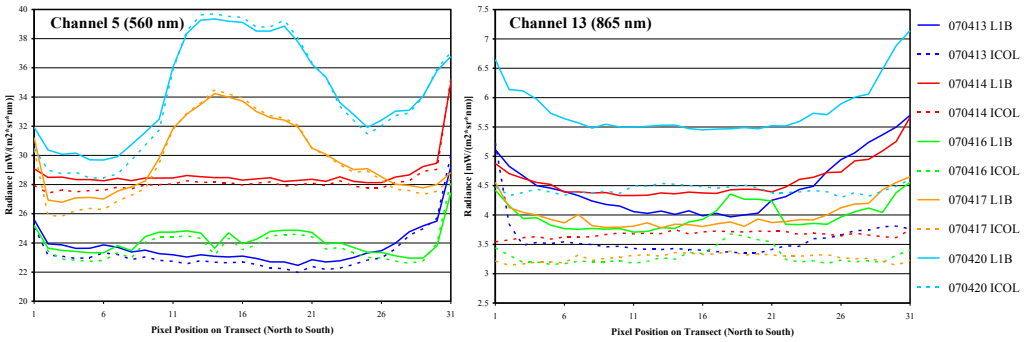

Figure 1-6: Radiance variations in MERIS band 5 (left) and 13 (right), along the North-South transect across Lake Constance as shown in Figure 1-7, on 13-20 April 2007 ('YYMMDD' in legend). Solid lines indicate uncorrected at-sensor radiances ('L1B'), dashed lines represent ICOL corrected at-sensor radiances. 560 nm radiance maxima in the center of the lake correspond to variations in water constituent concentrations (Odermatt et al., 2008b).

Adjacency effects are extensively studied by 5S model calculations in Santer and Schmechtig (2000). They remain significant to as far as 20 km off shore, and increase towards the shore, with wavelength, atmospheric optical thickness (AOT), solar zenith and reflectance difference. The corresponding ICOL algorithm applies these model calculations for the correction of MERIS L1B radiances into L1C radiances. The ICOL algorithm has been validated (Santer et al., 2007) and is available through the Basic ERS & Envisat (A)ATSR and MERIS toolbox (BEAM) (Santer and Zagolski, 2009).

Figure 1-6 shows that wavelengths around 560 nm are barely changed when correcting adjacency effects, as the reflectance of water and surrounding surfaces are at about the same magnitude. At 865 nm however, we observe spatially homogeneous, more than 15% reduced radiances after correction and significantly larger effects over the Southern than over the Northern shore. This confirms previous findings (Santer et al., 2007; Santer and Schmechtig, 2000), and emphasizes the need for adjacency effect correction for the NIR signal from natural waters. These NIR bands are widely used for estimating AOT over water bodies, where usually more than 90% of measured radiance are of atmospheric origin (Siegel et al., 2000).

In the first experiment in Chapter 2 (Odermatt et al., 2008a), AOT is calculated from a priori assumed aquatic backscattering, aerosol type and a single NIR band. Consequently, adjacency effects cause an immediate overestimation of AOT towards the shoreline as depicted in Figure 1-7 (left), and accordingly low, partly negative near-shore reflectances. The retrieval of water constituent concentrations from such underestimated and misshapen reflectances with the Modular Inversion and Processing system's (MIP) downhill simplex procedure is problematic, since outputs will often tend towards the algorithms minimum and maximum thresholds.

In the second experiment in Chapter 3 (Odermatt et al., 2010), the NN for atmospheric correction forces the retrieval of realistic water reflectance spectra, leaving near-shore AOT clearly underestimated (Figure 1-7, right). Interpretation of the propagation of this error is complicated by the black box properties of the NN inversion. The atmospheric correction of C2R and accordingly the retrieved R_{rs}^{-} are however significantly improved by the application of ICOL, as shown in Figure 3-4 and further literature (Guanter et al., 2010; Koponen et al., 2008; Ruiz-Verdu et al., 2008). However, it is also found that this enhanced reflectance spectral input does not consistently improve the water constituents finally retrieved by C2R (Binding et al., 2011; Koponen et al., 2008).

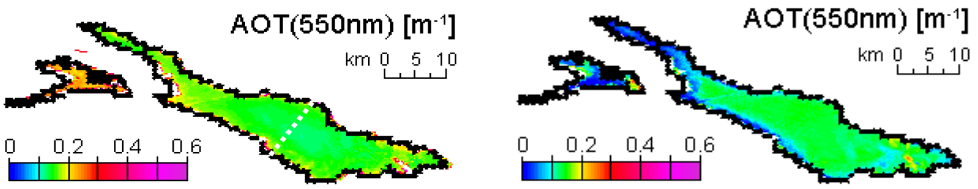

Figure 1-7: AOT estimates for uncorrected MERIS L1B radiances of Lake Constance on 13 April 2007. Left: AOT retrieval from Odermatt et al. (2008a), the dashed white line indicates the transect position for Figure 1-6; Right: AOT retrieval from Odermatt et al. (2010).

1.5 Objectives

1.5.1 Scope of research

Several inversion algorithms have been developed and evaluated for perialpine inland waters. They are typically validated in matchup campaigns, where reflectances and concentrations are measured and compared with one or a few

image acquisitions (Floricioiu et al., 2004; Gege and Plattner, 2004; Giardino et al., 2007; Heege and Fischer, 2004). Such dedicated validation experiments proof the basic validity of an algorithm, but they do not address the long-term consistency or reliable handling required for operational, unsupervised use. In particular the algorithm parameterization becomes essential with regard to such requirements, as optical properties of atmosphere and water may vary strongly during different acquisitions and are hardly represented in matchup validation experiments.

The work by Miksa et al. (2006) is the only corresponding application example for a larger number of MERIS images. Their validation is relatively scarce in statistical quantities, but applies long-term in situ *chl-a* monitoring timeseries from local authorities to overcome the limitations of matchup validation. Their algorithm is an advanced version of Heege and Fischer (2004), whereas appropriate parameterization of the latter has become even more demanding with the improvements introduced by the former. It was therefore decided to use the original algorithm by Heege and Fischer (2004) as a starting point towards timeseries-validation of an automatic *chl-a* retrieval algorithm MERIS data of perialpine lakes. Several further reference data from previous matchup field campaigns in 2007, 2008 and 2009 are used as described in Chapter 2. At a later stage, enhanced versions of the algorithm used by Gege and Plattner (2004) became available through a specific project by the European Space Agency's (ESA) (Doerffer and Schiller, 2008a; Ruiz-Verdu et al., 2008). An analogous evaluation experiment is thus described in Chapter 3.

1.5.2 Research questions

The first publication "*Water quality monitoring for Lake Constance with a physically based algorithm for MERIS data*" in Chapter 2 aims at the use of an experimental, airborne imaging spectrometry algorithm (Heege and Fischer, 2004) with state-of-the-art medium resolution satellite imagery acquired at high temporal resolution. The algorithm applies two separate modules for atmospheric correction and water constituent retrieval. They require several mensural, atmospheric and aquatic input parameters, such as band weighting and adjustment, aerosol model, AOT retrieval band and the contribution of aquatic backscattering therein, and abundancy and optical properties of constituents. These parameters vary for each image acquisition and exceed available previous knowledge. They are estimated as a qualified guess, optimization it-

erations and expert knowledge. A lake-specific, universally valid parameterization streamlines this procedure towards an unsupervised, automatic application.

The following research question is addressed in the first Section:

- Can a simple, physically based algorithm for water constituent retrieval be automatized with lake specifically universal input parameters?

The second publication "*Chlorophyll retrieval with MERIS Case-2-Regional in perialpine lakes*" in Chapter 3 is on the validation of dedicated, sensor-specific neural network algorithms (Doerffer and Schiller, 2008a, b) and an adjacency effect correction (Santer and Zagolski, 2009) for perialpine inland waters. The latter needs separate validation with regard to its effect on retrieved ground reflectances and their propagation to constituent concentrations. Both algorithms' inherent models represent a higher complexity than those applied in the previous experiment, and the neural network inversion ensures numerically stable outputs. However, they suffer typical black box properties, including reduced adjustability, intransparent internal processes and complicated failure interpretation, whose significance for operational processing need to be assessed. Validation with in situ measured *chl-a* timeseries is thus extended to a choice of 7 sufficiently large lakes North and South of the Alps.

The following main research questions are addressed in the second Section:

- Are the C2R neural networks appropriate for the routine processing of *chl-a* products for perialpine lakes?
- What are the effects of the adjacency effect correction, and how does their removal propagate to the results of the neural network algorithms?

The third publication "*Assessing remotely sensed chlorophyll-a for the implementation of the Water Framework Directive in European perialpine lakes*" in Chapter 4 evaluates the applicability of the results from Chapter 3 with regard to water quality monitoring as foreseen by regulations in the European Union. The trophic state of 12 perialpine lakes is therefore assessed with over 200 MERIS images acquired in 2003-2009. The spatio-temporal variability of each lake is estimated, and suggestions are derived regarding the scale of an effective monitoring program that resolves the peaks in seasonal variability as well as significant spatial variations. A combination of remote and in situ measurements thereby allows the synopsis of frequent, spatially detailed satellite meas-

urements, and knowledge of the vertical, especially metalimnic variations during the stratification period.

The following research questions are addressed in the third Section:

- What variations in *chl-a* concentrations occur in perialpine lakes?
- What is the spatial variability of *chl-a*, and how does it change at several temporal scales?
- Can the WFD be applied to remote observations of lakes in the perialpine region?

The fourth publication "*Review of constituent retrieval in optically deep and complex waters from satellite imagery*" completes the thesis with a comparison of contemporary imaging spectrometry application validations. Experiments for band ratio and spectral inversion algorithms are analyzed regarding their range of applicability, preferred instrumentation and accuracy. These criteria draw a large scheme of relevant remote sensing techniques and are at the same time a means for the evaluation of suitable approaches or research gaps. The review also enables a classification of case 2 waters at higher detail, that is a novel classification according primarily to optical properties and suitable imaging spectrometric approaches, and only to a smaller extent corresponding ecological types.

The following research questions are addressed in the fourth Section:

- Which recent spaceborne remote sensing sensors and according algorithms have been validated for case 2 waters since 2005?
- For what typical constituent concentration ranges are these methods valid?
- What typology can be applied to further classify case 2 waters with regard to applicable remote sensing methods?

1.6 Structure

The superordinate concept of this thesis is the realization of spaceborne optical inland water quality monitoring systems for integration with current in situ monitoring programs. Chapter 1 therefore briefly familiarizes with the general problem and state of the art of aquatic remote sensing, and introduces objectives and corresponding research questions for the present thesis. The four fol-

lowing peer-reviewed scientific publications in Chapter 2 to Chapter 5 address these research questions and are self-contained in terms of both, structure and content. Conclusions from the publications in Section 2 to Section 5 are finally summarized and synthesized in Section 6.

1.7 References

Albert, A., & Mobley, C.D. (2003). An analytical model for subsurface irradiance and remote sensing reflectance in deep and shallow case-2 water. *Optics Express,* 11/22, 2873-2890

Antoine, D., & Morel, A. (1999). A multiple scattering algorithm for atmospheric correction of remotely sensed ocean colour (MERIS instrument): principle and implementation for atmospheres carrying various aerosols including absorbing ones. *International Journal of Remote Sensing,* 20/9, 1875-1916

Austin, R.W. (1974). The remote sensing of spectral radiance from below the ocean surface. In N.G. Jerlov & E. Steemann Nielsen (Eds.), *Optical aspects of oceanography* (pp. 317-344). London, New York: Academic Press

Babin, M., Morel, A., Fournier-Sicre, V., Fell, F., & Stramski, D. (2003). Light scattering properties of marine particles in coastal and open ocean waters as related to the particle mass concentration. *Limnol. Oceanogr.,* 48/2, 843-859

BAFU (2011). Cantonal and regional water quality data, allocated by the Federal Office for the Environment.

BAG/BAFU (2010). Reporting for Switzerland under the Protocol on Water and Health. In: *Report to UNECE/WHO* (48 p.), BAG/BAFU

Binding, C.E., Greenberg, T.A., Jerome, J.H., Bukata, R.P., & Letourneau, G. (2011). An assessment of MERIS algal products during an intense bloom in Lake of the Woods. *Journal of Plankton Research,* 33/5, 793-806

Boss, E., Pegau, W.S., Lee, M., Twardowski, M., Shybanov, E., Korotaev, G., & Baratange, F. (2004). Particulate backscattering ratio at LEO 15 and its use to study particle composition and distribution. *J. Geophys. Res.,* 109/C1, C01014

Brando, V.E., & Dekker, A.G. (2003). Satellite hyperspectral remote sensing for estimating estuarine and coastal water quality. *IEEE Transactions on Geoscience and Remote Sensing,* 41/6, 1378-1387

Braun, C.L., & Smirnov, S.N. (1993). Why is water blue? *Journal of Chemical Education,* 70/8, 612-null

Bulgarelli, B., Kiselev, V., & Roberti, L. (1999). Radiative transfer in the atmosphere-ocean system: The finite-element method. *Appl. Opt.,* 38/9, 1530-1542

BWG (2005). Hydrologie der Schweiz: Ausgewählte Aspekte und Resultate. In: *Berichte des BWG, Serie Wasser*, *7* (138 p.), M. Spreafico & R. Weingartner (Eds.), BWG

Carder, K.L., Chen, F.R., Lee, Z.P., Hawes, S.K., & Kamykowski, D. (1999). Semianalytic Moderate-Resolution Imaging Spectrometer algorithms for chlorophyll a and absorption with bio-optical domains based on nitrate-depletion temperatures. *J. Geophys. Res.,* 104/C3, 5403-5421

Chami, M., McKee, D., Leymarie, E., & Khomenko, G. (2006). Influence of the angular shape of the volume-scattering function and multiple scattering on remote sensing reflectance. *Appl. Opt.,* 45/36, 9210-9220

Dekker, A.G., Malthus, T.J., & Hoogenboom, H.J. (1995). The Remote Sensing of Inland Water Quality. In F.M. Danson & S.E. Plummer (Eds.), *Advances in Environmental Remote Sensing* (pp. 123-142): John Wiley & Sons Ltd

Doerffer, R., & Schiller, H. (2007). The MERIS case 2 water algorithm. *International Journal of Remote Sensing,* 28/3, 517-535

Doerffer, R., & Schiller, H. (2008a). MERIS lake water algorithm for BEAM. In: *BEAM Algorithm Technical Basis Document* (17 p.), GKSS Forschungszentrum, Geesthacht, Germany

Doerffer, R., & Schiller, H. (2008b). MERIS regional coastal and lake case 2 water project atmospheric correction. In: *BEAM Algorithm Technical Basis Document* (42 p.), GKSS Forschungszentrum, Geesthacht, Germany

Downing, J.A., Prairie, Y.T., Cole, J.J., Duarte, C.M., Tranvik, L., Striegl, R., McDowell, W.H., Kortelainen, P., Caraco, N., Melack, J.M., & Middelburg, J. (2006). The global abundance and size distribution of lakes, ponds, and impoundments. *Limnology and Oceanography,* 51/5, 10

European Parliament (2000). Directive 2000/60/EC of the European Parliament and of the council of 23 October 2000 establishing a framework for community action in the field of water policy. Official Journal of the European Communities, L327, 1–72

Floricioiu, D., Rott, H., Rott, E., Dokulil, M., & Defrancesco, C. (2004). Retrieval of limnological parameters of perialpine lakes by means of MERIS data. *Proc. Proc. of the 2004 Envisat & ERS Symposium*, Salzburg, Austria

Fournier, G.R., & Forand, J.L. (1994). *Analytic phase function for ocean water*. Bergen, Norway

Fournier, G.R., & Jonasz, M. (1999). Computer-based underwater imaging analysis, Denver, CO, USA, 62-70

Freda, W., Król, T., Martynov, O.V., Shybanov, E.B., & Hapter, R. (2007). Measurements of Scattering Function of sea water in Southern Baltic. *The European Physical Journal - Special Topics,* 144/1, 147-154

Fukushima, H., Higurashi, A., Mitomi, Y., Nakajima, T., Noguchi, T., Tanaka, T., & Toratani, M. (1998). Correction of atmospheric effect on ADEOS/OCTS ocean color data: Algorithm description and evaluation of its performance. *Journal of Oceanography,* 54/5, 417-430

Gege, P., & Plattner, S. (2004). MERIS validation activities at Lake Constance in 2003. *Proc. MERIS User Workshop*, Frascati, Italy

Giardino, C., Brando, V.E., Dekker, A.G., Strömbeck, N., & Candiani, G. (2007). Assessment of water quality in Lake Garda (Italy) using Hyperion. *Remote Sensing of Environment,* 109/2, 183-195

Giardino, C., Pepe, M., Brivio, P.A., Ghezzi, P., & Zilioli, E. (2001). Detecting chlorophyll, Secchi disk depth and surface temperature in a sub-alpine lake using Landsat imagery. *The Science of The Total Environment,* 268/1-3, 19

Gleick, P.H. (1996). Water resources. In S.H. Schneider (Ed.), *Encyclopedia of Climate and Weather* (pp. 817-823). New York: Oxford University Press

Gordon, H.R. (1978). Removal of atmospheric effects from satellite imagery of the oceans. *Appl. Opt.,* 17/10, 1631-1636

Gordon, H.R. (1980). A preliminary assessment of the NIMBUS-7 CZCS atmospheric correction algorithm in a horizontally inhomogenous atmosphere. In J. Gower (Ed.), *Oceanography from space* (pp. 281-294). New York and London: Plenum Press

Gordon, H.R. (1989). Dependence of the Diffuse Reflectance of Natural Waters on the Sun Angle. *Limnology and Oceanography,* 34/8, 1484-1489

Gordon, H.R., & Brown, O.B. (1973). Irradiance Reflectivity of a Flat Ocean as a Function of Its Optical Properties. *Appl. Opt.,* 12/7, 1549-1551

Gordon, H.R., Brown, O.B., Evans, R.H., Brown, J.W., Smith, R.C., Baker, K.S., & Clark, D.K. (1988). A semianalytic radiance model of ocean color. *J. Geophys. Res.,* 93/D9, 10909-10924

Gordon, H.R., Brown, O.B., & Jacobs, M.M. (1975). Computed Relationships Between the Inherent and Apparent Optical Properties of a Flat Homogeneous Ocean. *Appl. Opt.,* 14/2, 417-427

Gordon, H.R., & Morel, A. (1983). *Remote assessment of ocean color for interpretation of satellite visible imagery*. New York, USA: Springer

Gordon, H.R., & Wang, M. (1994). Retrieval of water-leaving radiance and aerosol optical thickness over the oceans with SeaWiFS: a preliminary algorithm. *Applied Optics,* 33/, 443-452

Gould Jr, R.W., Arnone, R.A., & Martinolich, P.M. (1999). Spectral Dependence of the Scattering Coefficient in Case 1 and Case 2 Waters. *Appl. Opt.,* 38/12, 2377-2383

Guanter, L., Ruiz-Verdu, A., Odermatt, D., Giardino, C., Simis, S., Estelles, V., Heege, T., Dominguez-Gomez, J.A., & Moreno, J. (2010). Atmospheric correction of ENVISAT/MERIS data over inland waters: Validation for European lakes. *Remote Sensing of Environment,* 114/3, 467-480

Guenther, B., Xiong, X., Salomonson, V.V., Barnes, W.L., & Young, J. (2002). On-orbit performance of the Earth Observing System Moderate Resolution Imaging Spectroradiometer; first year of data. *Remote Sensing of Environment,* 83/1-2, 16-30

Hale, G.M., & Querry, M.R. (1973). Optical Constants of Water in the 200-nm to 200-µm Wavelength Region. *Appl. Opt.,* 12/3, 555-563

Heege, T., & Fischer, J. (2004). Mapping of water constituents in Lake Constance using multispectral airborne scanner data and a physically based processing scheme. *Canadian Journal of Remote Sensing,* 30/1, 77-86

Hooker, S.B., Firestone, E.R., Esaias, W.E., Feldman, G.C., Gregg, W.W., & McClain, C. (1992). An overview of SeaWiFS and ocean color In: *NASA Tech. Memo. 104566*, *1* (24 p.), S.B. Hooker & E.R. Firestone (Eds.), NASA Goddard Space Flight Center

Hovis, W.A., Clark, D.K., Anderson, F., Austin, R.W., Wilson, W.H., Baker, E.T., Ball, D., Gordon, H.R., Mueller, J.L., El-Sayed, S.Z., Sturm, B., Wrigley, R.C., & Yentsch, C.S. (1980). Nimbus-7 Coastal Zone Color Scanner: System Description and Initial Imagery. *Science,* 210/4465, 60-63

IOCCG (2000). Remote sensing of ocean colour in coastal, and other optically-complex, waters. In: *Reports of the International Ocean-Colour Coordinating Group* (140 p.), S. Sathyendranath (Ed.), IOCCG

IOCCG (2006). Remote Sensing of Inherent Optical Properties: Fundamentals, Tests of Algorithms, and Applications. In: *Reports of the International Ocean-Colour Coordinating Group* (122 p.), Z.P. Lee (Ed.), IOCCG

IOCCG (2008). Why ocean colour? The societal benefits of ocean-colour technology. In: *Reports of the International Ocean-Colour Coordinating Group*, *7* (141 p.), T. Platt, N. Hoepffner, V. Stuart & C. Brown (Eds.), IOCCG

IOCCG (2010). Atmospheric correction for remotely-sensed ocean-colour products. In: *Reports of the International Ocean-Colour Coordinating Group*, *10* (78 p.), M. Wang (Ed.), IOCCG

Jaquet, J.-M., & Zand, B. (1989). Colour analysis of inland waters using Landsat TM data. In, (pp. 57-67). (ESTEC, Noordwijk)

Jin, Z., Charlock, T.P., Rutledge, K., Stamnes, K., & Wang, Y. (2006). Analytical solution of radiative transfer in the coupled atmosphere-ocean system with a rough surface. *Appl. Opt.,* 45/28, 7443-7455

Jin, Z., & Stamnes, K. (1994). Radiative transfer in nonuniformly refracting layered media: Atmosphere-ocean system. *Appl. Opt.,* 33/, 431-442

Keller, P.A. (2001). Comparison of two inversion techniques of a semi-analytical model for the determination of lake water constituents using imaging spectrometry data. *The Science of The Total Environment,* 268/1-3, 189

Kirk, J.T.O. (1991). Volume scattering function, average cosines, and the underwater light field. *Limnology and Oceanography,* 36/3, 455-467

Kisselev, V., & Bulgarelli, B. (2004). Reflection of light from a rough water surface in numerical methods for solving the radiative transfer equation. *Journal of Quantitative Spectroscopy and Radiative Transfer,* 85/3-4, 419

Koponen, S., Ruiz-Verdu, A., Heege, T., Heblinski, J., Sorensen, K., Kallio, K., Pyhalahti, T., Doerffer, R., Brockmann, C., & Peters, M. (2008). Development of MERIS lake water algorithms. In: *ESA Validation Report* (65 p.)

Kou, L., Labrie, D., & Chylek, P. (1993). Refractive indices of water and ice in the 0.65- to 2.5-µm spectral range. *Appl. Opt.,* 32/19, 3531-3540

Lee, M.E., & Lewis, M.R. (2003). A New Method for the Measurement of the Optical Volume Scattering Function in the Upper Ocean. *Journal of Atmospheric and Oceanic Technology,* 20/4, 563-571

Lee, Z., Carder, K.L., Mobley, C.D., Steward, R.G., & Patch, J.S. (1998). Hyperspectral Remote Sensing for Shallow Waters. I. A Semianalytical Model. *Appl. Opt.,* 37/27, 6329-6338

Miksa, S., Haese, C., & Heege, T. (2006). Time Series of Water Constituents and Primary Production in Lake Constance using satellite data and a physically based modular inversion and processing system. *Proc. Ocean Optics Conference XVIII*, 10

Mobley, C.D. (1994). *Light and Water*. San Diego: Academic Press Inc.

Mobley, C.D. (1999). Estimation of the Remote-Sensing Reflectance from Above-Surface Measurements. *Appl. Opt.,* 38/36, 7442-7455

Mobley, C.D., Gentili, B., Gordon, H.R., Jin, Z., Kattawar, G.W., Morel, A., Reinersman, P., Stamnes, K., & Stavn, R.H. (1993). Comparison of numerical models for computing underwater light fields. *Appl. Opt.,* 32/36, 7484-7504

Mobley, C.D., Sundman, L.K., & Boss, E. (2002). Phase Function Effects on Oceanic Light Fields. *Appl. Opt.,* 41/6, 1035-1050

Moore, G.F., Aiken, J., & Lavender, S.J. (1999). The atmospheric correction of water colour and the quantitative retrieval of suspended particulate matter in Case II waters: application to MERIS. *International Journal of Remote Sensing,* 20/9, 1713 - 1733

Morel, A. (1988). Optical Modeling of the Upper Ocean in Relation to Its Biogenous Matter Content (Case I Waters). *Journal of Geophysical Research,* 93/C9, 10749-10768

Morel, A., Claustre, H., Antoine, D., & Gentili, B. (2007). Natural variability of bio-optical properties in Case 1 waters: attenuation and reflectance within the visible and near-UV spectral domains, as observed in South Pacific and Mediterranean waters. *Biogeosciences,* 4/5, 913-925

Morel, A., & Gentili, B. (1991). Diffuse reflectance of oceanic waters: Its dependence on Sun angle as influenced by the molecular scattering contribution. *Appl. Opt.,* 30/30, 4427-4438

Morel, A., & Gentili, B. (1993). Diffuse reflectance of oceanic waters. II Bidirectional aspects. *Appl. Opt.,* 32/33, 6864-6879

Morel, A., & Gentili, B. (1996). Diffuse reflectance of oceanic waters. III. Implication of bidirectionality for the remote-sensing problem. *Appl. Opt.,* 35/24, 4850-4862

Morel, A., & Maritorena, S. (2001). Bio-optical properties of oceanic waters: A reappraisal. *J. Geophys. Res.,* 106/C4, 7163-7180

Morel, A., & Prieur, L. (1977). Analysis of Variations in Ocean Color. *Limnology and Oceanography,* 22/4, 709-722

Mueller, J.L., Austin, R.W., Morel, A., Fargion, G.S., & McClain, C. (2003). Introduction, Background and Conventions. In: *Ocean Optics Protocols for Satellite Ocean Color Sensor Validation, Revision 4, vol. 1*, *NASA/TM-2003-21621* (56 p.), J.L. Mueller, G.S. Fargion & C. McClain (Eds.), NASA, Goddard Space Flight Center, Greenbelt, MD

Nicolas, J.-M., Deschamps, P.Y., Loisel, H., & Moulin, C. (2005). POLDER-2/Ocean Color atmospheric correction algorithms. In: *Algorithm Technical Basis Document* (17 p.)

O'Reilly, J.E., Maritorena, S., Mitchell, B.G., Siegel, D.A., Carder, K.L., Garver, S.A., Kahru, M., & McClain, C. (1998). Ocean color chlorophyll algorithms for SeaWiFS. *Journal of Geophysical Research,* 103/C11, 24937-24953

Odermatt, D., Giardino, C., & Heege, T. (2010). Chlorophyll retrieval with MERIS Case-2-Regional in perialpine lakes. *Remote Sensing of Environment,* 114/3, 607-617

Odermatt, D., Heege, T., Nieke, J., Kneubuehler, M., & Itten, K. (2008a). Water quality monitoring for Lake Constance with a physically based algorithm for MERIS data. *Sensors,* 8/8, 4582-4599

Odermatt, D., Kiselev, V., Heege, T., Kneubühler, M., & Itten, K.I. (2008b). Adjacency effect considerations and air/water constituent retrieval for Lake Constance. *Proc. 2nd MERIS/AATSR workshop*, Frascati, Italy

Park, Y., & Ruddick, K. (2005). Model of remote-sensing reflectance including bidirectional effects for case 1 and case 2 waters. *Appl. Opt.,* 44/7, 1236-1249

Pegau, W.S., Zaneveld, J.R.V., Mitchell, B., Mueller, J.L., Kahru, M., Wieland, J., & Stramska, M. (2003). Inherent Optical Properties: Instruments, Characterization, Field Measurements and Data Analysis Protocols. In: *Ocean Optics Protocols for Satellite Ocean Color Sensor Validation, Revision 4, vol. 4*, *NASA/TM-2003-211621* (83 p.), J.L. Mueller, G.S. Fargion & C. McClain (Eds.), NASA, Goddard Space Flight Center, Greenbelt, MD

Petzold, T.J. (1972). Volume scattering functions for selected ocean waters. *SIO Ref. 72–78* (79 p.), Scripps Institution of Oceanography, Univ. of Calif., San Diego

Pope, R.M., & Fry, E.S. (1997). Absorption spectrum (380 -700 nm) of pure water. II. Integrating cavity measurements. *Applied Optics,* 36/, 8710-8723

Preisendorfer, R.W. (1961). Application of Radiative Transfer Theory to Light Measurements in the Sea. *International Union of Geodesy and Geophysics Monograph* (pp. 11-29)

Prieur, L., & Sathyendranath, S. (1981). An optical classification of coastal and oceanic waters based on the specific spectral absorption curves of phytoplanktion pigments, dissolved organic matter, and other particulate materials. *Limnology and Oceanography,* 26/4, 671-689

Rast, M., & Bezy, J.-L. (1999). The ESA Medium Resolution Imaging Spectrometer MERIS a review of the instrument and its mission. *International Journal of Remote Sensing,* 20/9, 1681-1702

Rey, P., & Müller, E. (2007). EU-Wasserrahmenrichtlinie und Schweizer Wasser- und Gewässerschutzgesetzgebung. In: *BAFU Expertenbericht* (95 p.), Hydra AG Gewässerfragen und Umweltinformation (in German)

Ruddick, K., Ovidio, F., & Rijkeboer, M. (2000). Atmospheric correction of SeaWiFS imagery for turbid coastal and inland waters. *Applied Optics,* 39/6, 897-912

Ruiz-Verdu, R., Koponen, S., Heege, T., Doerffer, R., Brockmann, C., Kallio, K., Pyhälahti, T., Pena, R., Polvorinos, A., Heblinski, J., Ylöstalo, P., Conde, L., Odermatt, D., Estelles, V., & Pulliainen, J. (2008). Development of MERIS lake water algorithms: Validation results from Europe. *Proc. 2nd MERIS/AATSR workshop*, Frascati, Italy

Santer, R., Brockmann, C., & Zuhkle, M. (2007). ICOL Validation Report. (26 p.), Université du Littoral Côte d'Opale, Wimereux, France

Santer, R., & Schmechtig, C. (2000). Adjacency effects on water surfaces: Primary scattering approximation and sensitivity study. (43 p.), Laboratoire Interdisciplinaire de Sciences de l'Environnement, Wimereux

Santer, R., & Zagolski, F. (2009). ICOL Improve Contrast between Ocean & Land. In: *BEAM Algorithm Technical Basis Document* (15 p.), Université du Littoral Côte d'Opale, Wimereux, France

Sathyendranath, S., & Platt, T. (1991). Angular Distribution of the Submarine Light Field: Modification by Multiple Scattering. *Proceedings: Mathematical and Physical Sciences,* 433/1888, 287-297

Sathyendranath, S., & Platt, T. (1997). Analytic model of ocean color. *Appl. Opt.,* 36/12, 2620-2629

Schaepman-Strub, G., Schaepman, M.E., Painter, T.H., Dangel, S., & Martonchik, J.V. (2006). Reflectance quantities in optical remote sensing--definitions and case studies. *Remote Sensing of Environment,* 103/1, 27-42

Schalles, J.F. (2006). Optical remote sensing techniques to estimate phytoplankton chlorophyll a concentrations in coastal waters with varying suspended matter and CDOM concentrations. In L.L. Richardson & E. LeDrew (Eds.), *Remote Sensing of Aquatic Coastal Ecosystem Processes: Science and Management Applications* (pp. 27-79). Dordrecht, Netherlands: Springer

Schiller, H., & Doerffer, R. (1999). Neural Network for Emulation of an Inverse Model Operational Derivation of Case II Water Properties from MERIS Data. *International Journal of Remote Sensing,* 20/9, 1735-1746

Siegel, D.A., Maritorena, S., Nelson, N.B., & Behrenfeld, M.J. (2005). Independence and interdependencies among global ocean color properties: Reassessing the bio-optical assumption. *J. Geophys. Res.,* 110/C7, C07011

Siegel, D.A., Wang, M., Maritorena, S., & Robinson, W. (2000). Atmospheric correction of satellite ocean color imagery: The black pixel assumption. *Applied Optics,* 39/21, 3582-3591

Sogandares, F.M., & Fry, E.S. (1997). Absorption spectrum (340 -640 nm) of pure water. I. Photothermal measurements. *Applied Optics,* 36/33, 8699-8709

Sokolov, A., Chami, M., Dmitriev, E., & Khomenko, G. (2010). Parameterization of volume scattering function of coastal waters based on the statistical approach. *Opt. Express,* 18/5, 4615-4636

Stumpf, R.P., Arnone, R.A., Gould, R.W., Martinolich, P.M., & Ransibrahmanakul, V. (2003). A partially coupled ocean-atmosphere model for retrieval of water-leaving radiance from SeaWiFS in coastal waters. In: *SeaWiFS Postlaunch Tech. Rep. Ser.*, *22* (51-59 p.), S.B. Hooker & E.R. Firestone (Eds.), NASA Goddard Space Flight Cent.

Sullivan, J.M., & Twardowski, M.S. (2009). Angular shape of the oceanic particulate volume scattering function in the backward direction. *Appl. Opt.,* 48/35, 6811-6819

Tanré, D., Deschamps, P.Y., Duhaut, P., & Herman, M. (1987). Adjacency Effect Produced by the Atmospheric Scattering in Thematic Mapper Data. *J. Geophys. Res.,* 92/D10, 12000-12006

UN Secretary General (2000). We the peoples: the role of the United Nations in the 21st century. In: *Millenium Report* (80 p.), United Nations

UNEP (1994). *The pollution of lakes and reservoirs*: United Nations Environment Programme

UNEP GEMS (2008). Water quality for ecosystem and human health. (130 p.), UNEP GEMS/Water Programme

US Congress (1977). Clean Water Act. Amendment to the Federal Water Pollution Control Act, P.L. 95-217

US Congress (1987). Water Quality Act. Amendment to the Federal Water Pollution Control Act, P.L. 100-4

Van Zee, H., Hankins, D., & deLespinasse, C. (2002). ac-9 Protocol Document (Revision F). (41 p.), WET Labs Inc.

Vidot, J., & Santer, R.P. (2003). Atmospheric correction for inland waters: application to SeaWiFS and MERIS. *Proc. Ocean Remote Sensing and Applications*, Hangzhou, China, 536

Voss, K.J. (1989). Use of the Radiance Distribution to Measure the Optical Absorption Coefficient in the Ocean. *Limnology and Oceanography,* 34/8, Hydrologic Optics, 1614-1622

WHO/UNICEF (2004). Meeting the MDG drinking water and sanitation target: A mid-term assessment of progress. (36 p.), WHO/UNICEF Joint Monitoring Programme for Water Supply and Sanitation

Zhai, P.-W., Hu, Y., Chowdhary, J., Trepte, C.R., Lucker, P.L., & Josset, D.B. (2010). A vector radiative transfer model for coupled atmosphere and ocean systems with a rough interface. *Journal of Quantitative Spectroscopy and Radiative Transfer,* 111/7-8, 1025-1040

Zhai, P.-W., Hu, Y., Trepte, C.R., & Lucker, P.L. (2009). A vector radiative transfer model for coupled atmosphere and ocean systems based on successive order of scattering method. *Opt. Express,* 17/4, 2057-2079

Zhang, M., Tang, J., Song, Q., & Dong, Q. (2010). Backscattering ratio variation and its implications for studying particle composition: A case study in Yellow and East China seas. *J. Geophys. Res.,* 115/C12, C12014

Zilioli, E., & Brivio, P.A. (1997). The satellite derived optical information for the comparative assessment of lacustrine water quality. *Science of The Total Environment,* 196/3, 229-245

Zimmermann, G., Neumann, A., Suemnich, K.-H., & Schwarzer, H.H. (1993). MOS/PRIRODA: an imaging VIS/NIR spectrometer for ocean remote sensing, Orlando, FL, USA, 201-206

2 WATER QUALITY MONITORING FOR LAKE CONSTANCE WITH A PHYSICALLY BASED ALGORITHM FOR MERIS DATA

This Chapter has been published as: Odermatt, D., Heege, T., Nieke, J., Kneubühler M. & Itten, K. I. (2008). Water quality monitoring for Lake Constance with a physically based algorithm for MERIS data. Sensors, 8, 4582-4599

Abstract

A physically based algorithm is used for automatic processing of MERIS level 1B full resolution data. The algorithm is originally used with input variables for optimization with different sensors (i.e. channel recalibration and weighting), aquatic regions (i.e. specific inherent optical properties) or atmospheric conditions (i.e. aerosol models). For operational use, however, a lake-specific parameterization is required, representing an approximation of the spatio-temporal variation in atmospheric and hydro-optic conditions, and accounting for sensor properties. The algorithm performs atmospheric correction with a LUT for at-sensor radiance, and a downhill simplex inversion of *chl-a*, *sm* and *y* from subsurface irradiance reflectance. These outputs are enhanced by a selective filter, which makes use of the retrieval residuals. Regular *chl-a* sampling measurements by the Lake's protection authority coinciding with MERIS acquisitions were used for parameterization, training and validation.

2.1 Introduction

Monitoring of water quality in lakes is an integral part of water resource management. It ensures the sustainable use of water and allows tracking the effects of anthropogenic influences. Water quality monitoring of the large fluviglacial Swiss lakes was established in the 1950s and 1960s. A broad range of water quality parameters is sampled at decent temporal resolutions, but very limited in the spatial dimension. In the early 1990s, analytical methods applied to high spectral resolution airborne scanner data were found to bear the potential to overcome these limitations. But neither did these studies lead to operational algorithms, nor was an adequate space borne sensor for monitoring purposes available at the time [1]. The latest generation of medium resolution Earth observation sensors (i.e. Moderate Resolution Imaging Spectroradiometer MODIS, Medium Resolution Imaging Spectrometer MERIS) provide a nominal revisit time of 2-3 days at mid latitudes and could therefore be an effective means to provide spatial measurements. A recent MERIS algorithm based on neural networks [2] improved the applicability of remote sensing data to optically complex waters (i.e. case II), and validation experiments confirmed the potential of satellite remote sensing for inland water quality monitoring, but at the same time revealed shortcomings concerning especially atmospheric correction [3].

MIP (Modular Inversion and Processing System) is an alternative algorithm based on the minimization of the difference between satellite measured and modeled spectra. It was developed for use with airborne sensors, where changing image acquisition conditions require higher flexibility [4, 5]. MIP was originally designed for Lake Constance, but has been used for different industrial and research applications in several marine (e.g. coast of Western Australia, Indonesia) and limnic (e.g. Lake Sevan/Armenia, Mekong/Vietnam, Lake Starnberg and Lake Waging-Taching/Germany) environments. The aim of this work is to make MIP applicable for automatic processing by optimizing a single, lake specific parameterisation for MERIS data of Lake Constance.

Lake Constance is the second largest lake in Western Europe, covering an area of 535 km^2 shared by Austria, Germany and Switzerland. It is located at 395 m a.s.l., its average and maximum depth are 101 m and 253 m, respectively. 15% of its area is shallow water of less than 10 m depth. The Alpenrhein River is its main feeder, accounting for 62% of the total inflow. Originally oligotrophic, the eutrophication of Lake Constance reached a peak in the late 1970s, mainly

due to nutrient influxes, followed by 20 years of steady reoligotrophication [6, 7]. Bi-weekly water quality monitoring measurements are carried out by IfS, on behalf of IGKB. Total phosphorous concentrations are still decreasing, e. g. from 10 mg/m^3 in spring 2003 to 8 mg/m^3 in spring 2005. Highest chlorophyll-a concentrations are reached during spring blooms, with a maximum of 11.8 µg/l in the top 10 m layer on 19 March 2002, but possibly higher concentrations at the water surface. Apart from 2002, spring blooms occurred earlier and at a smaller extent in recent years. In 2005, it started in late March and reached its peak in mid April, two weeks earlier than in 2003 [8]. Other than that, seasonal variations of chlorophyll-a concentrations are between 1 µg/l in winter and 3-5 µg/l in summer and autumn [7].

2.2 Data

2.2.1 Satellite data

51 MERIS level 1B full resolution datasets [9] of Lake Constance with coinciding IGKB water quality measurements are used in total. Both 2241 square pixel scenes and 1153 square pixel quarter scenes ("imagettes") are processed. MERIS data consist of 15 spectral channels as described in Table 2-1, at a ground resolution of about 300 m, and metadata, including geolocation, geometry and quality flag layers. Smile correction was not applied.

In pre processing, MERIS geolocation metadata is searched for the center coordinates of Lake Constance. A 501 to 301 pixels subset of all channels is extracted where these coordinates are found (Figure 2-1). The clippings include scaled radiances of all channels and are saved in BIL (Band Interleaved by Line) format. Meta data such as observation date, time and geometry, geolocation data and pixel quality flags are added for use in MIP modules and post processing. Georeferencing is not performed.

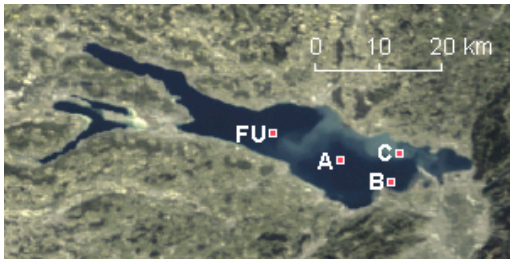

Figure 2-1: MERIS true color composite of Lake Constance, acquired 20 April 2007. Fischbach-Uttwil (FU) and the measurement sites A to C are located in the main basin called Obersee, with the finger-shaped Lake Überlingen in the top left corner of the image and the separated Untersee below. Geometric correction was not applied; the scale is averaged for the lake surface.

Table 2-1: Operational MERIS band set [9].

Band	Wavelength [nm]	Width [nm]	Potential Applications
1	412.5	10	Yellow substance, turbidity
2	442.5	10	Chlorophyll absorption maximum
3	490	10	Chlorophyll, other pigments
4	510	10	Turbidity, suspended sediment, red tides
5	560	10	Chlorophyll reference, suspended sediment
6	620	10	Suspended sediment
7	665	10	Chlorophyll absorption
8	681.25	7.5	Chlorophyll fluorescence
9	705	10	Atmospheric correction, red edge
10	753.75	7.5	Oxygen absorption reference
11	760	2.5	Oxygen absorption R-branch
12	775	15	Aerosols, vegetation
13	865	20	Aerosols corrections over ocean
14	890	10	Water vapor absorption reference
15	900	10	Water vapor absorption, vegetation

Among the total 51 images processed, a total of 18 images could not be further used in this study (Table 2-2). The data were excluded due to 3 different reasons:

(1) Sun glint occurs for certain observation geometries and rough water surfaces (i.e. high wind speed). It increases reflected NIR radiance, and thus causes errors in atmospheric correction. MERIS sun glint warning flags aren't set for inland waters, and wind speed metadata is not applicable over land. However, in the summer half-year, even 1 m/s wind speed on Lake Constance causes 1% sun glitter reflection at 20° eastward viewing zenith angle [10]. Eight erroneously processed images acquired at more than 20° eastward zenith in the summer half-year were therefore considered to be affected by sun glint.

(2) Cirrus clouds or contrails are visible in 6 images, although they are not identified by the MERIS bright pixel flags.

(3) MIP's atmospheric correction module is unable to process 4 images, in which aerosol optical thicknesses (AOT) is overestimated and reflectances in channels 1, 2, 6, 7 and 8 become zero [11].

Table 2-2: Overview of MERIS datasets used in this study.

Year	Initial set	Sun glint suspect	Cirrus or contrails	MIP error	Working set	Purpose
2003	11	1	1	1	8	Training
2004	10	2	2	1	5	Training
2005	12	3	0	1	8	Training
2006	16	2	2	1	11	IGKB Validation
2007	2	0	1	0	1	Field validation
Total	*51*	*8*	*6*	*4*	*33*	

2.2.2 Field campaign data

On 20 April 2007, up- and downwelling irradiances E_u and E_d, were measured in situ during MERIS overpass, R^- was calculated through (Eq. 2-1). The measurements with two RAMSES AAC instruments [12] onboard a research vessel of IfS were taken in the 4 sites depicted in Figure 2-1. Each dataset is an average of more than 20 5 s sampling intervals. The data is spectrally binned to 70 channels between 350 and 700 nm, at uniform intervals of 5 nm. Measurements were taken about 20 cm below the water surface and at 1 m depth. The relatively higher variations in the water column above the instrument during the 20 cm measurements caused generally smaller standard deviations than the low signal level at 1 m depth, the 20 cm data was thus preferred for further analysis (Figure 2-2). However, some instrument noise persists, even after manual removal of outliers, especially at 600-700 nm in the data of site B.

$$R^- = E_u^- / E_d^- \qquad \text{(Eq. 2-1)}$$

Reference measurements of constituents are taken from water samples. Suspended matter (*sm*) is measured as sum of organic and inorganic matter not passing a 1 μm glass fiber filter [5]. Gelbstoff (*y*) is filtered through a 0.2 μm filter and measured in a laboratory spectrometer [13]. However, the results are strongly inconsistent with one another, we can therefore only compare the *y* concentrations of MERIS and RAMSES inversion. Chlorophyll-a (*chl-a*) was measured with a fluorometer probe, which is cross-calibrated with HPLC (High Performance Liquid Chromatography) measurements by IfS.

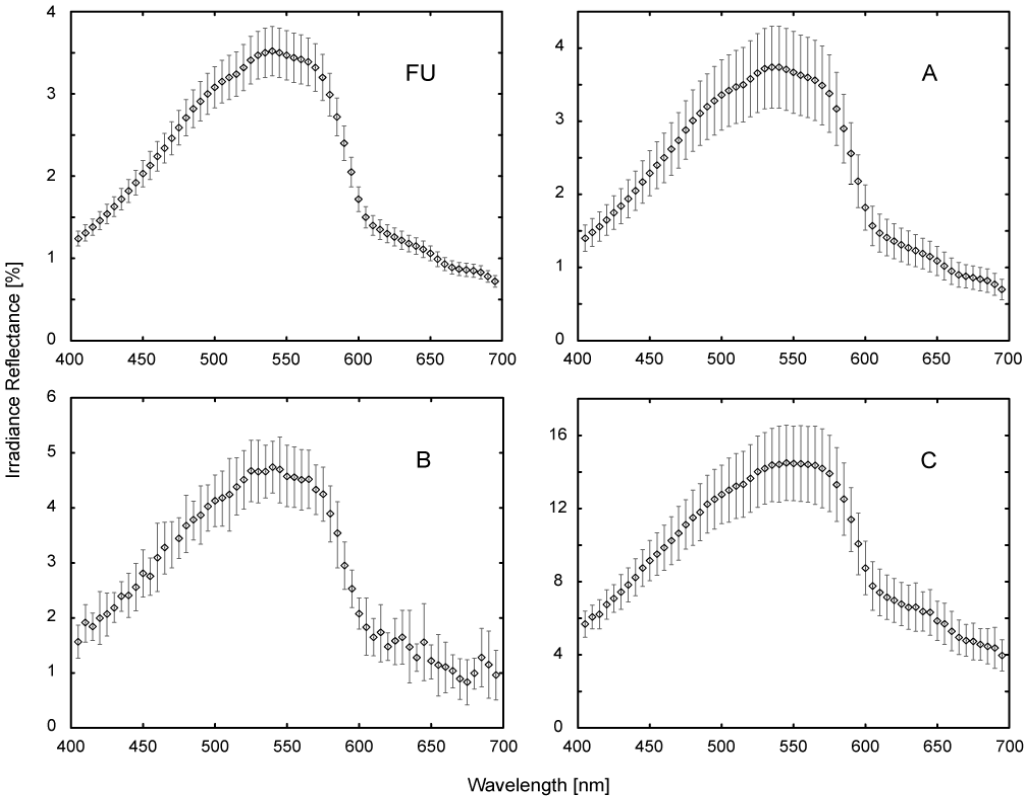

Figure 2-2: RAMSES data acquired in the sites FU and A-C (Figure 2-1) at a depth of 20 cm, on 20 April 2007.

2.2.3 Water quality monitoring data

In situ *chl-a* measurements carried out by IfS as part of the water quality monitoring by IGKB are used for training and validation of MERIS processing results. The data were sampled at the site Fischbach-Uttwil (FU, Figure 2-1, 47.62N / 9.37E), in approximately bi-weekly intervals. FU is located in the lake's deepest area and was chosen for comparison with satellite data because the disturbance by adjacency effects occurring in MERIS data is minimal in the pelagic [11]. The method used for *chl-a* determination is HPLC [14, 15]. 103 in situ measurements are available for the investigation period 2003-2006. Concurring measurements are available for 47 MERIS images; 4 dates in 2006 were interpolated from consecutive IGKB measurements with only small variation.

The *chl-a* concentrations measured by IfS represent an integral of the top 20 m layer, whereas the estimate from MERIS data represents only the top layer from which the signal originates. In Lake Constance, the top 2 (blue, red) to 8 m (green light) account for 90% of the reflected radiance, when the water is very clear. But in turbid waters, the same part of reflected radiance may be from only 1 and 2 m, respectively [5]. This means that vertical variations in water constituent concentrations, which are included in the 20 m column samples, will not be represented by estimates from remote sensing. However, the analysis of more than 350 profiles for both *chl-a* and *sm* in Lake Überlingen revealed a strong vertical correlation between the top layer at 0.5-1.5 m and the layers below [5, 16].

2.3 Methods

2.3.1 Algorithm description

The MERIS level 1B FR data are processed with two MIP modules [4, 5]. The first MIP module performs image based aerosol retrieval and atmospheric correction on at-sensor radiance data. It uses a look up table (LUT), which was simulated with a coupled, plane-parallel atmosphere-water model and the finite element method [17]. The module relates at-sensor radiances L_s to AOT of either continental, maritime or rural aerosol type, observation geometry, wavelength and the subsurface radiance reflectance R_L^-, which is mainly due to backscattering on suspended matter (*sm*) at large wavelengths. The resulting AOT map is used to retrieve the angularly dependent subsurface radiance reflectance R_L^- for channels 1-8 from the same LUT. Another LUT is used to account for the directionality of the underwater light field, thus to convert R_L^- to the angularly independent subsurface irradiance reflectances R^-. It consists of *Q*-factors for varying wavelengths, observation geometries and water constituent concentrations, and is applied to R_L^- according to (Eq. 2-2).

$$R^- = R_L^-(\Delta\phi,\theta_{obs},\theta_{sun})\pi / Q(\Delta\phi,\theta_{obs},\theta_{sun}) \qquad \text{(Eq. 2-2)}$$

The inherent optical properties (IOP) of water are related to R^- through Equation (Eq. 2-3) [18], where f is parameterized as a function of μ [19], and μ is calculated for $z = 0$ m as a function of a, b, and the mean cosine of the incident light field [20].

$$R^{-} = f\ b_b/(a+b_b) \qquad \text{(Eq. 2-3)}$$

The coefficients x_i for absorption ($x=a$), scattering ($x=b$) and backscattering ($x=b_b$) of pure water ($i=w$), chlorophyll-a ($i=chl\text{-}a$), suspended matter ($i=sm$), and gelbstoff absorption ($i=y$) are calculated by (Eq. 2-4), whereas a_{sm}, $b_{chl\text{-}a}$ and b_y can be neglected for Lake Constance [4, 5].

$$x = x_w + x_{chl-a}chl - a + x_{sm}sm + x_y y \qquad \text{(Eq. 2-4)}$$

The inversion of subsurface irradiance reflectance R^- to the coefficients x_i is accomplished by another MIP module. It adjusts modeled and input image spectra after atmospheric correction by means of a downhill simplex algorithm [21]. The algorithm starts with a set of initial concentrations. The spectrum modeled for these concentrations is linearly scaled to fit the input spectrum, leading to a first guess of concentrations, which is then optimized by two iterations of Q-factor correction and water constituent retrieval. The full processing scheme is illustrated in Figure 2-3.

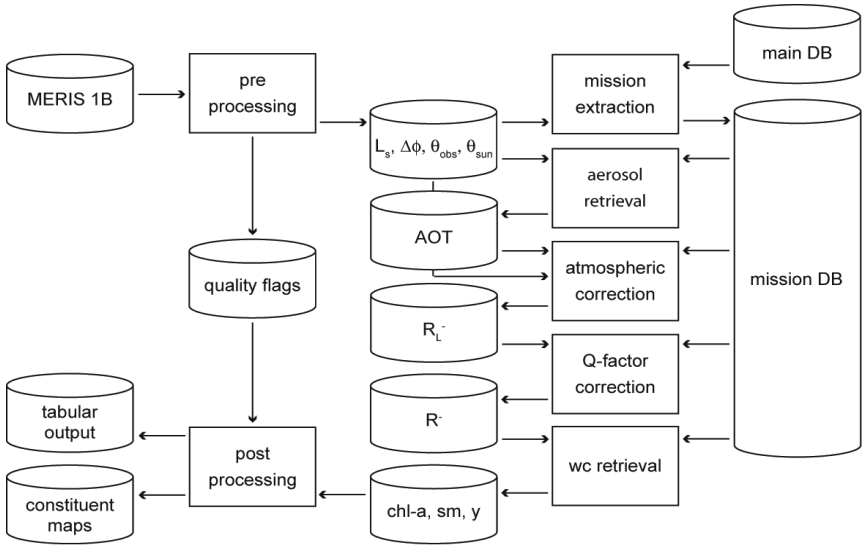

Figure 2-3: Flow chart of the automatic data processing chain. The mission DB contains the LUTs for atmospheric and Q-factor correction, for the data specifications defined in the mission extraction. The tabular output contains concentration and retrieval quality parameters for FU and lake means.

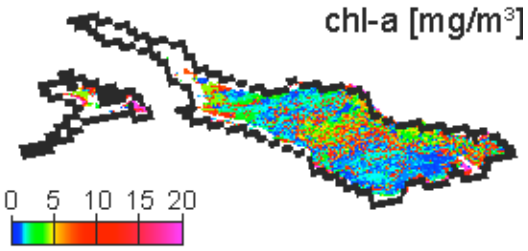

Figure 2-4: Chl-a map for 20 April 2007, prior to filtering.

MIP generates maps of *chl-a* and *sm* concentration, *y* absorption (400 nm) and AOT (550 nm). Furthermore, residuals of image and model spectra fits are calculated as a retrieval quality indicator. Occasional over- and under-estimation of AOT by the atmospheric correction module may cause zero reflectances in red bands or a shift of the reflectance peak towards the blue bands, respectively. This may force the constituent retrieval algorithm to approximate irregular spectral shapes, leading to high variations between neighboring pixels, and in places the algorithm reaches its threshold of 20 mg/m^3 (Figure 2-4). Such aberrations can be reduced by a low pass filter on input imagery [22], as SNR in MERIS channels 1-8 of reduced resolution (RR) data decreases from about 1:1100 to 1:500, but is very close to 4 times lower in FR data [23, personal communication]. In order to use the retrieval residual as an indicator of whether the atmospherically corrected R^- are valid water spectra reproducible by the model, we combined such spatial smoothing with a selective filter, which replaces each output concentration pixel by the average of the concentrations of the 3 pixels fitted at the lowest residual within a 5x5 neighborhood.

Figure 2-4 and Figure 2-5 show *chl-a* outputs for the field campaign date 20 April 2007 prior to and after filtering, respectively. This image is affected by the presence of cirrus clouds and thus suboptimal atmospheric conditions. This leads to a high variation in the atmospheric correction output and consequently to high *chl-a* variations, which are removed by selective filtering. The images also show two regional limitations of the data processing: (1) narrow Lake Überlingen is frequently excluded from processing due to the influence of adjacency effects, and (2) Untersee results are often missing or reaching the algo-

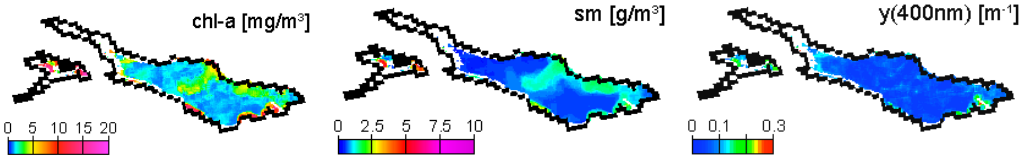

Figure 2-5: Chl-a, sm and y map for 20 April 2007, after application of the selective filter.

rithm threshold, due to large shallow water areas and possibly bad representation by the SIOP (specific inherent optical properties) optimized for Obersee.

2.3.2 Algorithm parameterization

MIP is originally used with input variables for individual optimization with sensors (i.e. channel weighting), aquatic regions (i.e. SIOP) or atmospheric conditions (i.e. aerosol models). For operational use, a lake-specific parameterization for best performance with all datasets is required, approximating the spatio-temporal variation of hydro-optic conditions. Iterative, image-based optimization is applied to determine aerosol model, AOT estimation channel and *sm* a priori assumption. Largest differences are found for different aerosol types, with continental aerosols leading to an underestimation of reflectances in short wavelength channels and finally to an overestimation of *chl-a* and low *sm*. Channel 14 (Table 2-1) measures in between the water vapor absorption bands, and has therefore performed best in the estimation of AOT with this algorithm [10]. The optimization of SIOP is done with the RAMSES measurements of 20 April 2007 and previous projects in Lake Constance [4, 24]. Measured R^- is inverted with absorption and scattering coefficients known from literature (Table 2-3).

Table 2-3: Parameters used for analysis of Lake Constance (1).

Process	Parameter	Value
Atmospheric Correction (L_S to R_L^-)	Aerosol model	Maritime [10]
	AOT estimation	MERIS channel 14 [10]
	sm assumption	1.5 g/m^3 [10]
Water Constituent Retrieval (R_L^- to *chl-a*, *sm*, *y*)	a_w	Buiteveld et al. [27]
	$a_{chl\text{-}a}$	Heege [5]*0.75
	a_y	S=0.014 [28]
	b_w	Smith and Baker [29]
	$b_{b,\,sm}$	$0.014(\lambda/400)^n$; n=$-0.8(\lambda/400)^{1.2}$; b_b/b=0.019 [5]

For $b_{b,\,sm}$, we started iterations with a known exponential function [25], and adjusted the constants in factor and exponent, for a constant b_b/b ratio of 0.0019 [4], which leads to a generally good agreement of modeled and measured RAMSES spectra (Figure 2-6). Reference spectra with high *sm* concentrations (i.e. Alpenrhein plume) are modeled less adequately than others, but an improved agreement for these sites can only be achieved by reducing the spectral exponent S [26] of *y* to 0.012 or by introducing an absorbing part of *sm* with

S=0.012. The reason for this could be a significant portion of detritus absorption, which is not the case in other parts Lake Constance. In order not to decrease the model quality for the typical range of conditions, we neglected this change in SIOP. Iterations within certain thresholds are started with initial values (Table 2-4) unless values of adjacent pixels are available.

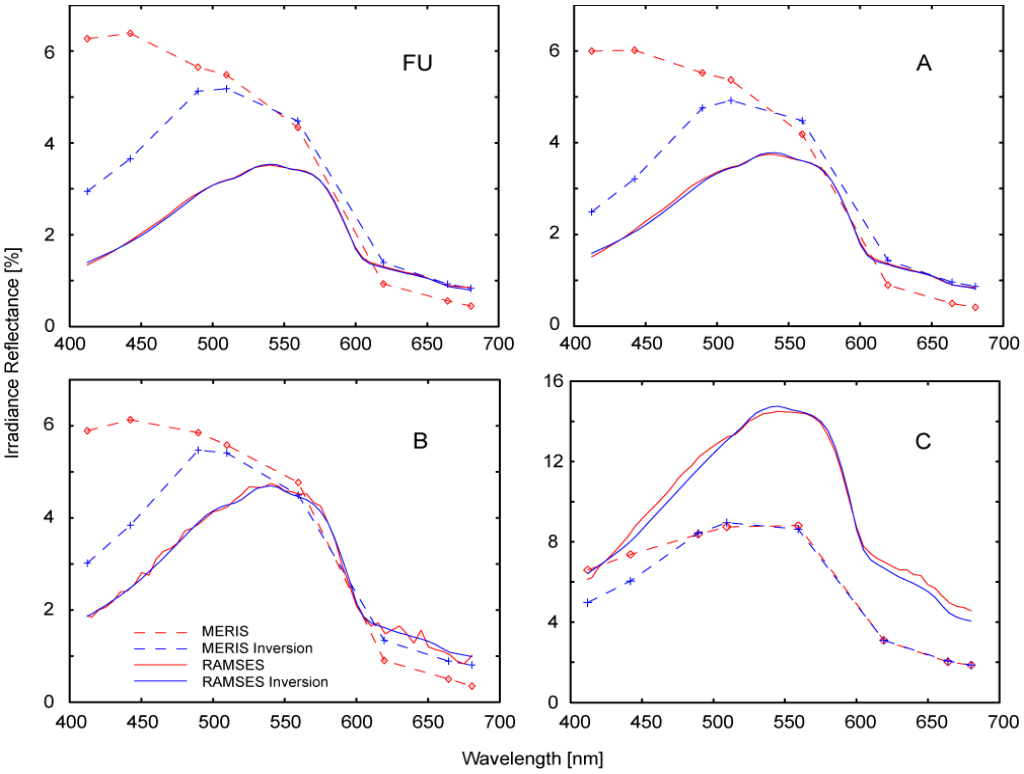

Figure 2-6: MERIS and RAMSES irradiance reflectance spectra for the sites FU and A-C (Figure 2-1) on 20 April 2007, with corresponding model spectra as resulting from inversion iterations. The concentrations calculated for inversion results are in Table 2-5.

Table 2-4: Parameters used for analysis of Lake Constance (2, values from [5]).

Constituent	**Initial value**	**Min. threshold**	**Max. threshold**
chl-a [mg/m^3]	3	0.3	20
sm [g/m^3]	1.5	0.2	10
y [m^{-1} (440 nm)]	0.2	0.1	0.35

Table 2-5: 20 April 2007 reference measurements (lab) sampled at 0.5 to 1 m depth, inversion results for RAMSES (ram, Figure 2-2) and MERIS (mer). MERIS acquisition time was at 9:46 UTC. MERIS pixel results are after filtering, results may thus vary slightly from the spectra in Figure 2-6.

Site	UTC ram	*chl-a* [mg/m^3]			*sm* [g/m^3]			*y* [m^{-1}] (400 nm)	
		situ	ram	mer	situ	ram	mer	ram	mer
FU	8:20	0.8	1.1	1.4	0.6	0.6	0.8	0.25	0.11
A	9:25	1.1	1.9	1.1	0.8	0.7	0.7	0.21	0.10
B	10:20	1.1	1.3	0.9	1.0	0.9	0.7	0.22	0.10
C	11:05	3.6	4.9	3.2	2.3	3.9	1.7	0.20	0.12

The *chl-a* concentrations of RAMSES and MERIS inversion and fluorometer measurements reveal an overestimation by RAMSES in sites A-C. In FU, the RAMSES inversion produced higher *y* absorption than in the other sites, but outputs a relatively low *chl-a* concentration. These two parameters can act as substitutes in the inversion and therefore cause certain discrepancies. Another uncertainty lies in the high spatio-temporal variation on the border of the plume in the center of the main basin, which is visible in Figure 2-1 and might have changed during the 3 hours of reference data acquisition. The *sm* concentrations agree better, with only the RAMSES estimate of site C revealing a larger offset. *Y* estimates by MERIS are impossible due to low reliability of the calculated R^- in channels 1 and 2, especially with difficult atmospheric conditions such as on 20 April 2007.

2.3.3 Inversion parameterization

Figure 2-6 displays a good agreement of RAMSES and MERIS in channels 5-8 for FU, A and B. Channels 1-4 are overestimated, possibly due to the thin cirrus clouds observed on that day, which are not accounted for in the atmospheric correction. The inversion algorithm enables individual weighting to account for systematic differences in the channels' reliability. In site C, AOT is overestimated because of significantly higher *sm* than assumed a priori. However, similar offsets occur also in most data with low *sm*, when using MERIS' original calibration. Empirical recalibration factors were thus applied to compensate for the bias found between calibrated radiances and model calculations. This adjustment was found necessary in previous work [22, personal communication], but only processing other sensors or lakes will reveal to what extent this is due to inaccuracy of model or calibration.

21 pairs of concurring *chl-a* measurements and MERIS images in 2003-2005 are used as training data. They are processed with varying weightings of channels 1-8 in the water constituent retrieval module, and with varying empirical recalibration factors for channel 1, 2, 3 (water constituents) and 14 (atmospheric correction). The optimization is started with channel 14, whose original radiance values lead to frequent overestimations of AOT, and thus to zero subsurface reflectance in channels 1, 2, 6-8. The datasets are processed in iterations with channel 14 lowered in intervals of 0.5%, which changes AOT only by few percent, but has a distinctive impact on short wavelength channel reflectances. Water constituent retrieval was performed for each AOT estimate, and *chl-a* outputs were compared to IGKB values. The best agreement was found for 0.97. Similar but multivariate optimization iterations are performed with the channels used by the water constituent module, using correlation coefficients as optimization measure. Channel 1 is excluded from the retrieval, since it displays random offsets from model results. Similar problems are encountered with channels 2 and 3, but reduction in weighting and individual recalibration leads to better results than their exclusion. The lowest R^- used is normally channel 8, which is thus the first to become zero when AOT is overestimated. Channel 8's weighting was therefore also slightly reduced. Table 2-6 is an overview of the weighting and recalibration values.

Table 2-6: Weighting and recalibration factors for MERIS bands 1-8 and 14 (Table 2-1), which were used for water constituents and AOT retrieval, respectively.

Channel	**1**	**2**	**3**	**4**	**5**	**6**	**7**	**8**	**14**
Recalibration	-	0.975	0.98	-	-	-	-	-	0.97
Weighting	-	0.2	0.5	1	1	1	1	0.8	0.97

2.4 Results

2.4.1 Training of empirical recalibration

The training data that were used in the recalibration reveal relatively low concentrations in 2003 and 2004, but high concentrations in 2005 (Figure 2-7). They contain data pairs for each spring bloom, but according to Lake Constance's natural variation, most data pairs represent *chl-a* concentrations between 1-4 mg/m^3. The largest relative differences between satellite and sampling results are found for the datasets of 29 March 2004 and 15 April 2005.

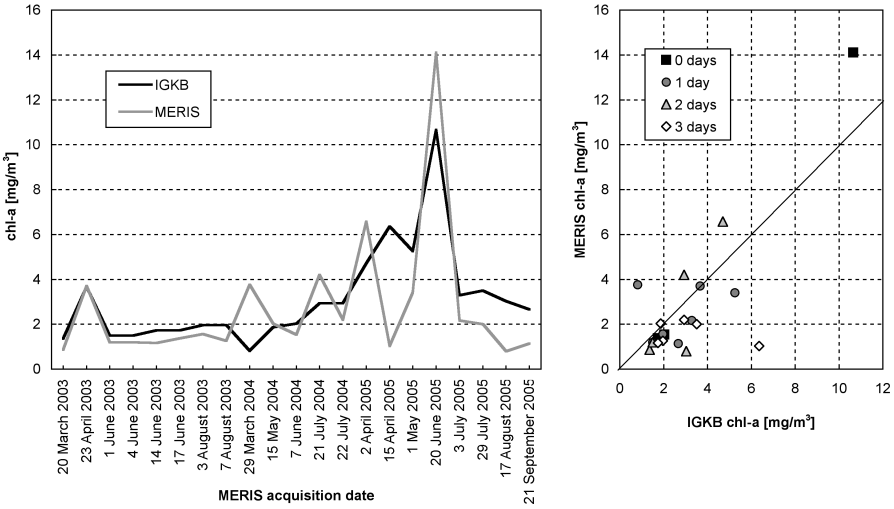

Figure 2-7: 21 chl-a data pairs for the site FU, 2003-2005. The number of days between data acquisition are indicated in the figure on the right. MERIS values are filtered outputs, as shown in Figure 2-5.

MERIS image of 29 March 2004 outputs high concentrations, while the corresponding IGKB measurement on 30 March 2004 is exceptionally low. However, a simultaneous probe profile reveals much higher values, and sample measurements acquired two weeks earlier and later confirm the spring bloom seen by MERIS. On 18 April 2005, IGKB measurements reach the spring bloom maximum of 6.4 mg/m^3, while the corresponding estimate of MERIS for the sampling station FU on 15 April 2005 is remarkably low. However, MERIS derived concentrations are up to 5 mg/m^3 in the eastern part of the main basin (Figure 2-8). A possible explanation could therefore be the spatio-temporal variation of algae, which can lead to significant differences for this data pair, where MERIS and IGKB acquisition lie 3 days apart (Figure 2-7, right). For the total 21 *chl-a* training data pairs, a correlation coefficient of 0.79 is achieved by iterative optimization of weighting and recalibration. If the images of 29 March 2004 and 15 April 2005 are excluded, the correlation coefficient increases to 0.94.

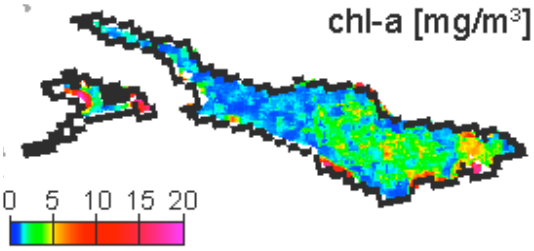

Figure 2-8: Chl-a concentration map for 15 April 2005.

2.4.2 Validation

11 datasets acquired in 2006 were processed with the weighting and recalibration optimized for 2003-2005 data. The agreement with IGKB data is good for the first 8 datasets from March to August, correlating at a coefficient of 0.89, and representing the spring bloom, low *chl-a* in summer and an increase in August. However, an extraordinary increase in autumn is found in IGKB data, which is not found in MERIS imagery, leading to a low overall correlation (Figure 2-9).

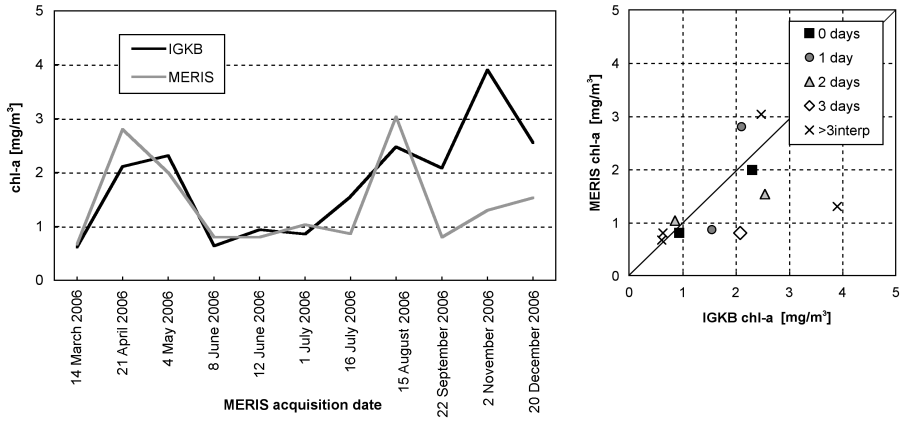

Figure 2-9: 11 chl-a data pairs for validation of IGKB and MERIS measurements, for the site FU, 2006. Number of days between in situ sampling and satellite overpass are indicated in the figure on the right.

On 22 September 2006, 1-3 mg/m^3 *chl-a* are calculated for the cloud free area around FU (Figure 2-10), thus a fairly good agreement with IGKB data. However, spatial variation is high, and the filtered FU geolocation pixel happens to output a significantly lower concentration value. The results for 2 November 2006 depict a more general explanation for the

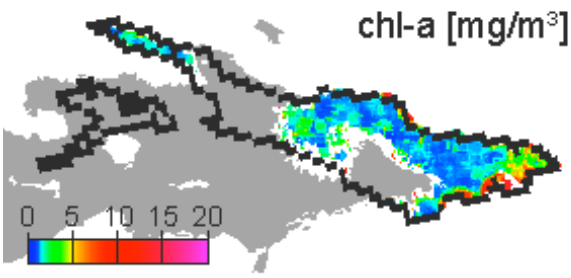

Figure 2-10: Chl-a concentration map for 22 September 2006. Grey color indicates bright pixel flags in MERIS data, white pixels within the shoreline are considered clouds by MIP's own masking algorithm.

large differences in late 2006 data. The image based AOT retrieval is about 0.05 only, leading to inadequate atmospheric correction, and subsequently to erroneous water constituent output (Figure 2-11). In the IGKB measurements on 7 November 2006, Secchi depth of 8.3 m at FU is slightly above average, while *chl-a* samples reveal the maximum annual concentrations of 4.5 mg/m^3 and 5.1 mg/m^3 in the same week. However, high *chl-a* concentrations in the pelagic of Lake Constance normally lead to increased extinction and therefore low Secchi depth. A significant change in SIOP could therefore be a possible explanation for both the unexpected combination of high *chl-a* and high Secchi depth and the error in AOT estimation.

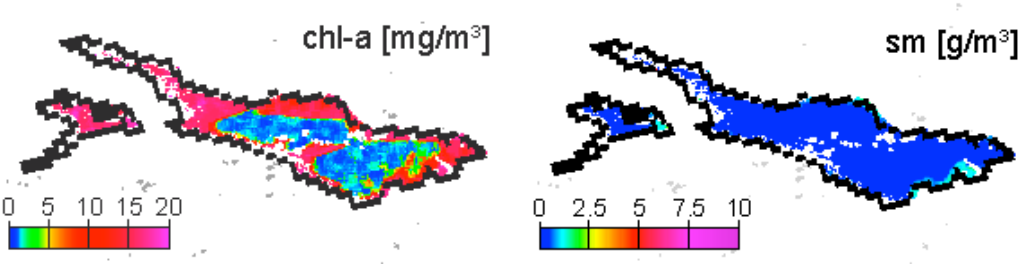

Figure 2-11: Chl-a and sm concentration maps for 2 November 2006. Pink and dark blue colors represent threshold concentrations allowed by the algorithm, which indicates erroneous processing.

2.5 Conclusions and Discussion

This study confirms the general applicability of MIP for automatic, operational processing by applying a lake specific parameterization. The correlation of *chl-a* estimates from MERIS with in situ water quality monitoring is sufficient, considering differences in methodology and spatial representation. MERIS processing results are most reliable, when satellite estimates are validated by concurring in situ measurements, and applied for their additional spatial significance. Alternatively, MERIS *chl-a* results can be used as additional estimates, and thus improve the temporal resolution of current water quality monitoring. However, this approach requires the analysis of unvalidated MIP results, which are occasionally affected by processing errors. Expert knowledge is thus required in the interpretation of unvalidated outputs.

We distinguish three potential error sources introduced by the present processor, i.e. atmospheric correction, bio-optical parameterization and filtering. At-

mospheric correction is the most fragile part. Errors in this module may be due to insufficient assumptions for atmospheric correction parameters (i.e. fixed aerosol model, *sm* a priori assumption). Adjacency effects are another source of atmospheric correction error and suspect of making most results of Lake Überlingen inadequate. Radiances in channel 14 thereby continuously increase towards the shore, leading to similarly increasing AOT estimates. This again leads to an underestimation of atmospherically corrected reflectances, especially in channels with high atmospheric scattering (1, 2) or low water reflectivity (6, 7, 8), where output reflectances can drop even to zero. The respective output concentrations are then either missing or equaling one of the threshold parameters, which are frequently found in areas within up to 5 pixels from the coastline [11]. Existing adjacency effect correction methods are currently considered for implementation [30, 31]. When large areas of the lake are unavailable in output, the reasons are either thin clouds ignored by MERIS quality flags or exceptionally high channel 14 radiances that cannot be accounted for with a constant *sm* backscattering assumption. A solution for the latter is the implementation of a more complex atmospheric correction module, which is iteratively coupled to the water constituent retrieval [22]. Neglecting MERIS' smile error could be another potential source of errors, although no camera border artifacts or correlation with observation zenith angle was found in the results.

The water constituent retrieval produces *chl-a* output that agrees well with FU sampling data, apart from the exceptional phytoplankton bloom in late 2006, where a change in SIOP seems to cause erroneous processing, with the simplified empirical parameterization being only a limited representation of the bio-optical complexity of the lake. However, the physical constitution enables arbitrary modifications to any single parameter where such problems occur, which could eventually lead to an alternative set of parameters to be specified for certain events that are known to lie out of range of the original parameterization.

The residual weighted filter improves the results significantly, by reducing aberrations by the algorithm due to atmospheric correction inaccuracies and at the same time performing spatial averaging to address the relatively low SNR in FR data. Moreover, the gap between spatially discrete laboratory samples and the complex representation of a spatially averaged, depth dependent estimate by remote sensing is hard to bridge. A conversion formula based on depth resolved profile measurements in Lake Überlingen [5] suggests that remote sensing generally underestimates sample measurements. This is not the case with our results, thus no conversion calculation was performed. However, the

optimization of the channel recalibration with original IGKB data can be excluded as reason for this discrepancy, since it leads to large modifications in the processing of certain images, but not to a general scaling of the results.

An empirical recalibration of level 1B radiances was found necessary for the processing of MERIS data, with a majority of datasets producing erroneous or unreasonable output with the original calibration. The exact significance of this recalibration will only clarify with further investigation. It is expected that the processing chain can be applied to other large, prealpine lakes with the same recalibration, and individually optimized parameterizations only. Other than that, we consider the complementary use of and adjustment for MODIS data, whereof experience is available from previous work with MIP.

Acknowledgements

The authors thank the Swiss National Science Foundation, Contract Nr. [200020-112626/1] for funding this project, Institute for Lake Research (IfS) Langenargen of LuBW and German Aerospace Center (DLR) Oberpfaffenhofen for active support with data, vessels, staff and instruments. The field campaigns in 2007 were supported by ESA, contract Nr. 20436/07/I-LG. Special thanks are due to Kirstin König and Andreas Schiessel (LuBW), Jörg Heblinski (EOMAP), Hanna Huhn, Esra Mandici, Thomas Agyemang, Klaus Schmieder (Univ. Hohenheim), Juliane Huth and Thomas Krauss (DLR) for their commitment in field work; Silvia Ballert (Univ. Konstanz), Brigitte Engesser (LuBW) and Anke Bogner (EOMAP) for their laboratory work; the Internationale Gewässerschutz Komission Bodensee IGKB for provision with ground truth data from the standard monitoring program; Steven Delwart for his information regarding MERIS SNR estimation experiments; Peter Gege for support with gelbstoff measurement interpretation and Andreas Hueni in the preparation of the manuscript.

2.6 References and Notes

1. Dekker, A.; Malthus, T.J.; Hoogenboom, H.J. The remote sensing of inland water quality. In Advances in Environmental Remote Sensing; Danson, F.M., Plumer, S.E., Eds.; Wiley & Sons: New York, 1995; pp. 123-142.

2. Doerffer, R.; Schiller, H. The MERIS Case 2 water algorithm. Int. J. Remote Sens. 2007, 28 (3), 517-535.

3. Gege, P.; Plattner, S. MERIS validation activities at Lake Constance in 2003. In Proc. of the MERIS User Workshop, Frascati, Italy, 10-13 November 2003; 2004.

4. Heege, T.; Fischer, J. Mapping of water constituents in Lake Constance using multispectral airborne scanner data and a physically based processing scheme. Can. J. Remote Sensing 2004, 30 (1), 77-86.

5. Heege, T. Flugzeuggestützte Fernerkundung von Wasserinhaltsstoffen am Bodensee; DLR-Forschungsbericht, 2000, 2000 (40), 141 pp. (in German).

6. Liechti, P. Der Zustand der Seen in der Schweiz; BUWAL Schriftenreihe Umwelt, 1994; Nr. 237, 159 pp. (in German).

7. Mürle, U.; Ortlepp, J.; Rey, P. Der Bodensee - Zustand, Fakten, Perspektiven; IGKB, 2004; 185 pp. (in German).

8. Bürgi, H.-R.; Buhmann, D.; Ehmann, H.; Güde, H.; Hetzenauer, H.; Kümmerlin, R.; Kuhn, G.; Obad, R.; Rossknecht, H.; Schröder, H.G.; Stich, H.B.; Wolf, T. Limnologischer Zustand des Bodensees; IGKB Jahresbericht Januar 2005 bis März 2006, 2006, 83 pp. (in German).

9. ESA. MERIS Product Handbook; Issue 2.1, 2006 (accessed 20 September 2007), http://envisat.esa.int/pub/ESA_DOC/ENVISAT/MERIS/meris.ProductHandbook.2_1.pdf.

10. Koepke, P. The reflectance factors of a rough ocean with foam. Comment on remote sensing of the sea state using the 0.8-1.1μm spectral band by Wald, L. and Monget. M. Int. J. Remote Sens. 1985, 6 (5), 787-799.

11. Odermatt, D.; Heege, T.; Nieke, J.; Kneubühler, M.; Itten, K.I. Parameterisation of an automized processing chain for MERIS data of

Swiss lakes. In Proc. Envisat Symposium, Montreux, Switzerland, 23-27 April 2007; 2007.

12. TriOS Mess- und Datentechnik GmbH. RAMSES Hyperspectral Radiometer Manual; Rel. 1.0, 2004, 27 pp.

13. Gege, P. Improved method for measuring gelbstoff absorption spectra. In Proc. Ocean Optics Conf. XVII, Freemantle, Australia, 25-29 October 2004.

14. Stich, H.B.; Brinker, A. Less is better: Uncorrected versus pheopigment-corrected photometric chlorophyll-a estimation. Arch. Hydrobiol. 2005, 162 (1), 111-120.

15. Utermöhl, H. Zur Vervollkommnung der quantitativen Phytoplankton-Methodik. Mitt. Int. Ver. Theor. Angew. Limnol. 1958, 38 pp. (in German).

16. Tilzer, M.M.; Beese, B. The seasonal productivity cycle of phytoplankton and controlling factors in Lake Constance. Schweiz. Z. Hydrol. 1988, 50 (1), 1-39.

17. Kiselev, V.; Bulgarelli, B. Reflection of light from a rough water surface in numerical methods for solving the radiative transfer equation. J. Quant. Spectrosc. Radiat. Transfer 2004, 85, 419-435.

18. Gordon, H.R.; Brown, O.B.; Jacobs, M.M. Computed relationships between the inherent and apparent optical properties of a flat homogeneous ocean. Appl. Opt. 1975, 14 (2), 417-427.

19. Kirk, J.T.O. Volume scattering function, average cosines, and the underwater light field. Limnol. Oceanogr. 1991, 36 (3), 455-467.

20. Bannister, T.T. Model of the mean cosine of underwater radiance and estimation of underwater scalar irradiance. Limnol. Oceanogr. 1992, 37 (4), 773-780.

21. Nelder, J.A.; Mead, R. A simplex method for function minimization. Comput. J. 1965, 7, 308-313.

22. Miksa, S.; Haese, C.; Heege, T. Time series of water constituents and primary production in Lake Constance using satellite data and a physically based modular inversion and processing system. In Proc. Ocean Optics Conf. XVIII, Montreal, Canada, 9-13 October 2006.

23. Delwart, S. Instrument characterization overview. Presented at NASA/NOAA MERIS US workshop, Silver Springs, United States, 14 July 2008.

24. Gege, P. Gewässeranalyse mit passiver Fernerkundung: Ein Modell zur Interpretation optischer Spektralmessungen. DLR-Forschungsbericht 1994, 1994-15, 171 pp. (in German).

25. Kallio, K.; Pulliainen, J.; Ylöstalo, P. MERIS, MODIS and ETM channel configurations in the estimation of lake water quality from subsurface reflectance with semi-analytical and empirical algorithms. Geophysica 2005, 41, 31-55.

26. Bricaud, A.; Morel, A.; Prieur, L. Absorption by dissolved organic matter of the sea (yellow substance) in the UV and visible domains. Limnol. Oceanogr. 1981, 26 (1), 43-53.

27. Buiteveld, H.; Hakvoort, J.H.M.; Donze, M. The optical properties of pure water. In Proc. Ocean Optics Conf. XII, Bergen, Norway, 13-15 June 1994; 2258, 174-183.

28. Gege, P. Gaussian model for yellow substance absorption spectra. In Proc. Ocean Optics Conf. XV, Monaco, 16-20 October 2000.

29. Smith, R.C.; Baker, K. S. Optical properties of the clearest natural waters (200-800 nm). Appl. Opt. 1981, 20 (2), 177-184.

30. Santer, R.; Schmechtig, C. Adjacency Effects on Water Surfaces: Primary Scattering Approximation and Sensitivity Study. Appl. Opt. 2000, 39 (3), 361-375.

31. Candiani, G.; Giardino, C.; Brando, V. Adjacency Effects and bio-optical Model Regionalisation: MERIS Data to assess Lake Water Quality in the Subalpine Region. In Proc. Envisat Symposium, Montreux, Switzerland, 23-27 April 2007.

3 CHLOROPHYLL RETRIEVAL WITH MERIS CASE-2-REGIONAL IN PERIALPINE LAKES

This Chapter has been published as: Odermatt, D., Giardino C. & Heege, T. (2010). Chlorophyll retrieval with MERIS Case-2-Regional in perialpine Lakes. Remote Sensing of Environment, 114/3, 607-617

Abstract

Semi-analytical remote sensing applications for eutrophic waters are not applicable to oligo- and mesotrophic lakes in the perialpine area, since they are insensitive to chlorophyll concentration variations between 1-10 mg/m^3. The neural network based Case-2-Regional algorithm for MERIS was developed to fill this gap, along with the ICOL adjacency effect correction algorithm. The algorithms are applied to a collection of 239 satellite images from 2003-2008, and the results are compared to experimental and official water quality data collected in six perialpine lakes in the same period. It is shown that remote sensing estimates can provide an adequate supplementary data source to in situ data series of the top 5 m water layer, provided that a sufficient number of matchups for a site specific maximum temporal offset is available.

3.1 Introduction

The glacial lake basins around the Alps are essential fresh water resources for Central Europe. Their ecological state vitally affects their value as drinking water reservoirs, for irrigation, fishery or recreation. For this reason, the European Commission (EC) has adopted the Water Framework Directive (Directive-2000/60/EC, 2000) which defines water quality categories as well

as monitoring parameters for the appropriate assignment of these categories. The Directive applies to all countries of the European Union (EU) and the European Economic Area (EEA), but not to Switzerland, where some of the feeder rivers of Europe's largest river systems (i.e. Danube, Po, Rhine, and Rhone) originate. However, due to its position in the Central Alps, Switzerland shares a long tradition of international water protection directives; with Austria and Germany on Lake Constance (since 1961), with France on Lake Geneva (1962) and with Italy on Lake Lugano and Lake Maggiore (1972). Consequently, the countries involved are experienced in the practice of water quality monitoring and most water bodies in and around Switzerland are considered to be of very good quality, although Switzerland's water protection laws are less consistent than the WFD and do not contain a mandatory definition of water quality monitoring requirements (Rey and Müller, 2007). Number and type of parameters, sites and intervals applied in such programs vary strongly among perialpine lakes. Chlorophyll-*a* concentrations (*CHL*) are however widely measured as an indicator for eutrophication and primary production. Ongoing efforts in reducing nutrient loads to these lakes trigger large interest in measuring biologic productivity on high-resolution temporal and spatial scales. Development of novel, reliable remote sensing techniques could thus provide a significant improvement in water quality and lake condition monitoring.

Various methods were developed to estimate the constituents of inland waters from remote sensing data, based on physical relations known from radiative transfer theory (Mobley, 1994). Most of them are based on absorption and scattering properties of *CHL*, total suspended matter (*TSM*) and gelbstoff (Y). Simple, semi-analytical methods for the retrieval of *CHL* apply band ratios of the secondary *CHL* absorption maximum at around 675 nm and adjacent spectral bands that are not affected by *CHL* absorption, such as the near-infrared (NIR) reflectance peak near MERIS' 709 nm band (Gons et al., 2002; Gons et al., 2005), MODIS' 748 nm and SeaWiFS' 765 nm band (Dall'Olmo et al., 2005) or a combination of MERIS' 709 nm and 754 nm bands (Gitelson et al., 2008; Gitelson et al., 2007). They are applicable to in situ measured or atmospherically corrected surface reflectances of eutrophic waters containing 10-200 mg/m^3. However, *CHL* in perialpine lakes varies only between 1 and 20 mg/m^3, and surface reflectances rarely display the needed NIR reflectance peak (Giardino et al., 2007; Odermatt et al., 2008a).

More complex, physically based inversion methods for simultaneous retrieval of *CHL*, *TSM* and *Y* were originally developed for airborne scanners (Heege

and Fischer, 2004; Hoogenboom et al., 1998). When applied to satellite sensors of lower spectral resolution, such as Landsat-TM5 and SPOT-HRV, such methods are adequate for the quantification of *TSM* by its strong scattering signal (Dekker et al., 2001). However, only more recent sensors were found to provide sufficient spectroradiometric properties for the estimation of low *CHL* concentrations in inland waters, for example Hyperion (Giardino et al., 2007) or MERIS (Odermatt et al., 2008a) in Lakes Garda and Constance, respectively. However, constant gelbstoff (Y) absorption had to be assumed in both studies, as its variation was not distinguishable from oligotrophic lakes' *CHL* patterns with those instruments.

An inversion technique based on neural networks (NN) is used in the MERIS ground segment to simultaneously retrieve case II water constituents. Current MERIS level 2 standard products (*algal_2*, *yellow_subs*, *total_susp*) are processed with such a sensor-specific NN algorithm (Doerffer and Schiller, 2007). Between January 2007 and June 2008, the European Space Agency (ESA) funded the "Development of MERIS Lake Water Algorithms" (MERIS Lakes) project on the elaboration and validation of inland water NN for BEAM (Fomferra and Brockmann, 2006). The project led to three plug-in algorithms based on the MERIS Case-2 Core Module: Case-2 Regional (C2R), Boreal Lakes and Eutrophic Lakes (Doerffer and Schiller, 2008a) and a dedicated atmospheric correction (Doerffer and Schiller, 2008b). At about the same time the Improved Contrast between Ocean and Land (ICOL) processor became available, which accounts for the correction of adjacency effects (Odermatt et al., 2008b; Santer and Zagolski, 2009). The corresponding validation campaign concludes that (1) atmospherically corrected and in situ measured reflectances agree well in the green and red spectral region, but worse in the blue region, (2) ICOL has a positive or neutral effect, and (3) the accuracy is sufficient for *TSM* and *CHL*, but still not for *Y* (Koponen et al., 2008; Ruiz-Verdu et al., 2008).

Against the background of this recent progress, the applicability of the current C2R *CHL* product for the support of water quality monitoring in perialpine lakes is tested in this study. In section 2, a collection of MERIS images of the alpine region in the years 2003-2008 is described, along with several field campaigns including in situ reflectance measurements coinciding MERIS overpasses and water quality monitoring datasets acquired by local authorities. Section 3 contains an overview of the automatic processing environment applied to the satellite imagery (Odermatt et al., 2008a), which was adapted for

the use with BEAM's command line routines. The same processing environment accounts for the comparison with reflectances and concentrations measured in field campaigns and for water quality monitoring concentrations. Results of all three types of matchups are discussed in section 4. Conclusions are given in section 5.

We specifically address the following questions: (1) Are the C2R and ICOL appropriate for the routine processing of *CHL* products, (2) what is the spatio-temporal validity of the findings, and (3) how does ICOL affect the outcome of the C2R processing for perialpine lakes.

3.2 Data

3.2.1 MERIS images

239 MERIS full resolution (FR) level 1B quarter and full scenes were used in this investigation. The data were originally collected for other experiments on Lake Constance (2003-2007), Garda, and Maggiore (2003-2008), which are covered by 121, 150 and 185 images, respectively. The study includes 7 lakes, which were chosen for their regional relevance and are therefore regularly monitored. This ensures the availability of *CHL* monitoring reference data along with experimental spectroradiometric reference data. The lakes have a size adequate for the 300 m spatial resolution of MERIS FR (Figure 3-2). Partial coverage, inappropriate atmospheric conditions or sun glint affected geometries may occur especially over lakes that the data was not originally chosen for, leading to the lowest temporal coverage for Lake Geneva (86). The temporal coverage in winter is lower than in summer (Figure 3-1), since the images were chosen mainly to observe phytoplankton growth, and clouds and fog reduce the availability of data in the winter half year.

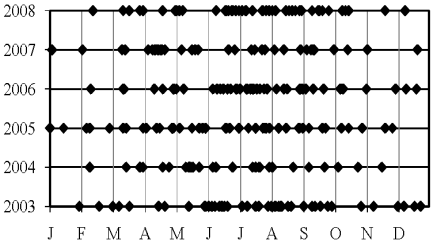

Figure 3-1: Temporal distribution of the 239 images used in this study.

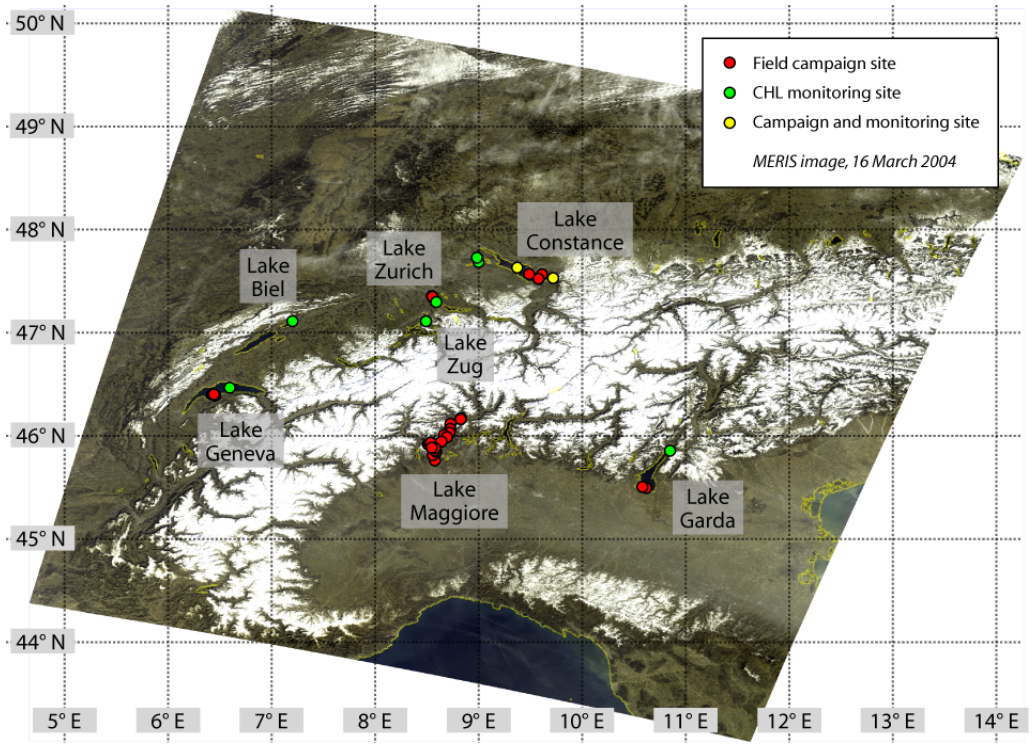

Figure 3-2: Example MERIS L1B full scene of the almost cloud free alpine area, showing the distribution of investigated lakes around the Alps, with the snow line at about 1000 m asl in average.

3.2.2 Field campaign data

35 spectroradiometric measurements with coinciding MERIS images were used in this study. They were converted to remote sensing reflectance R_{rs} (i.e. the ratio between the water leaving radiance and the incoming irradiance flux) for comparison with the C2R calculated reflectance. The field campaign data represent 5 lakes and were gathered on 8 field campaigns in the years 2005-2008. No spectroradiometric measurements are available for Lake Biel and Lake Zug.

In the northern perialpine region, MERIS coinciding spectroradiometric measurements were taken during 4 campaigns in 2007; in Lake Constance (14 and 20 April, henceforth addressed as con070414 and con070420), Lake Geneva (gen070910) and Lake Zurich (zur070815). Lake Geneva and Lake Constance

are the two largest freshwater reservoirs in Western Europe, while Lake Zurich is the most important drinking water storage for the city of Zurich. Lake Constance is considered oligotrophic; Lake Geneva and Lake Zurich are mesotrophic. In situ *CHL* concentrations were only measured on the Lake Constance field campaign. All field campaigns took place within 3 hours of MERIS image acquisition. RAMSES ARC and ACC instruments were used to measure downwelling irradiance as well as upwelling radiance and irradiance below the water surface (Koponen et al., 2008).

Field campaigns in the southern perialpine region were carried out on Lake Garda and Lake Maggiore. The two lakes are the largest of Italy, situated in the northern part of the country, which accounts for 80% of Italy's total freshwater storage. Both are in an oligotrophic state, although Lake Garda tends to mesotrophic conditions (Premazzi et al., 2003). Lake Garda was visited on two field campaigns (gar050726, gar080506), making available three in situ spectroradiometric measurements. Lake Maggiore field campaigns cover the northern half of the lake with 6 R_{rs} measurements (mag060710), and its southern half with another 12 measurements (mag080803). Half of the measurements in Lake Maggiore were taken in littoral sites, at only a few hundred meters from the shore and thus at a critical distance for MERIS' spatial resolution. The measurements were done within 5 hours of the acquisition of a MERIS image. Underwater downwelling irradiance and upwelling radiance were measured with an ASD-FR.

Both RAMSES and ASD-FR underwater measurements were corrected for the emersion factor to derive reflectance values that are comparable to C2R results. Self-shading was not accounted for, as they are minimal in clear waters (Leathers et al., 2004).

3.2.3 CHL monitoring data

A heterogeneous collection of water quality monitoring data was used for the long time validation of the C2R *CHL* product with meaningful, official water quality monitoring estimates. However, French, German, Italian and Swiss agencies and commissions responsible for their acquisition are manifold, and the different measurement methods and standards may lead to variations in the comparability with remote sensing estimates (Table 3-1).

Table 3-1: List of the lakes investigated, with corresponding water directives, the institutions in charge and the methods and intervals applied for the monitoring of CHL concentrations for the timeframe investigated.

Lake	Directive	Executing institution	Method	Interval	Timeframe
Biel	Cantonal	Bernese Cant. Water Protection and Waste Management Office	HPLC (15 m)	30 d	2003-2008
Constance	IGKB[1]	Institute for Lake Research, Langenargen (Germany)	HPLC (20 m)	14-30 d	2003-2007
Garda	WFD	APPA Trento (Italy)	Spectrophotometer (0-1 m)	30 d	2003-2008
Geneva	CIPEL	INRA, Thonon-Les-Bains (France)	Fluorescence probe (1-5 m)	14-30 d	2003-2007
Zug	Cantonal	Zug Cant. Environmental Protection Office	Fluorescence probe (1-5 m)	30 d	2005-2007
Zurich	Cantonal	Zurich Municipal Water Utility	HPLC profile (0-5 m)	30 d	2006-2008

The HPLC method applied to vertical composite water samples as in the monitoring program of Lake Biel, Lake Constance and Lake Zurich gives a precise laboratory measurement of constituent concentrations in a sample. In Lake Zurich, such samples are taken at 0, 1, 2.5 and 5 m depth and thus represent vertical variations in the top water layer; in case of Lake Biel and Lake Constance the water samples are taken as a vertical mixture of the topmost water layer, i.e. 20 m and 15 m, respectively. In Lake Garda, *CHL* is derived from spectrophotometer measurements of water samples of the top 1 m water layer (ISO-10260E, 1992). Finally, submersible fluorescence probes such as the SCUFA used in Lake Zug and the CTD90 used in Lake Geneva allow the depth profiling of *CHL* and other limnic parameters in the field.

3.3 Processing chain

Four BEAM routines are used in a processing chain for the automatic calculation of the C2R water constituent products. The BEAM tools are controlled by IDL routines, which account for the definition of parameters in the BEAM processor xml files, but also for the post processing of geometrically corrected L2 subsets (Figure 3-3).

1 International Commission for the Protection of Lake Constance

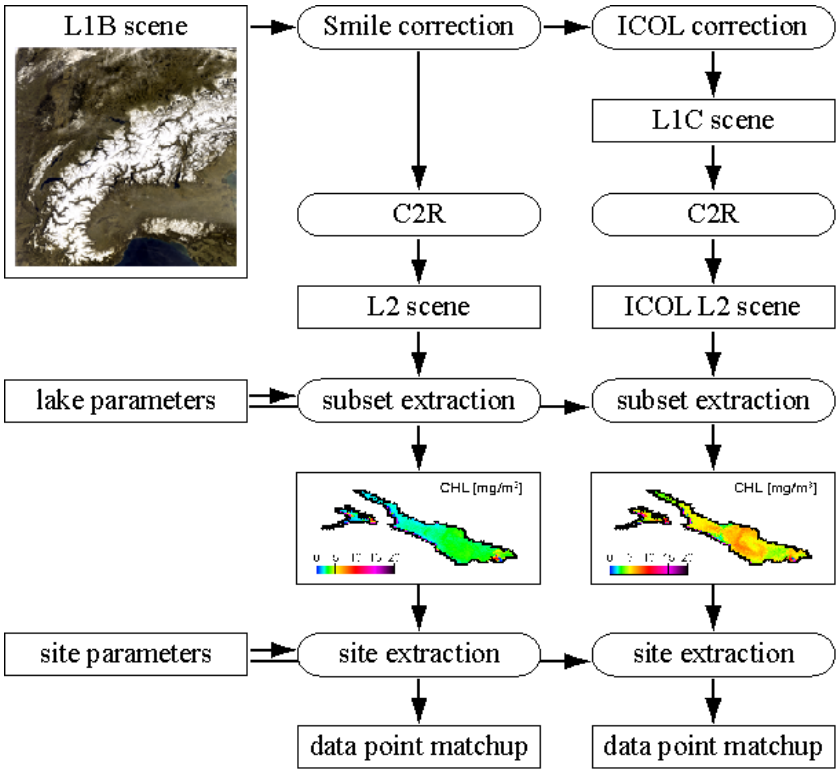

Figure 3-3: Flow chart of the processing scheme applied to the MERIS data.

3.3.1 Preprocessing

In a first step, BEAM's smile correction *meris-smile.bat* (version 1.1.101) is applied to the original L1B data. This command line algorithm is identical to the MERIS smile correction used in L2 products. It applies an irradiance correction to all bands, which accounts for the difference between actual and nominal wavelengths of the solar irradiance in each channel. A reflectance correction is also applied, based on spectral interpolation of reflectances in two adjacent bands. The default for water targets is to apply the reflectance correction to all bands apart from 8, 11, 14 and 15 (Fomferra and Brockmann, 2006).

The smile corrected L1B data are processed with ICOL (version 1.0.4) as implemented in BEAM's *gpt.bat* command line routine. ICOL calculates top of atmosphere (TOA) reflectance and applies a regular Rayleigh correction as done in the MERIS atmospheric correction over land of the MERIS ground

segment (Santer et al., 1999). This is done for the entire image, while the rest of the procedure is only applied to water pixels within 30 km of land surface areas. Rayleigh and aerosol adjacency effects are corrected by means of a look-up-table simulated with a primary scattering model (Santer and Schmechtig, 2000). MERIS bands 12 and 13 are thereby used for the estimation of aerosol type and optical thickness (AOT). The reduction of the surface reflectance caused Rayleigh and aerosol scattering over adjacent land is also accounted for. Finally, the adjacency effect corrected TOA reflectance is converted back into at-sensor radiances for all 15 bands, creating an L1C product according to ESA definitions (Santer and Zagolski, 2009).

3.3.2 Atmospheric correction and water constituent retrieval

The smile corrected L1B and L1C data are processed with C2R (version 1.3.2, Case 2 core module version 1.0), resulting in two sets of water constituent products, one with and one without ICOL correction (Figure 3-3). A C2R batch processing routine was therefore customized as described in the BEAM Lakes Wiki (Peters, 2008). It makes use of an adapted parameter file that switches C2R's internal smile correction off. C2R applies a dedicated NN based atmospheric correction built on more than 200'000 simulations for 15 input neurons, including radiance reflectance at top of a 50 layer standard atmosphere after Ozone and Rayleigh correction in 12 visible and NIR bands. Only bands 11, 14 and 15 are excluded. This helps to avoid the over-correction of visible bands occurring in earlier versions, which were based on the extrapolation of NIR retrieved atmospheric parameters to shorter wavelengths. 43 neurons are defined as output, consisting of water leaving radiance and downwelling irradiance (i.e., the terms to derive R_{rs}) as well as path-scattered radiance for the 12 input bands, AOT in 4 bands (given at 550 nm hereafter), and a sun glint parameter. The scattering by ice crystals in cirrus clouds is also accounted for. Performance tests across the entire range of values of atmospheric parameters included in the NN show that largest inaccuracies occur for low water leaving reflectances, i.e. at short wavelengths, under hazy conditions and over absorption dominated, low scattering waters. Therefore, the atmospheric correction was found to be applicable for atmospheric conditions up to AOT=0.5 under normal circumstances, but might fail even at AOT=0.2 over very dark water, such as in Finnish lakes (Doerffer and Schiller, 2008b).

C2R's water constituent retrieval NN uses the R_{rs} in MERIS bands 1-8 after atmospheric correction. It was trained with a LUT consisting of more than 80'000 *Hydrolight* simulations (Mobley, 1994). Natural variations in IOP and unavoidable errors in input R_{rs} are accounted for, but fluorescence effects are neglected. A so-called *invNN* is applied to invert given directional R_{rs} into concentrations, and a *forwNN* models R_{rs} for given concentrations and geometries. The *invNN* provides a first guess of instant concentrations. They fed in the *forwNN* together with the acquisition geometry, producing an R_{rs} spectrum to verify the inversion procedure. The difference in these R_{rs} is minimized by means of a Levenberg-Marquardt algorithm until an accuracy threshold is met, or up to a maximum of 10 iterations. The L2 products calculated in this way include *CHL*, *TSM* and *Y*, but also the minimum irradiance attenuation coefficient and the signal depth z_{90}. Furthermore, retrieval quality flags are set according to failures in meeting quality check thresholds for both atmospheric correction and water constituent retrieval (Doerffer and Schiller, 2008a).

3.3.3 Post processing

The optical closure of in situ R_{rs} measurements and corresponding C2R R_{rs} pixel spectra is quantified by means of the absolute and relative spectral Root Mean Square Error (RMSE) of MERIS channels 1-9:

$$RMSE = \sqrt{\frac{\sum_{i=1}^{N} (\overline{X}_i - \hat{X}_i)^2}{N-1}} \qquad [3\text{-}1]$$

$$Rel.RMSE = \sqrt{\frac{RMSE}{\frac{1}{N}\sum_{i=1}^{N} \overline{X}_i}} \cdot 100 \qquad [3\text{-}2]$$

where N is the number of bands (i.e. 9) and $\overline{X}_i$ and $\hat{X}_i$ are the remote sensing reflectances measured in situ and retrieved by C2R, respectively.

Once the water constituent concentrations are calculated, the subsequent post processing steps make use of two tables for the creation of map products and point wise comparison with in situ data. The lake parameter table contains geographic information for each lake to be extracted from the MERIS L2 images, i.e. name, altitude, pixel size, geographical coordinate subset boundaries in

each direction and UTM zone. This information is used for geometric correction and image clipping by means of the BEAM tool *mapproj.bat*. The DIMAP format lake clippings are then illustrated with legend and color table templates according to the variation of concentrations expected in each lake and saved as JPEG.

The second table with site parameters contains local *CHL* monitoring time series along with site name, acquisition method and latitude and longitude coordinates. It enables the extraction of spatio-temporal matchups between in situ *CHL* measurements and corresponding MERIS pixels. Where cloud free matchup pixels are found, the values of acquisition date, L1B flags, C2R flags, viewing zenith angle, C2R's chi square, AOT, *CHL*, *TSM*, *Y* and z_{90} are extracted and simple statistics such as R^2 and RMSEs are calculated. Corresponding values extracted from a 3x3 neighborhood instead of a single pixel do not consistently lead to improved results. Channel 13 quick looks of each MERIS image are automatically generated and manually searched for cirrus and contrail contaminations that were not identified by the MERIS flags. About 10 images per reference site were blacklisted and excluded from processing in this way. Additional criteria for data exclusion in the automatic process were sun glint suspect geometries (i.e. above 10° east in summer or 20° east in winter), C2R's error indicating retrieval flags (i.e. *ATC_OOR* and *RAD_ERR*) and unrealistic *CHL* levels (i.e. below 0.1 mg/m^3). The latter two may differ between ICOL corrected and uncorrected data, causing differences in the number of matchups available.

3.4 Results

3.4.1 Field campaign R_{rs} matchups

The comparison between 35 spectroradiometric measurements and corresponding image derived R_{rs} spectra for ICOL corrected and uncorrected MERIS data allows for a direct validation of the performance of ICOL and the C2R atmospheric correction. A qualitative evaluation of four cases can be given (Figure 3-4): [1] In situations with AOT around 0.05, the effect of ICOL is small, even for narrow basins such as Lake Zurich (zur070815). [2] When AOT increases to moderate values such as 0.14 over the eastern bay of Lake Constance on 13 April 2007, ICOL significantly improves the retrieved reflectance spectrum. [3] Underestimations of adjacency effects by ICOL were found for Lake Mag-

giore, where relatively low water reflectance leads to at-sensor radiances as small as the noise of MERIS (Guanter et al., 2010) and the surrounding topography further increases the intensity of adjacency effects (Candiani et al., 2007). [4] The retrieval for Lake Geneva on 10 September 2007 is carried out for a similar AOT (0.13) as in example 2. However, the shape of the Lake Geneva reflectance spectra with a secondary maximum in the 681 nm chlorophyll fluorescence band and an inflection point around 500 nm is generally not well reproduced, possibly due to the neglect of fluorescence and SIOP variations that C2R's forward simulations do not account for, respectively.

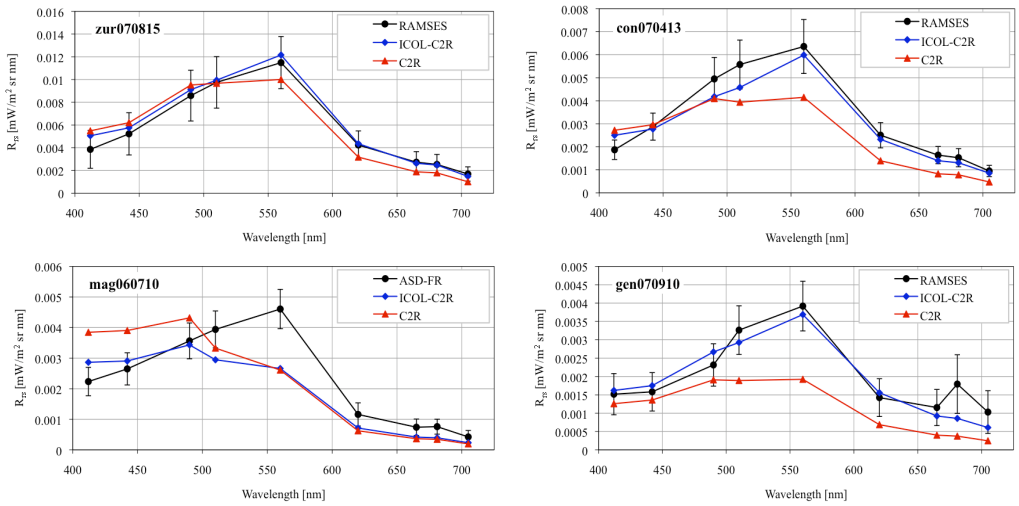

Figure 3-4: Example spectral matchups for weak (zur070815) and strong (con070413) adjacency effects, and assumingly underestimated adjacency effects (mag060710) and inadequate SIOP (gen070910).

The optical closure according to Equation [3-1] and [3-2] was calculated for both adjacency effect corrected and uncorrected data. In 32 of 35 cases, both absolute and relative RMSEs decrease when ICOL is applied (Figure 3-5). But through normalization of the RMSEs, higher relative inaccuracies for darker waters such as Lake Maggiore become visible. In the case of gen060910 and mag080803, the application of ICOL reduces the average relative RMSEs from 55% and 54%, respectively, to 24% for both lakes. Only for mag060710, the average relative RMSE is not sufficiently improved (57% to 43%), displaying case [3] in Figure 3-4. Among brighter waters, the relative RMSEs for Lakes Zurich and Constance decrease to an average of 12% and 19%, respectively,

whereas the spectral fits for Lake Garda are not improved by ICOL. The relative RMSEs for ICOL corrected data of Lake Constance, Lake Garda, Lake Geneva and Lake Zurich are more or less in the range of the 10-21% calculated for the visible spectral range in a previous experiment on Lake Garda, where a customized atmospheric correction using actual AOT measurements was applied to a single Hyperion image (Giardino et al., 2007).

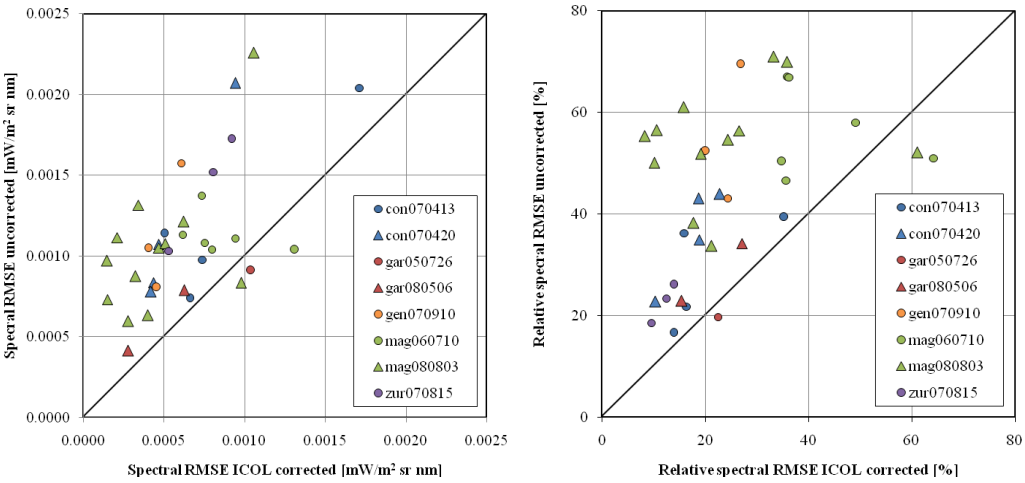

Figure 3-5: Spectral RMSEs and relative spectral RMSEs for 35 in situ spectral measurements and the corresponding R_{rs} spectra calculated by C2R for ICOL corrected and uncorrected input data.

3.4.2 Field campaign CHL matchups

The results of the Lake Constance field campaign *CHL* matchups confirm the moderate correlation for *CHL* without ICOL (Figure 3-6) as found in the MERIS Lakes validation study. The correlation coefficient of R=0.74 for the ICOL corrected *CHL* product is even slightly higher, where the validation study revealed only R=0.32. The absolute and relative RMSEs of ICOL corrected *CHL* are more than twice that of the uncorrected estimate, since the ICOL correction generally increases the water constituent concentration estimate (Koponen et al., 2008). But when the individual bias in the linear relationship between in situ data and the two C2R estimates is taken into account, the ICOL corrected estimate is again insignificantly better with an RMSE of 0.78 against 0.81 mg/m^3. In general, the results confirm the contradictory find-

ing that ICOL significantly improves the retrieval of R_{rs} (Figure 3-5) but not the determination of water constituents (Koponen et al., 2008).

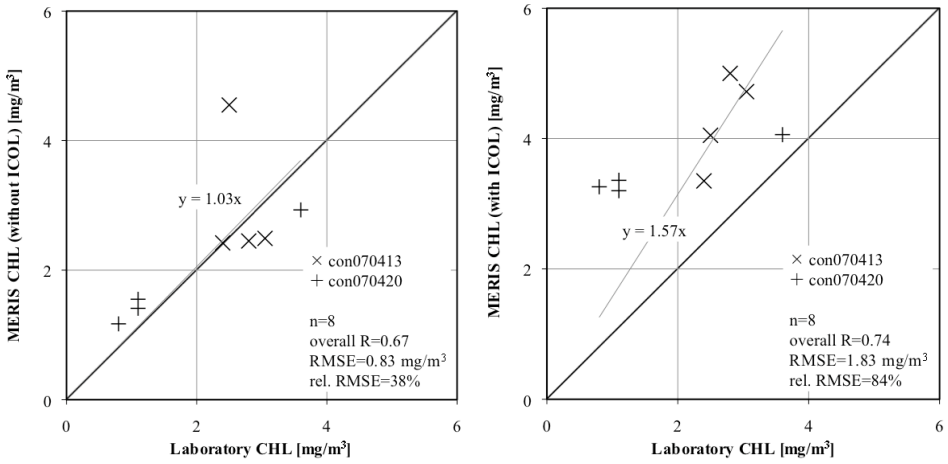

Figure 3-6: Lake Constance plots of laboratory CHL with uncorrected (left) and ICOL corrected (right) MERIS C2R estimates. When the linear regressions are applied to the MERIS estimates, absolute RMSEs are 0.81 and 0.78 mg/m³ and relative RMSEs are 37% and 36% for data without and with ICOL, respectively.

3.4.3 CHL monitoring matchups

The general comparability of C2R results with 0-5 m depth resolved reference data from official water quality monitoring is demonstrated using the example of Lake Zurich (HPLC reference, Figure 3-7). Correlation coefficients and absolute RMSEs are higher and the relative RMSEs lower than those found in the field campaign matchups for Lake Constance, which can be explained with the higher range of concentrations occurring in Lake Zurich. The main difference due to ICOL can be expressed by a difference in linear regression similar to the Lake Constance field campaign (Figure 3-6), only that this time ICOL is closer to the 1:1 line. Some outliers among the 3-5 days offset matchups can be identified for the occurrence of spatio-temporal variations in the *CHL* patterns observed by MERIS, but are not discussed individually.

The matchups for Lake Zug in Figure 3-8 represent an aggregation of low concentration cases and only a few algae bloom events, making the correlation less reliable than for Lake Zurich. Nevertheless, the correlations similar and the lin

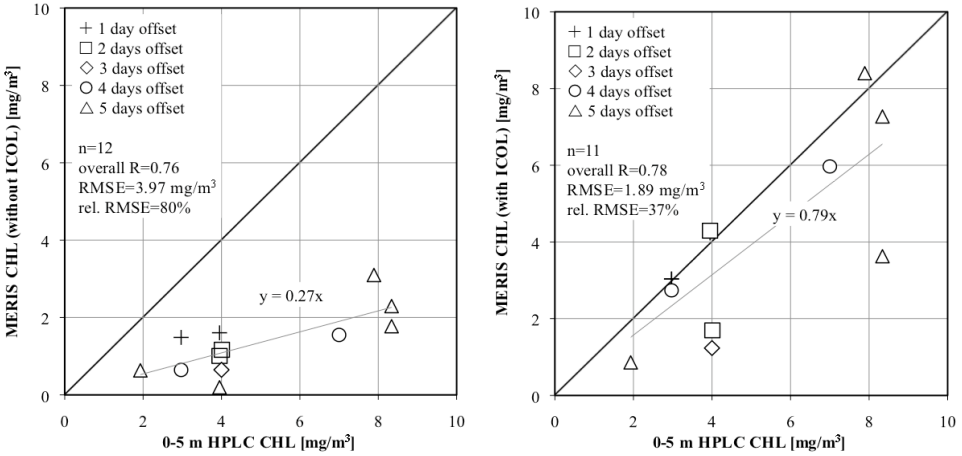

Figure 3-7: Lake Zurich plots of official water quality CHL with uncorrected (left) and ICOL corrected (right) MERIS C2R estimates. When the linear regressions are applied to the MERIS estimates, absolute RMSEs are 1.85 and 1.87 mg/m³ and relative RMSEs are 38% and 37% without and with ICOL, respectively.

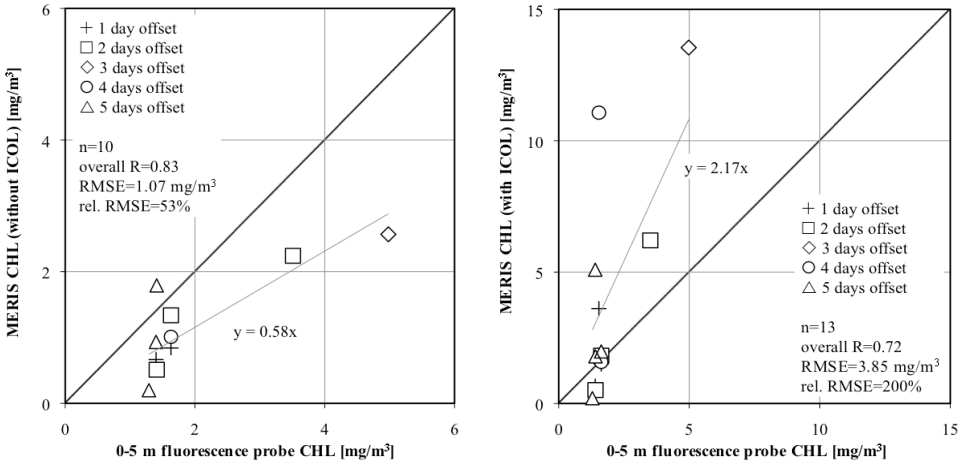

Figure 3-8: Lake Zug plots of official water quality CHL with uncorrected (left) and ICOL corrected (right) MERIS C2R estimates. When the linear regressions are applied to the MERIS estimates, absolute RMSEs are 0.71 and 1.32 mg/m³ and relative RMSEs are 35% and 69% without and with ICOL, respectively.

ear regression is again considerably steeper for ICOL corrected than for uncorrected data, whereas both are off the 1:1 line in this example. The main differences are due to the strong overestimation of concentrations by C2R for ICOL

corrected data, leading to high RMSEs. However, the two maximum values by C2R with ICOL correspond to spring bloom events in April 2005 and 2007, where increased (6-8 mg/m^3) *CHL* concentrations are found at 7-12 m depth, but not in the top 5 m layer averaged for the reference dataset. When comparing to the average of the top 20 m probe profile data, ICOL corrected estimates improve to R=0.84, while it decreases to 0.74 without ICOL.

For Lake Geneva, 98 in situ measurements in 2003-2007 are available for a sampling station in the center of the lake, allowing for the reduction of maximum temporal offset for data matchups to two days. However, the entire investigation period reveals correlations of only R=0.33 without and 0.26 with ICOL. But when only the first 3 of 5 years are analyzed, the correlation without ICOL improves, and the ICOL corrected R=0.89 becomes the highest of all lakes (Figure 3-9). It is assumed that the SIOPs of Lake Geneva have significantly shifted in 2006-2007. Several indications support this hypothesis, such as the obvious change in phytoplankton variability visible in the *CHL* reference data (Figure 3-13), the inability to differentiate AOT, *CHL*, *TSM* and *Y* patterns in some images, the difference between the spectral shape of gen070910 compared to the other reference spectra and the poor retrieval of that spectrum by C2R (Figure 3-4, type [4]), and finally the observation of exceptional blooms of filamentous Mougeotia algae in 2007 by local limnologists (Rimet et al., 2008; Tadonleke, pers. comm.).

In Lake Garda, the sampling station is very close to the inflow of River Sarca in the narrow northern part of the lake. 0-1 days offset would have to be allowed in order to get enough matchups, but cannot account for the temporal variability in this estuary region (R=0.50, n=11). A local comparison with remote sensing estimates is thus impossible unless the temporal agreement of image and in situ sample acquisition can be improved.

In Lake Biel and Lake Constance, water quality monitoring data is measured as HPLC analysis of 20 m composite profiles. A reduced comparability with remote sensing estimates is indicated by matchups for 4 different sites in Lake Constance (Figure 3-10), where the correlation is only about half of that found for the 0-5 m profile matchups. The largest RMSEs are found for the 4 ICOL corrected matchups of the site BR in the eastern bay of the lake, close to the River Rhine estuary. If removed, the other 3 sites achieve R=0.67 with ICOL. The small number of Lake Biel reference measurements requires a 2-day offset threshold to analyze 12 matchups, which correlate even less (R<0.26).

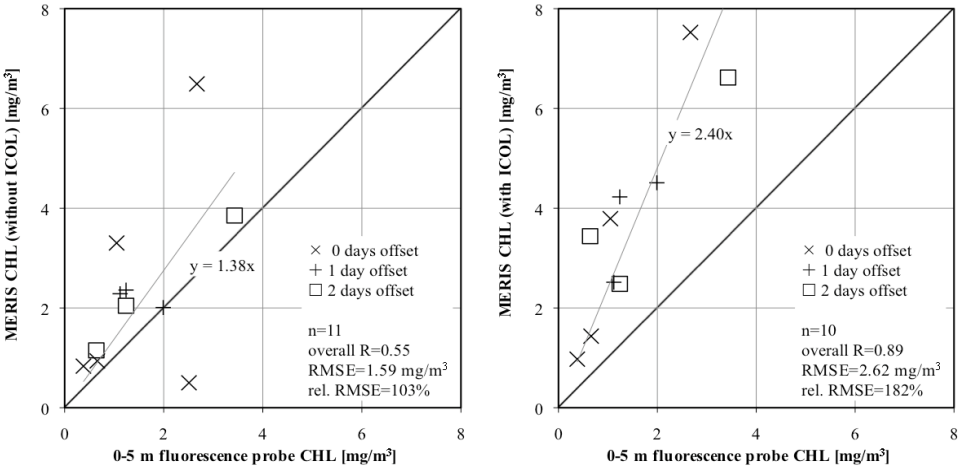

Figure 3-9: Lake Geneva plots of official water quality CHL with uncorrected (left) and ICOL corrected (right) MERIS C2R estimates (only 2003-2005). When the linear regressions are applied to the MERIS estimates, absolute RMSEs are 1.04 and 0.44 mg/m³ and relative RMSEs are 68% and 30% without and with ICOL, respectively.

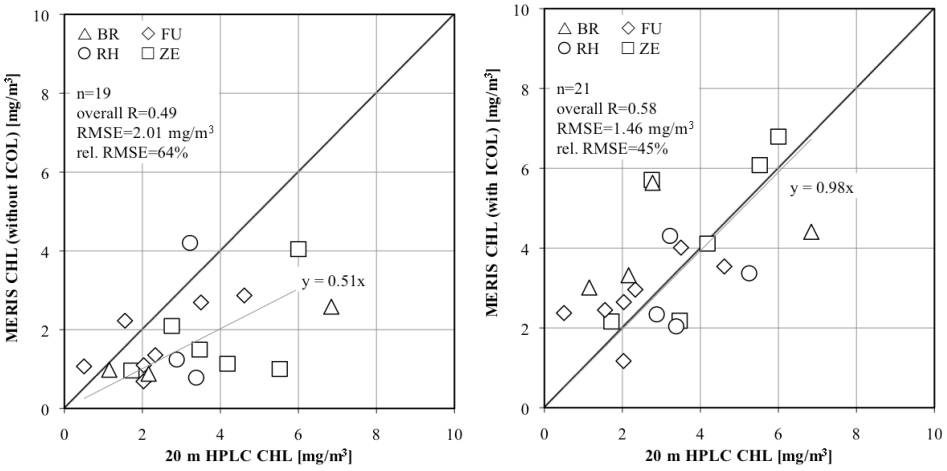

Figure 3-10: Lake Constance plots of 20m HPLC water quality data, measured in 4 different sites, with uncorrected (left) and ICOL corrected (right) MERIS C2R estimates of images taken on the same day. When the linear regressions are applied to the MERIS estimates, absolute RMSEs are 1.94 and 1.48 mg/m³ and relative RMSEs are 56% and 41% for data without and with ICOL, respectively.

3.4.4 Fusion of CHL time series

The correlation found for 0-5 m monitoring data and C2R *CHL* estimates are additionally examined by means of their seasonal and interannual variation. The linear gain factors found for the *CHL* monitoring matchups in Figure 3-7, Figure 3-8 and Figure 3-9 are applied to the C2R estimates, and the standard deviations of the averaged profile data are displayed as error bars of in situ *CHL*. In Lake Zurich, most images are available for the second half of 2006, where the in situ concentrations show a steady increase (Figure 3-11). Another cluster is related to the minimum concentrations in summer 2007 and the relative maxima before and after. Both situations are well reproduced by the C2R estimates, without a significant difference for ICOL corrected (n=39) and uncorrected (n=33) data. A difference in the number of observations occurs because C2R L2 flags *ATC_OOR* and *RAD_ERR* are less frequent in the corrected (11) than in the uncorrected (17) data, whereas about half of the flagged non-ICOL *CHL* concentrations would be in a reasonable range, while the other half is mostly above 20 or below 1 mg/m^3. Furthermore, the C2R estimates seem to underestimate low concentrations, while they overestimate higher concentrations. Again, this applies to both types of satellite estimates.

The Lake Zug time series of in situ *CHL* data consists of relatively constant 2-4 mg/m^3 concentrations with annual short periods of increased concentrations in spring and autumn. For the years 2005 and 2007, these events are well reproduced by the C2R estimates, with occasional overestimations by both non-ICOL and ICOL processed *CHL*. The spring maximum in 2006 measured on 24 April in situ is not confirmed by any valid MERIS observation. A MERIS image acquired on 21 April indicates above average *CHL* concentrations of 4.3 (non-ICOL) and 4.7 mg/m^3, but is not displayed in Figure 3-12 due to sun glint suspect geometry. The autumn maximum in 2007 is not visible in the in situ data, since no fluorescence probe measurements were taken between 18 July and 29 October. MERIS estimates indicate that this algae growth event has taken place to a similar extent as in the year before.

For the Lake Geneva time series, ICOL results (n=50) are more accurate than non-ICOL (n=49) results, as already found for the correlation of matchups. In the years 2003-2005, only two events of concentrations above 4 mg/m^3 are documented by in situ data, while the variations at low concentrations are very volatile (Figure 3-13). Nevertheless, a good agreement is visible especially in

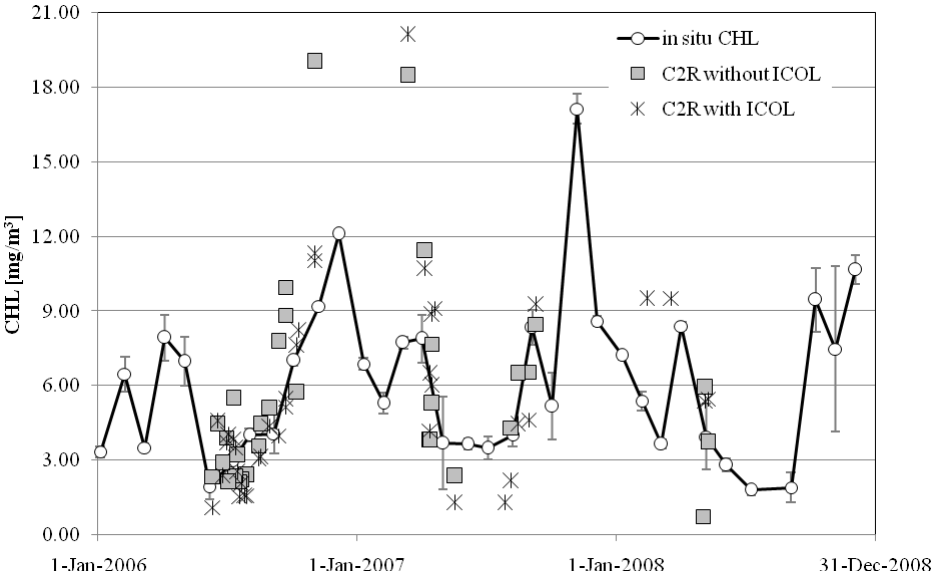

Figure 3-11: Lake Zurich time series of 0-5 m averaged HPLC samples and C2R estimate after application of the linear regression found in Figure 3-7.

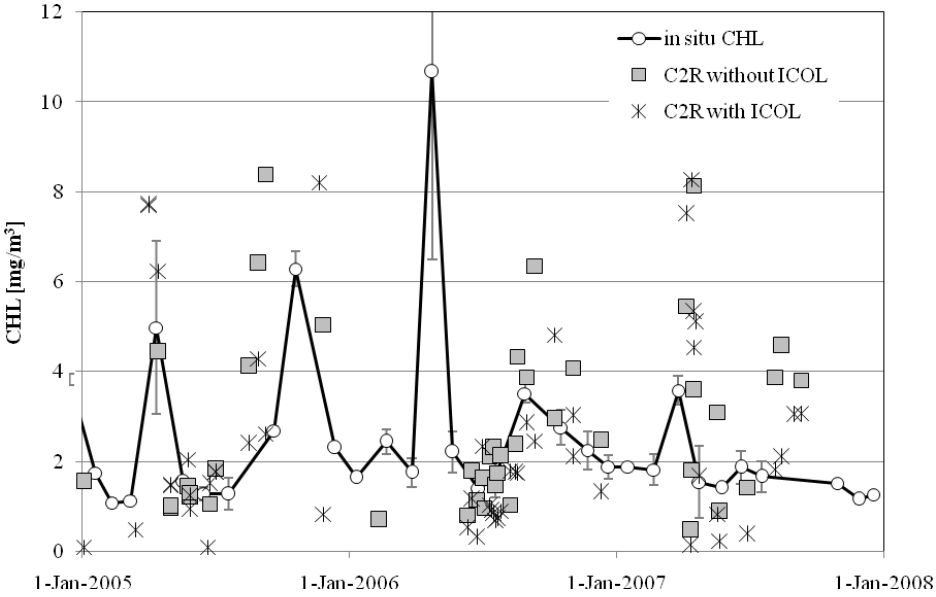

Figure 3-12: Lake Zug time series of 0-5 m fluorescence in situ measurements and C2R estimate after application of the linear regression found in Figure 3-8.

2004, where all but the first C2R estimates are in the range between the previous and the subsequent in situ measurement. The years 2006 and 2007 introduce increased average and maximum *CHL* reference concentrations and an increased seasonal variability. C2R retrieved *CHL* concentrations cannot account for these changes, although the MERIS images still depict many spatial features as relative concentration differences.

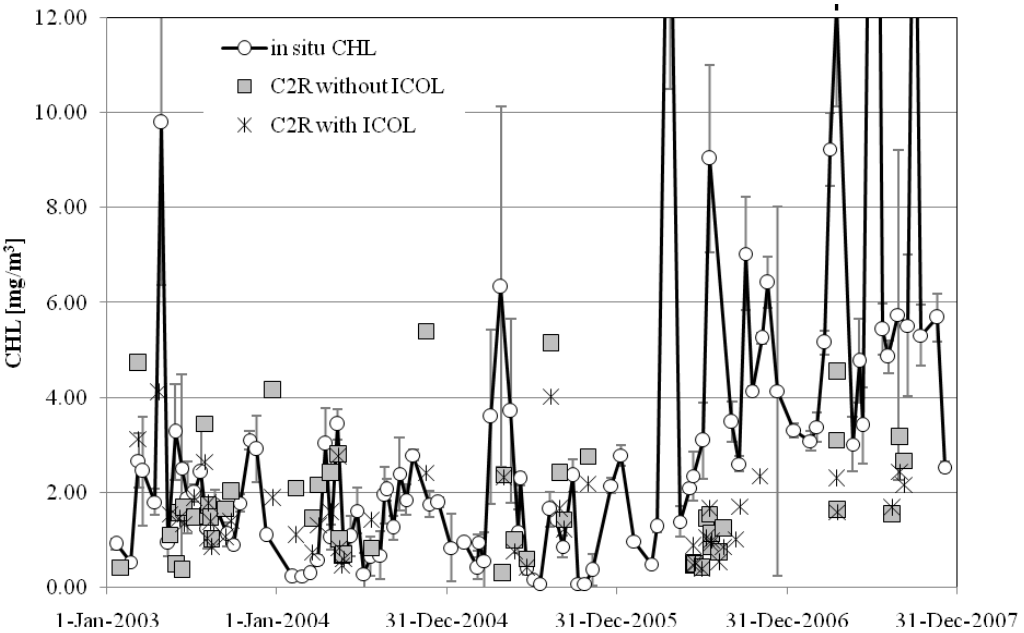

Figure 3-13: Lake Geneva time series of 0-5 m fluorescence in situ measurements and C2R estimate after application of the linear regression found in Figure 3-9.

3.5 Conclusions and discussion

It was shown that both C2R and ICOL are well automatable algorithms, allowing for the supply of relatively accurate *CHL* products for most of the larger perialpine lakes. The potential for their use for in situ water quality monitoring is considerable, also taking into account the near real-time availability from ESA's rolling archives. The application of simplified automatic quality checks regarding sun glint suspect and flagged pixels has strongly reduced the number of outliers in the MERIS data, although it lead to the loss of some significant datasets, which could be avoided by means of manual data quality control or

an improved C2R flagging system, e.g. for sun glint affected pixels. Extraordinarily complex cases like the strong adjacency effects over Lake Maggiore (Candiani et al., 2007; Guanter et al., 2010) or the change in SIOP in Lake Geneva in the years 2006 and 2007 require further investigation. Especially the changing environmental conditions in Lake Geneva demonstrate that remote sensing means for water constituent estimation will hardly replace in situ measurements in the near future. At the same time, it could strongly improve the current monitoring if in situ observations would include the estimation of the water's optical properties.

In terms of purposeful water quality monitoring, reliability and significance of remote sensing estimates cannot substitute in situ estimates, as they are strongly depending on atmospheric conditions and do not represent identical quantities, regarding area representation and penetration depth. Nevertheless, this study showed that the combination of in situ and spaceborne inland water *CHL* monitoring can improve our knowledge of the current state of our freshwater reservoirs with both temporally and spatially improved resolution. Depth resolved data are thereby clearly more suitable for comparison (R=0.71 to 0.89 and rel. RMSEs between 30% and 69% with ICOL) with remote sensing estimates than 15 or 20 m composite samples (ICOL R<0.58). The signal depth z_{90} calculated by the C2R algorithm in the present study (not shown) was between 5 to 12 m for all lakes. Vertically resolved in situ measurements of the topmost 5-12 m are accordingly the most suitable reference datasets when it comes to combining in situ and remotely sensed water quality estimates (Lindell et al., 1999). Temporal offsets up to 5 days turned out to be adequate for the majority of matchups in Lake Zug and Lake Zurich, whereas a very high temporal agreement is required in estuary sites such as BR in Lake Constance or the Lake Garda site. Regarding other water constituents, it is known from the outcome of the MERIS Lakes validation campaign and was confirmed by our estimates, that the *TSM* estimates by C2R are even more accurate than *CHL*, while the *Y* product is faulty, probably due to atmospheric correction issues at short wavelengths (Koponen et al., 2008).

The role of the ICOL adjacency effect correction in the processing of MERIS data is consistently positive as far as the retrieval of accurate R_{rs} by C2R is concerned. It also increases the correlation coefficient for *CHL* comparisons in 5 out of 6 examples, but not to a comparable extent. This finding confirms the conclusions of the MERIS Lakes validation study (Koponen et al., 2008), but lacks a simple explanation since the inversion criteria of the NN are relatively

intransparent. However, C2R was originally developed for use without ICOL, and adjacency effects remained unconsidered in the forward NN, among other parameters. The reflectance inversion is therefore an approximation, in which neglected optical effects may be erroneously compensated by other parameters. In the present study, the correlation between adjacency effect corrected and uncorrected *Y* estimates (e.g. R=0.38 for Lake Zurich matchups) is considerably lower than in the case of *CHL* and *TSM* (R=0.70 and 0.67, respectively). C2R's *Y* was also found to be the most inaccurately retrieved constituent in the MERIS Lakes validation study (Koponen et al., 2008). Average values without adjacency effect correction are twice to three times lower than found in previous studies (Heege and Fischer, 2004; Odermatt et al., 2008a) or when ICOL is applied. Therefore, we assume that *Y* buffers a large portion of the inaccuracy of R_{rs} derived without ICOL, while the *CHL* retrieval suffers only minor damages in relation to other error sources and the limited comparability of in situ and remote sensing measurements.

Acknowledgements

We are very grateful to all those who provided us with their measurements or helped in corresponding field campaigns and data analyses, namely Brigitte Engesser, Kirstin König and Andreas Schiessel (LuBW), Anke Bogner and Jörg Heblinski (EOMAP), Hanna Huhn, Esra Mandici, Thomas Agyemang and Klaus Schmieder (Univ. of Hohenheim), Peter Gege, Juliane Huth and Thomas Krauss (DLR), Silvia Ballert (Univ. Konstanz); Luca Fila (CRA Sirmione), Alessandro Oggioni and colleagues from CNR-ISE; Mariano Bresciani and Mauro Musanti (CNR-IREA).For the in situ *CHL* monitoring data we thank Markus Zeh and the water and soil protection laboratory of the Canton of Berne (GBL); Hans Güde, the Regional Office for Environment, Measurements and Nature Conservancy of Baden-Württemberg (LuBW) and the International Water Protection Commission for Lake Constance (IGKB); Ghislaine Monet, Remy Tadonleke, the Lacustrian Hydrobiology Station in Thonon-les-Bains (INRA UMR CARRTEL) and the International Commission for the Protection of Lake Geneva (CIPEL); Chiara Defrancesco, the Environmental Protection Agency of Trento (APPA) and the International Commission for the Protection of Italo-Swiss Waters (CIPAIS), Peter Keller and the Office of Environmental Protection of the Canton of Zug (AfU); and Richard Forster and the Zurich Water Supply Authority (WVZ).This work was funded by the Swiss

National Science Foundation, Contract Nr. [200020-112626/1]. MERIS data were made available through the ESA projects AO-553 and AO-1107.

3.6 References

Candiani, G., Giardino, C., & Brando, V.E. (2007). Adjacency effects and bio-optical model regionalisation: MERIS data to assess lake water quality in the subalpine ecoregion. *Proc. ENVISAT Symposium 2007*, Montreux, Switzerland, 6

Dall'Olmo, G., Gitelson, A.A., Rundquist, D.C., Leavitt, B., Barrow, T., & Holz, J.C. (2005). Assessing the potential of SeaWiFS and MODIS for estimating chlorophyll concentration in turbid productive waters using red and near-infrared bands. *Remote Sensing of Environment,* 96/2, 176-187

Dekker, A.G., Vos, R.J., & Peters, S.W.M. (2001). Comparison of remote sensing data, model results and in situ data for total suspended matter (TSM) in the southern Frisian lakes. *The Science of The Total Environment,* 268/1-3, 197-214

Directive-2000/60/EC (2000). Water Framework Directive of the European Parliament and of the Council of 23 October 2000 establishing a framework for community action in the field of water policy. In: *Official Journal L* (327 p.)

Doerffer, R., & Schiller, H. (2007). The MERIS case 2 water algorithm. *International Journal of Remote Sensing,* 28/3, 517-535

Doerffer, R., & Schiller, H. (2008a). MERIS lake water algorithm for BEAM. In: *BEAM Algorithm Technical Basis Document* (17 p.), GKSS Forschungszentrum, Geesthacht, Germany

Doerffer, R., & Schiller, H. (2008b). MERIS regional coastal and lake case 2 water project atmospheric correction. In: *BEAM Algorithm Technical Basis Document* (42 p.), GKSS Forschungszentrum, Geesthacht, Germany

Fomferra, N., & Brockmann, C. (2006). The BEAM project web page [Internet]. Carsten Brockmann Consult, Hamburg, Germany. http://www.brockmann-consult.de/beam/, accessed 23 April 2009

Giardino, C., Brando, V.E., Dekker, A.G., Strömbeck, N., & Candiani, G. (2007). Assessment of water quality in Lake Garda (Italy) using Hyperion. *Remote Sensing of Environment,* 109/2, 183-195

Gitelson, A.A., Dall'Olmo, G., Moses, W., Rundquist, D.C., Barrow, T., Fisher, T.R., Gurlin, D., & Holz, J. (2008). A simple semi-analytical model for remote estimation of chlorophyll-a in turbid waters: Validation. *Remote Sensing of Environment,* 112/9, 3582-3593

Gitelson, A.A., Schalles, J.F., & Hladik, C.M. (2007). Remote chlorophyll-a retrieval in turbid, productive estuaries: Chesapeake Bay case study. *Remote Sensing of Environment,* 109/4, 464-472

Gons, H., J., Rijkeboer, M., & Ruddick, K. (2002). A chlorophyll-retrieval algorithm for satellite imagery (Medium Resolution Imaging Spectrometer) of inland and coastal waters. *Journal of Plankton Research,* 24/9, 947-951

Gons, H.J., Rijkeboer, M., & Ruddick, K.G. (2005). Effect of a waveband shift on chlorophyll retrieval from MERIS imagery of inland and coastal waters. *Journal of Plankton Research,* 27/1, 125-127

Guanter, L., Ruiz-Verdu, A., Odermatt, D., Giardino, C., Simis, S., Estelles, V., Heege, T., Dominguez-Gomez, J.A., & Moreno, J. (2010). Atmospheric correction of ENVISAT/MERIS data over inland waters: Validation for European lakes. *Remote Sensing of Environment,* 114/3, 467-480

Heege, T., & Fischer, J. (2004). Mapping of water constituents in Lake Constance using multispectral airborne scanner data and a physically based processing scheme. *Canadian Journal of Remote Sensing,* 30/1, 77-86

Hoogenboom, H.J., Dekker, A.G., & De Haan, J.F. (1998). Retrieval of chlorophyll and suspended matter from imaging spectrometry data by matrix inversion. *Canadian Journal of Remote Sensing,* 24/2, 144-152

ISO-10260E (1992). Water quality measurement of biochemical parameters - spectrophotometric determination of chlorophyll-a concentration. Geneva, Switzerland

Koponen, S., Ruiz-Verdu, A., Heege, T., Heblinski, J., Sorensen, K., Kallio, K., Pyhalahti, T., Doerffer, R., Brockmann, C., & Peters, M. (2008). Development of MERIS lake water algorithms. In: *ESA Validation Report* (65 p.)

Leathers, R.A., Downes, T.V., & Mobley, C.D. (2004). Self-shading correction for oceanographic upwelling radiometers. *Optics Express,* 12/20, 4709-4718

Lindell, T., Pierson, D., Premazzi, G., & Zilioli, E. (1999). Manual for monitoring European lakes using remote sensing techniques. In: *Official Publications of the European Communities, EUR Report n. 18665* (164 p.), Luxembourg

Mobley, C.D. (1994). *Light and Water*. San Diego: Academic Press Inc.

Odermatt, D., Heege, T., Nieke, J., Kneubuehler, M., & Itten, K. (2008a). Water quality monitoring for Lake Constance with a physically based algorithm for MERIS data. *Sensors,* 8/8, 4582-4599

Odermatt, D., Kiselev, V., Heege, T., Kneubühler, M., & Itten, K.I. (2008b). Adjacency effect considerations and air/water constituent retrieval for Lake Constance. *Proc. 2nd MERIS/AATSR workshop*, Frascati, Italy

Peters, M. (2008). Technical note - run processor in batch mode [Internet]. Carsten Brockmann Consult, Hamburg, Germany. http://www.brockmann-consult.de/beam-wiki/display/LAKES/Home., accessed 19 February 2009

Premazzi, G., Dal Miglio, A., Cardoso, A.C., & Chiaudani, G. (2003). Lake management in Italy: The implications of the Water Framework Directive. *Lakes & Reservoirs: Research and Management,* 8/1, 41-59

Rey, P., & Müller, E. (2007). EU-Wasserrahmenrichtlinie und Schweizer Wasser- und Gewässerschutzgesetzgebung. In: *BAFU Expertenbericht* (95 p.), Hydra AG Gewässerfragen und Umweltinformation (in German)

Rimet, F., Druart, J.C., & Moreau, L. (2008). Phytoplancton du Léman - The phytoplankton of Lake Geneva. In: *Rapport Commission International pour la Protection des eaux du Léman contre la pollution - Campagne 2007* (85-95 p.), INRA-UMR/CARRTEL, Thonon-Les-Bains, France

Ruiz-Verdu, R., Koponen, S., Heege, T., Doerffer, R., Brockmann, C., Kallio, K., Pyhälahti, T., Pena, R., Polvorinos, A., Heblinski, J., Ylöstalo, P., Conde, L., Odermatt, D., Estelles, V., & Pulliainen, J. (2008). Development of MERIS lake water algorithms: Validation results from Europe. *Proc. 2nd MERIS/AATSR workshop*, Frascati, Italy

Santer, R., Carrère, V., Bubuisson, P., & Roger, J.C. (1999). Atmospheric correction over land for MERIS. *International Journal of Remote Sensing,* 20/9, 1819-1840

Santer, R., & Schmechtig, C. (2000). Adjacency effects on water surfaces: Primary scattering approximation and sensitivity study. (43 p.), Laboratoire Interdisciplinaire de Sciences de l'Environnement, Wimereux

Santer, R., & Zagolski, F. (2009). ICOL Improve Contrast between Ocean & Land. In: *BEAM Algorithm Technical Basis Document* (15 p.), Université du Littoral Côte d'Opale, Wimereux, France

4 ASSESSING REMOTELY SENSED CHLOROPHYLL-A FOR THE IMPLEMENTATION OF THE WATER FRAMEWORK DIRECTIVE IN EUROPEAN PERIALPINE LAKES

This Chapter has been published as: Bresciani, M., Stroppiana, D., Odermatt, D., Morabito, G. & Giardino, C. (2011). Assessing remotely sensed chlorophyll-a for the implementation of the Water Framework Directive in European perialpine lakes. Science of the Total Environment, 409/17, 3083-3091. The contribution of D. Odermatt to this article is 5% methods, 30% data analysis and 10% writing.

Abstract

The lakes of the European perialpine region constitute a large water reservoir, which is threatened by the anthropogenic pressure altering water quality. The Water Framework Directive of the European Commission aims to protect water resources and monitoring is seen as an essential step for achieving this goal. Remote sensing can provide frequent data for large scale studies of water quality parameters such as chlorophyll-a (*chl-a*). In this work we use a dataset of maps of *chl-a* derived from over 200 MERIS (MEdium Resolution Imaging Spectrometer) satellite images for comparing water quality of 12 perialpine lakes in the period 2003 - 2009. Besides the different trophic levels of the lakes, results confirm that the seasonal variability of *chl-a* concentration is particularly pronounced during spring and autumn especially for the more eutrophic lakes. We show that relying on only one sample for the assessment of lake water quality during the season might lead to misleading results and erro-

neous assignments to quality classes. Time series MERIS data represents a suitable and cost-effective technology to fill this gap, depicting the dynamics of the surface waters of lakes in agreement with the evolution of natural phenomena.

4.1 Introduction

Lentic ecosystems are inestimable renewable natural resources for biodiversity and can be significantly altered by human activities and climate change (Kaiblinger et al., 2009). Their ecological status vitally affects their value as drinking water reservoirs, for irrigation, fishery or recreation; any effort placed for preserving and/or improving the quality of these resources in the years to come and for increasing monitoring capability is justified. For this reason, the European Commission (EC) has adopted the Water Framework Directive (WFD) (Directive, 2000) with the main objective of maintaining 'good' and non-deteriorating status for all waters (surface, ground and coastal) (Chen et al., 2004). The Directive applies to all countries of the European Union (EU) and it has to be implemented at the catchment scale (river basin district) thus taking into account hydrological rather than geographical or political boundaries (Premazzi et al., 2003). Monitoring is an essential part of the implementation of the WFD (Premazzi et al., 2003). Surveillance monitoring aims at assessing the status of surface and ground waters. Operational monitoring is undertaken to evaluate the effects of measures undertaken to improve critical situations and to evaluate the level of achievement of the Directive's objectives; systematic monitoring has to be done through monitoring networks (Chen et al., 2004). So the starting step is the classification of water bodies into 'ecological quality status' using biological indicators (Kaiblinger et al., 2009). Lake classification under the WFD is based from the deviation of the present state from type specific reference conditions (Wolfram et al., 2009). Moreover, the WFD forces the member states to monitor systematically all natural and artificial lakes with surface area$\geq$0.5 km_2 (Premazzi et al., 2003). Field measurements of the indicators of lake water quality are to be carried out every three months although recent works suggest that the time interval between samplings should be reduced.

The sampling protocols adopted across EU suggest a minimum number of yearly samples for phytoplankton analysis. Sampling is usually carried out on a seasonal basis, therefore four samples is the most common option, although

some Member States (such as Italy) decided to increase the minimum frequency up to 6 samples per year, trying to include those periods when phytoplankton is rapidly changing, due to the transition between two seasonal phases of relative stability in the assemblage composition. Because phytoplankton structure can be particularly variable from day to day during these transitional phases (Salmaso, 1996), the choice of the sampling dates is crucial, because it can significantly affect the outcome of the classification.

The number of samplings during the year is a compromise between the effort/cost required from the agencies in charge of monitoring and the need of describing the seasonal ecological variability with at least four to six sampling for all lakes. Within the time frames set by the Directive for measurements, the choice of the date is often dictated by the organizational needs hence the picture of water ecological conditions might be biased especially in the case of parameters which can vary significantly over small time periods, such as chlorophyll-a (*chl-a*).

The classification of the ecological status of lakes is based on the values measured for physicochemical and chemical parameters, which are related to the trophic level of the water: transparency, hypolimnetic oxygen, chlorophyll-a and total phosphorus. In the WFD *chl-a* concentration is therefore recognized as an essential parameter for the classification of the quality of lake waters (Jeppesen et al., 2003; Søndergaard et al., 2005) since together with phytoplankton species composition (Salmaso et al., 2006) is essential for an exhaustive description of the waters ecological status (Carvalho et al., 2008). In fact, these latter parameters are related to nutrient availability within waters (Vollenweider and Kerekes, 1980).

However, the estimation of *chl-a* concentrations in waters is often carried out with different methods for both sampling and laboratory analyses (Lindell et al., 1999) thus leading to the need of intercalibration of different monitoring systems as also required by the WFD (Nõges et al., 2010). Remote sensing technology is a tool for collecting consistent/homogeneous spatial and temporal data for the assessment of water quality parameters in lakes (e.g., Bukata et al., 1991; Cavalli et al., 2009; Dekker et al., 2001; Koponen et al., 2004; Gons et al., 2008; Giardino et al., 2010). It allows us to monitor large water areas (from local to global scale) with systematic and cost-effective acquisitions. Salmaso and Mosello (2010) reviewed over 200 articles published in the field of limnology and draw the conclusion that synoptic analyses on a macroregional scale in the sub alpine region need to be further addressed by re-

searchers. Remote sensing can certainly provide the data to achieve this goal. Moreover, it offers archives of data which are suitable for the re-construction of historical trends (Chen et al., 2007). Several works have in particular focused on the satellite-inferred estimation of the concentration of *chl-a* (Baban, 1993; Giardino et al., 2001; Gons et al., 2002; Strömbeck and Pierson, 2001; Doerffer and Schiller, 2007; Gitelson et al., 2007; Gower and King, 2007; Bilgehan et al., 2009; Bresciani et al., 2009). In fact, changes in the concentration of *chl-a* are associated to changes in the amount of water leaving radiance in the photosynthetically active radiation region of the electromagnetic spectrum and these changes can be detected with optical remote sensors (Baban, 1999). Therefore remote sensing can be a tool for collecting data to support the implementation of the monitoring activities outlined in the EC WFD. However, despite the undisputable advantages offered by satellite sensors, remote sensing relies on the collection of in situ data for the development and the validation of algorithms and models (Brando and Dekker, 2003; Chen et al., 2004). The systematic collection of in situ data should be performed as an integral part of operational monitoring build on remote sensing technology for lake management strategies such those as required by the WFD.

This work relies on the availability of a large dataset of maps of *chl-a* over 12 perialpine lakes for the period 2003–2009. Maps were derived from over 200 images acquired by the MEdium Resolution Imaging Spectrometer (MERIS) onboard the Envisat-1 mission of the European Space Agency (ESA) (Odermatt et al., 2010). The objectives are i) to compare water quality of the subalpine lakes of the study area by analysing *chl-a* concentrations, ii) to analyze the spatial variability of *chl-a* concentration during the season and over the years, and iii) to simulate the application of the WFD to this sub-alpine region through the information supplied by remotely sensed data.

4.2 Study area

The European perialpine region around the Alps comprises a significant number of glacial and tectonic lakes, which constitute an inestimable reservoir of freshwater. The 12 lakes selected in the study area (Figure 4-1) belong to four countries: Italy, Switzerland, France and Germany. They have a size suitable for the geometric characteristics of the MERIS sensor (spatial full resolution is 300 m) and they are greater than 0.5 km_2, which is the minimum size required by the WFD for enforcing quality monitoring. Water of these lakes is exten-

sively used for the production of hydroelectric power, is intensively used in agriculture and industry, becoming a life-sustaining element for the economy of the surrounding areas. Waters from the largest lakes (e.g., Lake Zurich and Lake Como) are even used directly as fresh water supply of the nearby cities. In addition, these water bodies are one of the key elements for the tourist economy of the Alpine region.

Figure 4-1: Study area with indication of Region of Interest (ROI) for every lakes.

The lakes included in this study are oligotrophic by nature (Guilizzoni et al., 1983) but they underwent intense processes of cultural eutrophication started in the 1960s, which reached a maximum at the end of the '70s. The major cause of the ecological deterioration was phosphorus loads from sewage, which triggered the increase of annual primary productivity, of algal biovolume and growth of cyanobacteria. Since the early 1980s, nutrient loads have been gradually reduced mainly by adopting treatment plants and by reducing the phosphorus contained in domestic detergents. Since then most of the lakes (i.e. the largest lakes) have started a reoligotrophication process. Obviously each lake has had its own ecological history, which is extensively described in

the scientific literature (e.g. Binelli et al., 1997; Ruggiu et al., 1998; Pugnetti et al., 2006; Anneville et al., 2007; Eckmann et al., 2007; Manca et al., 2007; Salmaso and Mosello, 2010; Stich and Brinker, 2010).

The deep lakes of the Alps could be classified as warm monomictic lakes (e.g. Maggiore and Garda), the shallow lakes could be classified dimictic (e.g. Varese). Some common morphological features can be identified: the lakes are narrow and elongated, with steep sides and generally a flat bottom. The thalwegs of the largest Italian lakes are roughly oriented North-South whereas the others are mainly oriented East–West (Figure 4-1). Except for Pusiano and Varese, which were included in the study for their peculiar trophic levels and their morphology, all lakes are characterized by high depth (both mean and maximum). The principal morphometric and hydrological features of the lakes are listed in Table 4-1. The lakes differentiate for their water circulation patterns, which lead to highly different residence times (0.7–26.8 years). In the table we also identify the lake typology (L-AL3 and L-AL4),which is mainly assigned based on the above sea level (a.s.l.) altitude and on the water mean depth as described by Wolfram et al. (2009): only lakes Pusiano and Varese are classified as L-AL4 lakes because of their shallow waters.

Table 4-1: The major characteristics of the perialpine lakes object of this study. Lake typology ("Type") is assigned based on Wolfram et al. (2009).

Lake	Surface (km2)	Volume (km3)	Max depth (m)	Mean Depth (m)	Altitude (m a.s.l.)	Catchment area (km3)	Residence time (year)	Type
Como	145	22.5	410	154	198	4508	4.5	L-AL3
Constance	536	55	254	90	395	11500	4.3	L-AL3
Garda	370	50.35	346	136	65	2290	26.8	L-AL3
Geneva	582.4	89	310	154	372	7975	11.4	L-AL3
Interlaken	48.3	6.5	217	136	558	2500	1.85	L-AL3
Iseo	65.3	7.6	251	124	185	1777	4.2	L-AL3
Lucerne	113.6	11.8	214	104	434	2124	3.4	L-AL3
Maggiore	212	37	370	177	193	6599	4	L-AL3
Pusiano	5.2	0.07	27	14.5	257	94.3	0.7	L-AL4
Varese	14.5	0.1	26	11	238	112	1.8	L-AL4
Zug	38.3	3.2	198	83.2	413	204	14.7	L-AL3
Zurich	88.66	3.9	143	49	406	1829	1.2	L-AL3

4.3 Materials and methods

The maps of *chl-a* concentration for the lakes of the study area were produced by Odermatt et al. (2010) from a dataset of over 200 MERIS images for the period 2003–2009. MERIS is a medium resolution imaging spectrometer carried onboard the ESA-Envisat-1 satellite and operating since 2002 within a mission covering open oceans, coastal zone and land surfaces. The instrument has a field of view around nadir of about 68.5° and it covers a swath width of 1150 km.MERIS is designed to acquire 15 spectral bands in the visible and near-infrared wavelengths with a spatial resolution of about 300m at nadir. All images were processed with the procedure available in the ESA Basic Envisat/ERS ATSR and MERIS (BEAM) that accounts for instrument smile, geometric, adjacency and atmospheric effects as described and validated in Odermatt et al. (2010). In particular, the adjacency effects were corrected with the Improved Contrast between Land and Ocean (ICOL) processor (Santer and Schmechtig, 2000; Santer and Zagolski, 2009). For the atmospheric correction and the retrieval of *chl-a* concentrations the Case-2 Regional (C2R) module (Doerffer and Schiller, 2008a,b), which implements a neural network for the inversion of both radiative transfer and bio-optical models, was used. C2R provided accurate reflectance values and consistent retrieval of *chl-a* concentrations in the study area (Odermatt et al., 2010). Outputs are given in the form of map products as well as in tabular form, whereas the latter allows the extraction of all relevant parameters and simple statistical variables for several sampling sites. Datasets were excluded i) if acquired at sun glint suspect geometries (i.e. above 10° east in summer or 20° east in winter), ii) if indicated by the C2R error flags, iii) if *chl-a* was below 0.1 mg/m3 or iv) if contrails or cirrus clouds were visible in a channel 13 quicklook.

For the definition of the sampling sites we first defined a set of Regions Of Interest (ROIs) of the size of 3x3 MERIS pixels over the lakes of the study area. For lakes with a surface area≥0.5 km_2, the WFD locates the sampling point for monitoring water quality at the centre of the lake. This position is also ideal for optical measurements since it minimizes the adjacency effect, avoids mixed land/water pixels and ensures the least interference from the signal of the bottom of the lake. Therefore, we selected one ROI located at the centre of each lake of the study area. Moreover, for the largest lakes (surface area≥80 km_2) and for lakes of irregular shape, the WFD imposes additional sampling points to be defined case by case. For this reason we selected multiple ROIs for the

largest lakes and we located them where the *chl-a* spatial variability might increase due to the presence of local factors (e.g. tributary water).

We extracted the temporal profiles of *chl-a* concentration for each ROI and analysed statistic metrics globally and for each season (spring, summer, autumn and winter) to compare the different trophic levels of the lakes. We chose to divide the year into the four seasons because hydrodynamic features and eutrophication are highly seasonal phenomena.

In order to achieve the third objective of this work (simulation of the application of the WFD with information supplied by remotely sensed data), we classified the lakes based on *chl-a* concentrations estimated for the seasonal periods given in Table 4-2. These periods are those suggested in the Italian official protocol for sampling lake phytoplankton, according to WFD (Buraschi et al., 2008). Within each season, we selected one date (Option A) mainly based on the quality and coverage of the satellite images. The ecological status classes were assigned based on reference values given by Wolfram et al. (2009). Since one major advantage of remote sensing is the availability of frequent observations at a low additional cost of acquisition, we applied the same classification by selecting a different date within the same periods of the year. Finally, we perform the same exercise by averaging all dates available from satellite images to simulate a condition of a full integration of remotely sensed data into a monitoring system of lake water quality as proposed by the WFD.

Table 4-2: The dates selected for each monitoring period defined by the Italian national protocol for sampling lake phytoplankton. If the MERIS acquisition were not available on the exact date shown here we chose the closest in time, which generally falls in an interval of ±3 days. These sampling periods correspond to Option A in Table 4-3.

Season	**Reference range**	**2003**	**2004**	**2005**	**2006**	**2007**	**2008**	**2009**
Winter	1 January - 20 March	10/03	10/02	01/03	11/02	03/02	13/02	13/02
Spring	1 April - 15 May	23/04	20/04	02/04	13/04	16/04	02/05	14/04
Summer	1 July - 31 August	03/08	15/07	28/07	10/07	18/07	05/07	16/07
Autumn	1 October - 31 November	28/10	24/10	29/10	10/10	15/10	09/10	25/10
Spring-summer transition	15 May - 15 June	31/05	25/05	29/05	08/06	19/05	10/06	19/05
Summer-autumn transition	1 September - 1 October	14/09	07/09	21/09	12/09	10/09	16/09	08/09

4.4 Results and discussion

Figure 4-2 shows some example maps of *chl-a* concentration over the largest lakes of the study area (i.e. Constance, Garda, Maggiore, Como and Geneva). The temporal trends observed in correspondence with the ROIs are presented in Figure 4-3.

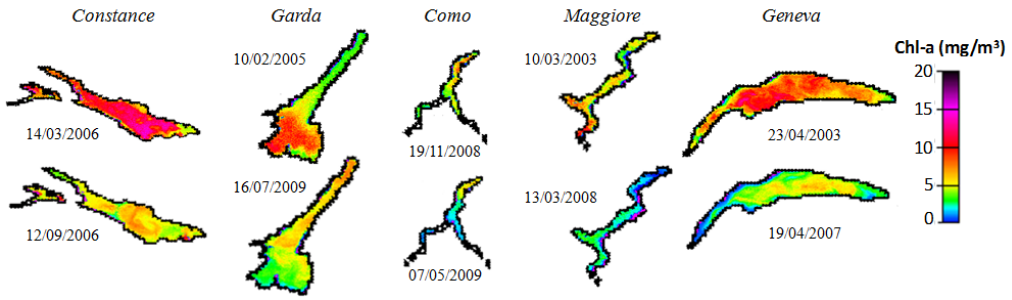

Figure 4-2: Some example maps of chl-a concentration over the largest lakes of the study area on key dates of the period 2003-2009.

Figure 4-2 shows an algal bloom occurring in March and September 2006 in the central area of lake Constance where water is deepest. The map also shows the location of both the inflow (south east end) and outflow (west end) of the Rhein river as red spots of high concentration of *chl-a* (N10 mg/m3). In fact, the difference of the profiles extracted for the ROIs is statistically different (**pb0.01). Indeed, the description of the spatial patterns of water quality parameters is one of the major contributions of remote sensing techniques for environmental monitoring. The oligotrophication of Lake Constance has begun at the beginning of this century as a consequence of the treatments of wastewater. This progressive process leads to low concentrations of *chl-a* and little fluctuations as shown by our results for the last seven years (Figure 4-3). Moreover, our results highlight that in the very recent years and with the exception of the bloom observed in 2006, *chl-a* has stabilized below 5 mg/m3 confirming findings by Stich and Brinker (2010).

Chl-a concentration in Lake Como have decreased between 2003 and 2006 (Figure 4-3) and have maintained stable after 2006: seasonal maxima have in fact decreased from above 10 mg/m3 to below 5 mg/ m3 with a reduction of seasonal fluctuations. Moreover, the two sampled ROIs appear to have diffe-

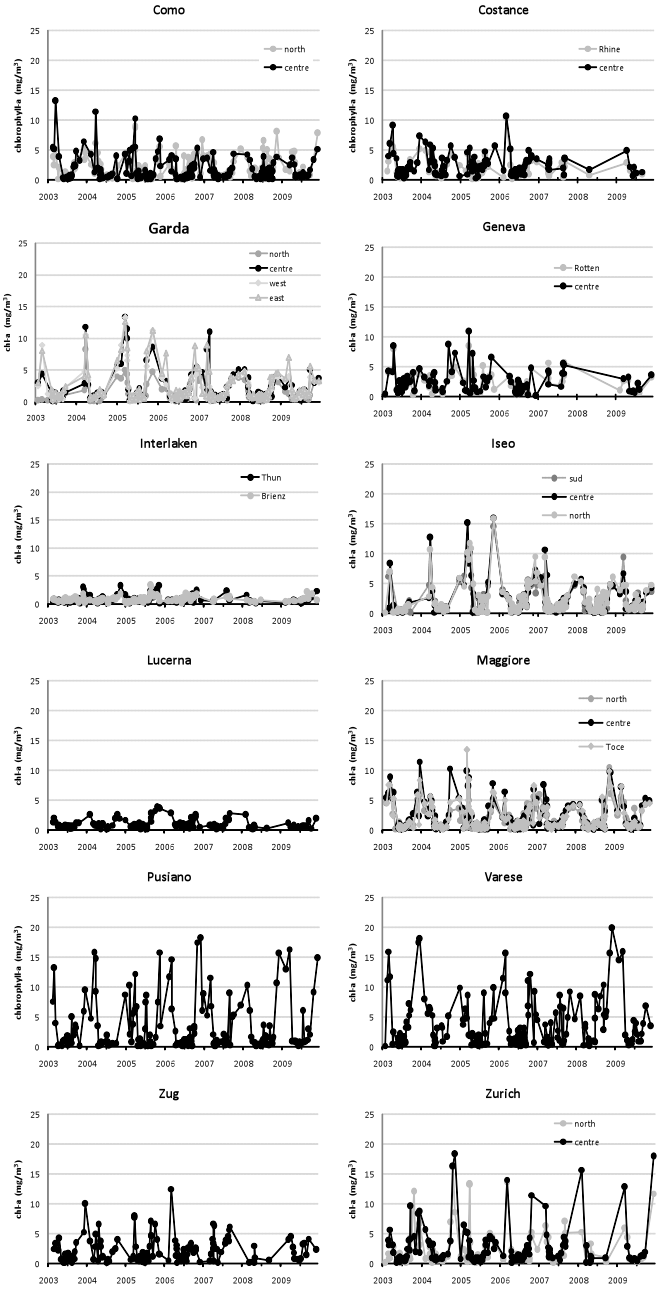

Figure 4-3: Trends of chl-a concentrations for the ROIs extracted for the lakes of the study area. The gaps within the time series are due to persistent cloud cover over the lakes or lack of data. The discontinuity affects in particular some of the lakes in 2008-2009.

rent values after 2006 although the difference is not statistically significant (p=0.66). This deep lake is geographically divided into three sub-basins (northern, western and eastern), which can be identified in Figure 4-2; of these sub-basins, the deepest south-western Como branch is characterised by the lack of an outflow river and therefore by a longer water exchange time. By looking at the entire dataset, it appears rather difficult to identify regular, persistent and interpretable spatial patterns of *chl-a* concentration in Lake Como. The cause might be related to the atmospheric interference and quickly changing winds which modify the constituent patterns very frequently. The narrow y-shaped lake Como determines a behaviour similar to the typical behaviour of smaller lakes which are characterised by wide variability and unpredictability (Salmaso, 2010).

On the contrary, the size of Lake Garda leads to a minor susceptibility to the influence of hydrological and meteorological events hence more regular distribution of physical and chemical cycles (Salmaso, 2005). The map in Figure 4-2 (16 July 2009) clearly shows the effect of inflow waters from the Sarca tributary at the northern edge of the lake with high concentration of *chl-a* (red colour key, *chla*~10 mg/m$_3$) while the effect of water mixing is clearly visible on 10 February 2005 (Figure 4-2). The temporal trends collected over the three ROIs (Figure 4-3) show a seasonal cycle with maxima generally occurring in spring. The difference between the northern ROI and each of the other two sampling points of the lake is statistically significant (***pb0.001): in fact, the northern region is characterised by lower concentrations with values below 5 mg/m$_3$ whereas the other two regions have seasonal maxima above 10 mg/m$_3$. This difference might be determined by several anthropic and geographical factors among which: the southern lake is the most densely populated and touristic area, the sewage collection is channelled towards the southern lake and winds favour the mixing of the shallower waters of the southern sub-basin.

Lake Maggiore shows a very high spatial variability of *chl-a* concentration from the lowest on one side to the highest values of the scale on the other side of the lake (i.e. west to east direction). This spatial variability is more comparable to the variability observed for Lake Como rather than Lake Garda as it would be expected for the similar dimensions. These changes might be the consequence of some residual adjacency effects (Odermatt et al., 2010) or they might be due to the effect of local meteorological conditions such as winds. Even the hydrodynamics of these basins could play a role, taking into account the strong differences in the residence times of the three lakes (Table 4-1).

In Lake Geneva, the largest of the study area, the spring algal bloom occurred in 2007 when in less than a week the concentration of chlorophyll a increased on average from 5 mg/m$_3$ up to 10 mg/m$_3$ and returned down to the initial values. The temporal trend (Figure 4-4) highlight that maxima of *chl-a* concentrations (>5 mg/m$_3$) mainly occurred in either spring or autumn in the period 2003 to 2005, the spring peak in 2003 was also observed by Personnic et al. (2009); note that the lack of data in 2008 and 2009 might bias this results.

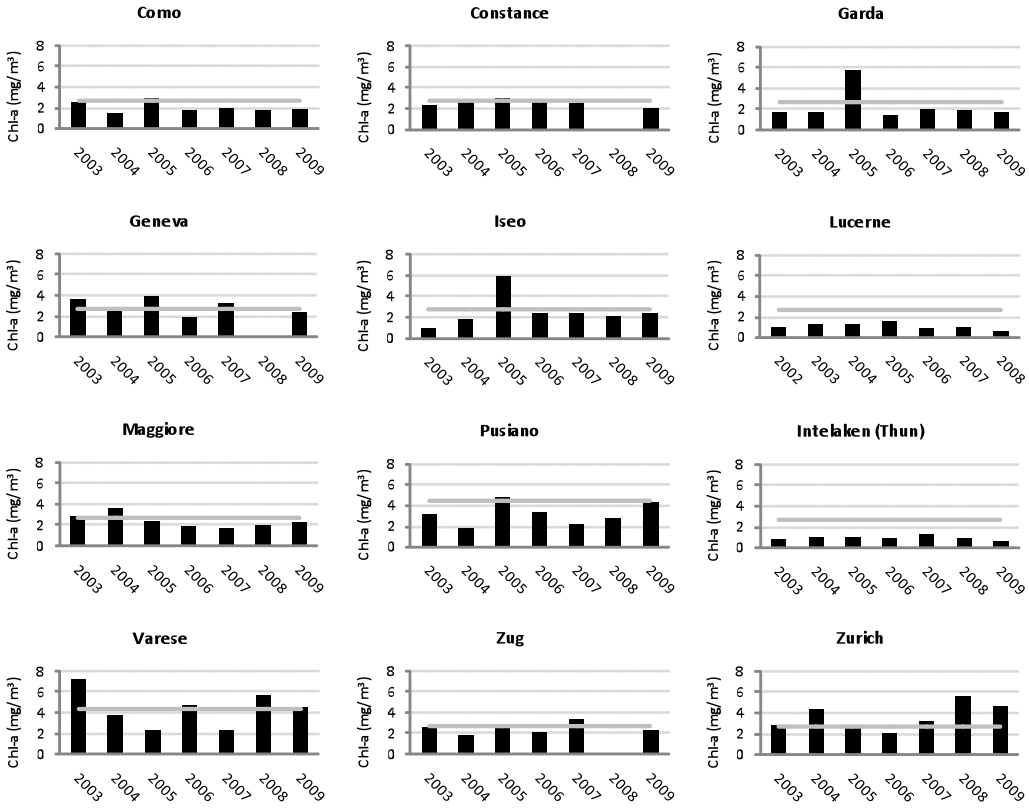

Figure 4-4: Chl-a concentrations derived from MERIS images (acquisition dates are given in Table 2) to support the application of the WFD. Values are the estimate of the central ROI for each lake. The straight line shows the limit between the classes high and good water quality as defined after the intercalibration exercise carried out inside the Alpine Geographic Intercalibration Group (Wolfram et al., 2009).

For the smaller lakes, we focused our analysis on the temporal trends (Figure 4-3). Lakes Zurich, Zug and Lucerne are geographically very close to each

other covering an area about 100 km wide. However, Lake Lucerne is the most oligotrophic while lakes Zurich and Zug are mesotrophic to eutrophic. Our estimates confirm the greatest concentrations of *chl-a* in lake Zurich with seasonal maxima close to or above 15 mg/m3 and the lowest values, always below 5 mg/m3, in lake Lucerne; in Lake Zug *chl-a* concentrations are generally below 5 mg/m3 but occasionally seasonal peaks can reach values of 10 mg/m3. Note that these peaks appear to be concentrated in the first three years of our analysis suggesting that this lake is still recovering from the severe eutrophication in the 1970s and 80s.

The Interlaken area comprises lakes Thun and Brienz, which are located at around 560 m a.s.l. (i.e. the highest lakes of the study area); many feeder rivers are of direct alpine origin (Kander, Lombach and Lütschine) and the ecological status is accordingly oligotrophic. Concentration of *chl-a* is very low (b3.5 mg/m_3), with the lowest values estimated for Lake Brienz, and variations are minimal.

Finally, the smallest Italian lakes Iseo, Pusiano and Varese, all of them in eutrophic status, have the greatest *chl-a* concentrations and the highest level of fluctuation. In particular, in Lake Pusiano an algal bloom event occurs almost every year during 2003–2009 with *chl-a* concentrations above 15 mg/m_3. These extreme conditions are mainly concentrated during either spring or autumn. The peaks of high chlorophyll a concentration of Lake Iseo are limited to sporadic events in winter compared to Pusiano and Varese.

We also computed the coefficient of variation ($CV=\sigma/\mu$) for each estimate within the 3°—3 ROIs to evaluate the spatial variability of *chla* estimates. In the small lakes with high *chl-a* concentrations CV is greater than 15% for almost half of the dates, meaning that water quality parameters can vary also over small scales. As pictured in Figure 4-2, the synoptic view of the sensors allows the description of the spatial variability of water quality parameters; this is indeed a major advantage offered by remote sensing techniques for the integration with field data collection, which, on the contrary, relies on the definition of representative sampling schemes.

The temporal trends do not show a tendency to either an increase or decrease of *chl-a* concentration. The regression lines have a slope not significantly different than zero and therefore the tendency is to maintain stable conditions. We computed the Hurst (H) exponent as an indicator of the expected tendency to confirm/reject the hypothesis of a stable behaviour. The results highlight that

only in lakes Pusiano, Varese and Zug have high values close to 0.5 thus suggesting an unpredictable behaviour.

The WFD foresees that the classification of the ecological status of a lake should be based on the annual average *chl-a* concentration derived from six seasonal samplings. We simulated the application of the WFD by using estimates of *chl-a* concentration derived from satellite images in correspondence with the central ROI of each lake and acquired on the dates shown in Table 4-2. Results are shown in Figure 4-4 and compared to the limit set by theWFD between the classes "high" and "moderate" water quality (straight grey line in the graphs).

These results show that the chlorophyll concentration is often below the threshold established as boundary between high and good quality classes (as reported in Wolfram et al., 2009), even in lakes usually classified as meso- or eutrophic. In particular, lakes Lucerne and Thun are characterised by stable oligotrophic conditions (Friedrich et al., 1999; Finger et al., 2007). Among the most eutrophic lakes, only Lake Zurich is, in some year, classified as good and only in one situation (i.e. 2008) as moderate. However, Lake Zurich is mesotrophic as a consequence of the anthropogenic pressure along the shores and has had some significant events of cyanobacteria blooms (Peter et al., 2009). Lake Varese, in spite of his long history of water quality deterioration due to cultural eutrophication (Premazzi et al., 2003), is classified as good in most cases.

On the other side, the classification of lakes Garda and Iseo as moderate in 2005, derived from MERIS images, properly mirrors the exceptional worsening of water quality in 2005 caused by cyanobacteria blooms in the first (Salmaso, 2010) and by high nutrient loads, phosphorus in particular, in the second (Salmaso et al., 2007).

Since the WFD identifies only the large periods of the year when monitoring activity should be carried out, any value made available by satellite acquisitions within these periods is eligible for the classification. We therefore selected alternative dates to those given in Table 4-2 (hereafter named Option B). The results clearly show that this choice can be influential on the final classification especially in key seasons of the year when *chl-a* concentrations can significantly vary from day to day such as spring. Table 4-3 shows the example case of Lake Como where the ecological status assigned to the lake can change even from high to moderate/poor and vice versa.

Table 4-3: Chl-a concentration for the lake Como for the two Options (i.e. A and B in the table) of date selection made possible by the availability of frequent MERIS acquisitions during the periods outline by the WFD for monitoring lake water quality.

	2003		**2004**		**2005**		**2006**		**2007**		**2008**		**2009**	
Season	A	B	A	B	A	B	A	B	A	B	A	B	A	B
Winter	5.13	5.38	4.22	4.22	0.72	4.90	3.31	4.16	3.63	3.44	4.29	3.39	2.46	2.46
Spring	3.81	3.81	1.90	11.4	10.3	5.58	0.96	3.47	1.27	4.67	0.50	1.78	3.78	2.63
Summer	0.45	0.20	0.38	1.27	0.59	0.32	0.41	0.28	0.65	0.65	0.55	0.55	0.36	0.71
Autumn	0.50	0.13	0.57	0.82	0.22	0.93	0.50	0.49	0.56	0.70	1.34	3.86	0.52	1.12
Spring-summer transition	2.43	4.71	1.08	1.08	0.73	0.80	2.50	1.44	1.58	1.18	2.11	0.78	0.62	0.78
Summer-autumn transition	3.22	6.47	0.17	3.93	4.81	6.83	2.33	5.26	4.43	1.93	1.37	2.81	3.36	5.21
Mean	2.59	3.45	1.38	3.80	2.90	3.23	1.67	2.52	2.02	2.09	1.70	2.20	1.85	2.15

The high variability of *chl-a* concentration in spring is confirmed by the standard deviation of the estimates derived from satellite data available for each period shown in Figure 4-5. In the same figure the standard deviation computed for the summer season is given for comparison. Spring is characterised by the highest variability and summer by the lowest due to stratification processes that reduce water flow between the strata. These dynamics are particularly effective in water resilience of the largest and deepest lakes (e.g. Garda). The most eutrophic lakes, such as Pusiano and Varese, are characterised by high variability of *chl-a* concentrations in both seasons. This would indicate that in the two lakes, summer chlorophyll concentration is less conservative than in the other lakes. The reason of this higher variability can be found in the differences in nutrient cycling across the trophic gradient. In eutrophic lakes, where the P supply at spring overturn is high, spring phytoplankton growth can produce high *chl-a* concentrations. The model suggested by Kufel (2001) can, probably, be applied also in our case: at the end of the growth phase, there is a strong nutrient flux towards the bottom of the lake, due to the sedimentation of decaying algal populations. This would remove a large amount of the nutrients from the upper water layers, thus limiting the phytoplankton growth. Under P limitation, a decline of *chl-a* is commonly observed in early summer in eutrophic lakes, until a new P input (i.e. from the metalimnion when the thermocline is deepening) refuels the algal population. On the other side, in the oligo- and mesotrophic lakes the spring growth is lower, therefore the downward P flux is less important and an higher amount of nutrients remain in the upper water layers and can be continuously recycled and exchanged between epilimnion and metalimnion: this would maintain a rather constant P availability,

avoiding strong *chl-a* fluctuations during summer. The weaker temperature gradient in oligo- and mesotrophic lakes could enhance the probability of nutrient exchange between epilimnion and metalimnion.

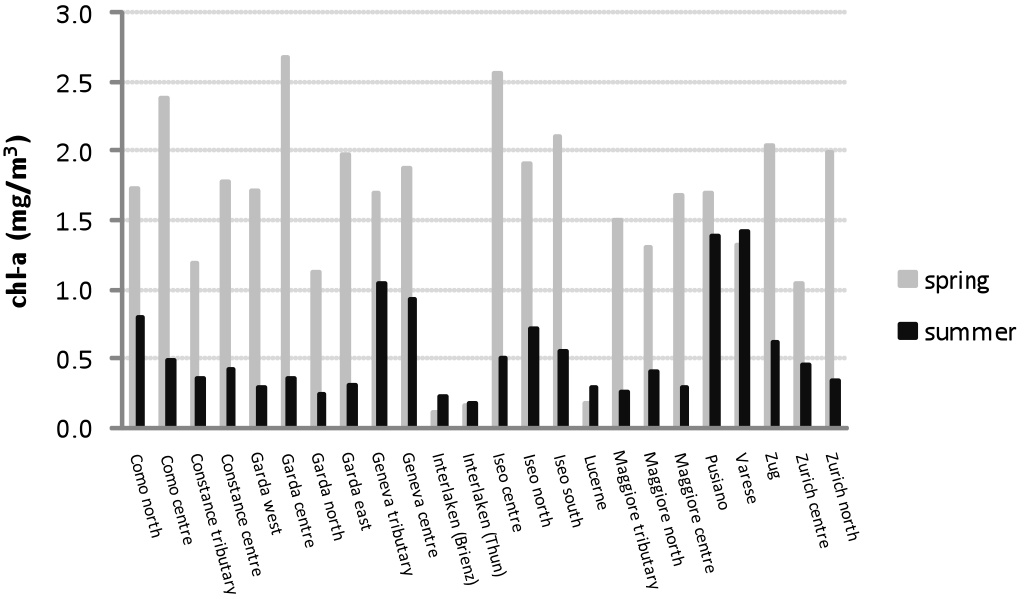

Figure 4-5: Standard deviation of the chl-a estimates derived from MERIS images available for spring and autumn seasons of the 2003-2009 period.

The finding of higher variability in the most eutrophic systems seems to confirm the hypotheses made by Cottingham et al. (2000), who, by analysing paleoecological data, showed that nutrient enrichment results in much more marked fluctuations in *chl-a* concentration.

Figure 4-6 shows the average, maximum and minimum values of *chl-a* concentrations estimated using all maps available for the six periods of the year outlined by the Italian sampling protocol. In Figure 4-6 we compare these values to *chl-a* concentration assessed for the single date of Option A (Table 4-3). These results highlight that the high temporal dynamic of phytoplankton which should be captured by the monitoring system. In those lakes which have a significant variability one sampling date during the season might not describe accurately the trophic conditions of the lake. One sampling might in fact capture either negative or positive outliers; the former describe the individual extreme event while the latter provide reference good quality parameters. However, in

both cases, the classification would be driven towards the erroneous quality class.

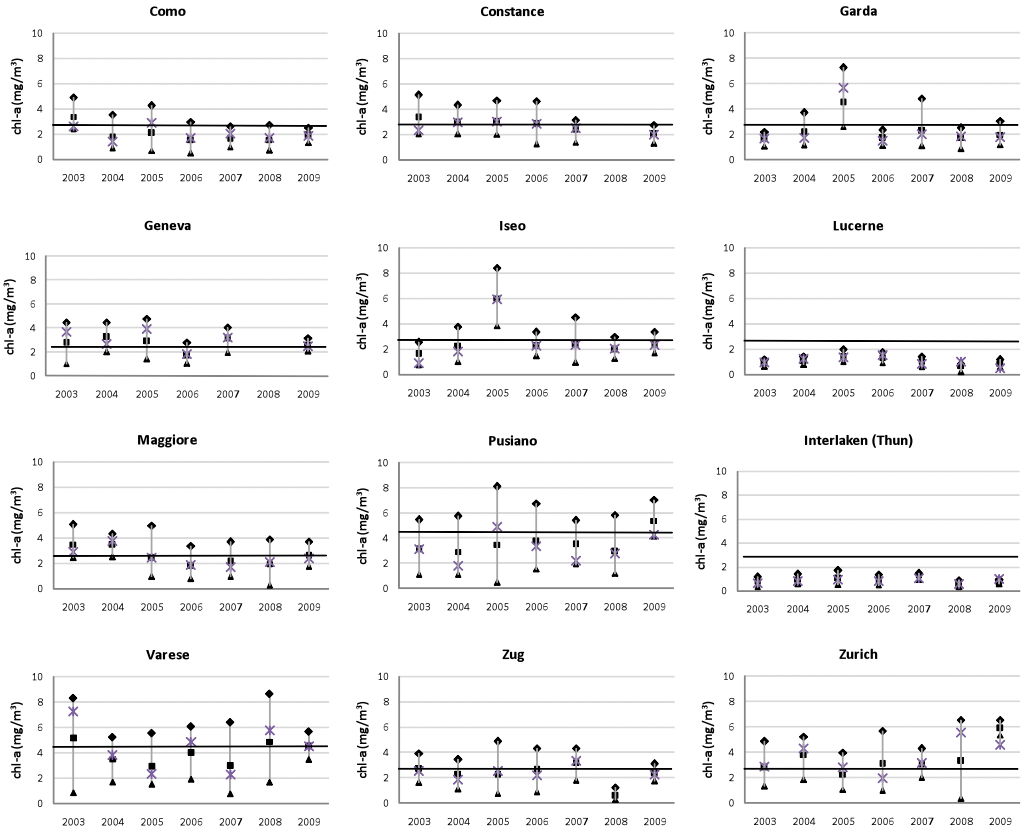

Figure 4-6: Average (squares), minimum (triangle) and maximum (rhombus) chl-a concentration in coincidence of the central ROIs derived from all product images available for the six key periods of the year. The estimates derived for the option A dates are shown for comparison with the cross markers. The straight line shows the limit between the classes high and good water quality as defined after the intercalibration exercise carried out inside the Alpine Geographic Intercalibration Group (Wolfram et al., 2009).

Besides the small lakes (Pusiano and Varese) and the case of lake Como already shown in Table 4-3, an example is lake Zurich where in 2006 the quality class varies depending on the use of either one date (Option A) or the average values.

4.5 Conclusions

Environmental monitoring of surface waters can take advantage of remote sensing techniques which provide a synoptic view over large areas and frequent acquisitions. In situ data can provide a snapshot of local water conditions, which are however necessary for calibration and validation of satellite based models. Maps of *chl-a* concentration were obtained from processing more than 200 MERIS images over 12 perialpine lakes encompassing four countries for the seven year period 2003–2009. Results show the largest lakes (Constance, Garda, Como, Maggiore and Geneva) to be meso- to oligotrophic with occasional events of high *chl-a* concentration. These lakes show a clear seasonal trend of the concentrations with the highest values estimated in winter and during seasonal transitions from winter to spring and from autumn to winter; the lowest concentrations occur in summer. Lucerne and Thun and Brienz, which form the Interlaken area, are the lakes with the best ecological conditions: the lowest *chl-a* concentration (bb5 mg/m_3) and the least fluctuations. On the other hand, the smaller Italian lakes, Iseo, Pusiano and Varese are characterised by high level of *chl-a* concentrations with peaks often above 10 mg/ m_3 and significant fluctuations in time. Despite the short time period of analysis, we observed that lakes are in stable conditions with the exception of Como, for which *chl-a* concentrations appear to have being decreasing.

We showed how remote sensing could be exploited for the implementation of the EU-WFD for classifying lake waters into quality classes. The small lakes are more frequently above the limit set for the high/good water quality class. On the contrary, larger lakes are in general high conditions with the exception of extreme events of algal blooms which temporarily worsen lake water quality during winter/spring. The use of remote sensing techniques for investigating phytoplankton abundance may overcome the problem of misclassification due to the *chl-a* seasonal variability and to the possibility of missing significant events when using the standard monitoring protocols with a low sampling frequency. On the other side, the vertical distribution of phytoplankton that in deep lakes is usually characterised by a metalimnetic chlorophyll maximum, often located around 10–15 m depth, could have an impact on the remotely sensed signal (Stramska and Stramski, 2005) so that during the stratification period the satellite-inferred estimates of *chl-a* might be lower than in situ measurements.

In order to assess water quality according to WFD criteria, the Members States monitoring programs suggest performing between four and six seasonal samplings during the year to average *chl-a* concentrations to identify a global quality class. We show that the assignment to a quality class can significantly depend on the date chosen for *chl-a* measurement/estimation since phytoplankton dynamics can vary from day to day. Since field campaigns significantly impact on the budget available for the implementation of the monitoring activities, remote sensing can be exploited to better describe these dynamics with multiple acquisitions with a lower marginal cost. If remotely sensed data are to be implemented in a monitoring system such as the one proposed by the WFD, research should focus on i) routine and extensive validation of the remotely sensed products through field data, ii) development of standard policies for satellite data acquisitions and criteria for interpreting products.

4.6 Acknowledgements

This study was co-funded by the EULAKES Project (EU Central Europe Programme 2010–2013). MERIS data were made available through the ESA projects AO-553 (MELINOS) and AO-1107. We are grateful to two anonymous reviewers for their useful comments on the manuscript.

4.7 References

Anneville O, Molinero JC, Souissi S, Balvay G, Gerdeaux D. Long-term changes in the copepod community of Lake Geneva. J Plankton Res 2007;29:49–59.

Baban MSJ. Detecting water quality parameters in Norfolk Broads, UK, using Landsat imagery. Int J Remote Sens 1993;14:1247–67.

Baban MSJ. Use of remote sensing and geographical information systems in developing lake management strategies. Hydrobiologia 1999;395/396:211–26.

Bilgehan N, Karabork H, Ekercin S, Berktay A. Mapping chlorophyll-a through in-situ measurements and Terra ASTER satellite data. Environ Monit Assess 2009;157:375–82.

Binelli A, Provini A, Galassi S. Trophic modifications in Lake Como (N. Italy) caused by the Zebra Mussel (Dreissena Plymorpha). Water Air Soil Pollut 1997;99:633–40.

Brando VE, Dekker AG. Satellite hyperspectral remote sensing for estimating estuarine and coastal water quality. IEEE Trans Geosci Remote 2003;41:1378–87.

Bresciani M, Giardino C, Longhi D, Pinardi M, Bartoli M, Vascellari M. Imaging spectrometry of productive inland waters. Application to the lakes of Mantua. Ital J Remote Sens 2009;41:147–56.

Bukata RP, Jerome JH, Kondratyev KY, Pozdnyakov DV. Satellite monitoring of opticallyactive components of inland waters: an essential input to regional climate change impact studies. J Great Lakes Res 1991;17:470–8.

Buraschi E, Buzzi F, Garibaldi L, Legnani E, Morabito G, Oggioni A, et al. Protocollo di campionamento di macrofite acquatiche in ambiente lacustre. Protocollo per il campionamento di fitoplancton in ambiente lacustre. Metodi biologici per le acqueAPAT (Italian Agency for the Environmental Protection); 2008. Parte 1.

Carvalho L, Solimini A, Phillips G, van den Berg M, Pietiläinen O-P, Lyche Solheim A, et al. Chlorophyll reference conditions for European intercalibration lake types. Aquat Ecol 2008;42:203–11.

Cavalli RM, Laneve G, Fusilli L, Pignatti S, Santini F. Remote sensing water observation for supporting Lake Victoria weed management. J Environ Manage 2009;90: 2199–211.

Chen Q, Zhang Y, Ekroos A, Hallikainen M. The role of remote sensing technology in the EU Water Frame Work Directive (WFD). Environ Sci Policy 2004;7:267–76.

Chen Q, Zhang Y, Hallikainen M. Water quality monitoring using remote sensing in support of the EU Water Framework Directive (WFD): a case study in the Gulf of Finland. Environ Monit Assess 2007;124:157–66.

Cottingham KL, Rusak JA, Leavitt PR. Increased ecosystem variability and reduced predictability following fertilisation: evidence from palaeolimnology. Ecol Lett 2000;3:340–8.

Dekker AG, Peters SWM, Vos RJ, Rijkeboer M. Remote sensing for inland water quality detection and monitoring: state-of-the-art application in Friesland waters. In: Van Dijk A, Bos MG, editors. GIS and Remote Sensing Technology in Land and Water Management. Netherlands: Kluwer Academic Publishers; 2001. p. 17–38.

Directive. Directive 2000/60/EC of the European Parliament and of the council of 23 October 2000 establishing a framework for community action in the field of water policy. Off J Eur Communities 2000;L327:1-72.

Doerffer R, Schiller H. The MERIS Case 2 water algorithm. Int J Remote Sens 2007;28:517–35.

Doerffer R, Schiller H. MERIS Regional Coastal and Lake Case 2 Water Project Atmospheric Correction ATBD, vol. 1.0; 2008a. May.

Doerffer R, Schiller H. MERIS LakeWater Algorithm for BEAM ATBD, vol. 1.0; 2008b. May.

Eckmann R, Gerdeaux D, Müller R, Rösch R. Re-oligotrophication and whitefish fisheries management—a workshop summary. Adv Limnol 2007;60:353–60.

Finger D, Bossard P, Schmid M, Jaun L, Müller B, Steiner D, et al. Effects of alpine hydropower operations on primary production in a downstream lake. Aquat Sci 2007;69:240–56.

Friedrich U, Schallenberg M, Holliger C. Pelagic bacteria–particle interactions and community-specific growth rates in four lakes along a trophic gradient. Microb Ecol 1999;37:49–61.

Giardino C, Bresciani M, Villa P, Martinelli A. Application of remote sensing in water resource management: the case study of lake Trasimeno, Italy. Water Res Manage 2010;24:3885–99.

Giardino C, Pepe M, Brivio PA, Ghezzi P, Zilioli E. Detecting chlorophyll, Secchi disk depth and surface temperature in a Subalpine lake using Landsat imagery. Sci Total Environ 2001;268:19–29.

Gitelson AA, Schalles JF, Hladik CM. Remote chlorophyll-a retrieval in turbid, productive estuaries: Chesapeake bay case study. Remote Sens Environ 2007;109:464–72.

Gons HJ, Auer MT, Effler SW. MERIS satellite chlorophyll mapping oligotrophic eutrophic waters Laurentian Great Lakes. Remote Sens Environ 2008;112:4098–106.

Gons HJ, Rijkeboer M, Ruddick K. A chlorophyll-retrieval algorithm for satellite imagery (medium resolution imaging spectrometer) of inland and coastal waters. J Plankton Res 2002;24:947–51.

Gower J, King S. Validation of chlorophyll fluorescence derived from MERIS on the west coast of Canada. Int J Remote Sens 2007;28:625–35.

Guilizzoni P, Bonomi G, Galanti G, Ruggiu D. Relationship between sedimentary pigments and primary production: evidence from core analysis of 12 Italian lakes. Hydrobiologia 1983;103 130-106.

Jeppesen E, Jensen JP, Jensen C, Faafeng B, Hessen DO, Søndergaard M, et al. The impact of nutrient state and lake depth on top-down control in the pelagic zone of lakes: a study of 466 lakes from the temperate zone to the Arctic. Ecosystems 2003;6: 313–25.

Kaiblinger C, Anneville O, Tadonleke R, Rimet F, Druart JC, Guillard J, et al. Central European water quality indices applied to long-term data from peri-alpine lakes: test and possible improvements. Hydrobiologia 2009;633:67–74.

Koponen S, Kallio K, Pulliainen J, Vepsäläinen J, Pyhälahti T, Hallikainen M. Water quality classification of lakes using 250-m MODIS data MERIS data. IEEE Geosci Remote Sens 2004;1:287–91.

Kufel L. Uncoupling of chlorophyll and nutrients in lakes—possible reasons, expected consequences. Hydrobiologia 2001;443:59–67.

Lindell T, Pierson D, Premazzi G, Zilioli E. Manual for monitoring European lakes using remote sensing techniques. EUR Report n.18665 EN. Luxembourg: Office for Official Publications of the European Communities; 1999.

Manca M, Torretta B, Comoli P, Amsinck S, Jeppesen E. Major changes in trophic dynamics in large, deep sub-alpine Lake Maggiore from 1940 s to 2002: a high resolution comparative palaeo-neolimnological study. Freshwater Biol 2007;52: 2256–69.

Nõges P, Poikane S, Kõiv T, Nõges T. Effect of chlorophyll sampling design on water quality assessment in thermally stratified lakes. Hydrobiologia 2010;649:157–70.

Odermatt D, Giardino C, Heege T. Chlorophyll retrieval with MERIS Case-2 Regional in perialpine lakes. Remote Sens Environ 2010;114:607–17.

Personnic S, Domaizon I, Dorigo U, Berdjeb L, Jacquet S. Seasonal and spatial variability of virio-, bacterio- and picophytoplanktonic abundances in three peri-alpine lakes. Hydrobiologia 2009;627:99-116.

Peter A, Kösterc O, Schildknechtc A, von Gunten U. Occurrence of dissolved and particle-bound taste and odor compounds in Swiss lake waters. Water Res 2009;43:219-2200.

Premazzi G, Dal Miglio A, Cardoso AC, Chiaudani G. Lake management in Italy: the implications of the Water Framework Directive. Lakes Reservoirs Res Manage 2003;8:41–59.

Pugnetti A, Camatti E, Mangoni O, Morabito G, Oggioni A, Saggiomo V. The phytoplankton production in Italian freshwater and marine ecosystems: state of the art and perspectives. Chem Ecol 2006;22:49–69.

Ruggiu D, Morabito G, Panzani P, Pugnetti A. Trends and relations among basic phytoplankton characteristics in the course of the long-term oligotrophication of Lake Maggiore (Italy). Hydrobiologia 1998;369/370:243–57.

Salmaso N, Mosello R. Limnological research in the deep southern subalpine lakes:synthesis, directions and perspectives. Adv Oceanogr Limnol 2010;1:1-47.

Salmaso N, Morabito G, Garibaldi L, Mosello R. Trophic development of the deep lakes south of the Alps: a comparative analysis. Fund Appl Limnol 2007;170:177–96.

Salmaso N. Effects of climatic fluctuations and vertical mixing on the interannual trophic variability of Lake Garda, Italy. Limnol Oceanogr 2005;50:553–65.

Salmaso N. Long-term phytoplankton community changes in a deep subalpine lake: responses to nutrient availability and climatic fluctuations. Freshwater Biol 2010;55:825–46.

Salmaso N. Seasonal variation in the composition and rate of change of the phytoplankton community in a deep subalpine lake (Lake Garda, Northern Italy). An application of nonmetric multidimensional scaling and cluster analysis. Hydrobiologia 1996;337:49–68.

Salmaso N, Morabito G, Buzzi F, Garibaldi L, Simona M, Mosello R. Phytoplankton as an indicator of the water quality of the deep lakes south of the Alps. Hydrobiologia 2006;563:167–87.

Santer R, Schmechtig C. Adjacency effects on water surfaces: primary scattering approximation and sensitivity study. Appl Opt 2000;39:361–75.

Santer R, Zagolski F. ICOL—improve contrast between ocean & land ATBD. Wimereux, France: Université du Littoral; 2009. Version 1.1, 6 January.

Søndergaard M, Jeppesen E, Jensen JP, Amsinck SL. Water Framework Directive: ecological classification of Danish lakes. J Appl Ecol 2005;42:616–29.

Stich HB, Brinker A. Oligotrophication outweighs effects of global warming in large, deep, stratified lake ecosystems. Global Change Biol 2010;16:877–88.

Stramska M, Stramski D. Effects of non-uniform vertical profile of chlorophyll concentration on remote-sensing reflectance of the ocean. Appl Opt 2005;44: 1735–47.

Strömbeck N, Pierson D. The effects of variability in the inherent optical properties on estimations of chlorophyll a by remote sensing in Swedish freshwater. Sci Total Environ 2001;268:123–37.

Vollenweider RA, Kerekes J. The loading concept as a basis for controlling eutrophication philosophy and preliminary results of the OECD programme on eutrophication. Prog Water Res 1980;12:5-38.

Wolfram G, Argillier C, de Bortoli J, Buzzi F, Dalmiglio A, Dokulil MT, et al. Reference conditions and WFD compliant class boundaries for phytoplankton biomass and chlorophyll-a in Alpine lakes. Hydrobiologia 2009;633:45–58

5 REVIEW OF CONSTITUENT RETRIEVAL IN OPTICALLY DEEP AND COMPLEX WATERS FROM SATELLITE IMAGERY

This Chapter has been submitted for publication as: Odermatt, D., Gitelson, A., Brando, V. E. & Schaepman, M. E. (2011). Review of constituent retrieval in optically deep and complex waters from satellite imagery. Submitted to Remote Sensing of Environment, September 2011

Abstract

We provide a comprehensive overview of water constituent retrieval algorithms and underlying definitions and models for optically deep and complex (i.e. case 2) waters using earth observation data. Predominant progress of retrieval potential is assessed in the period from 2006 to May 2011. Band arithmetic and spectral inversion algorithms for waters of different eutrophic states are classified using a method based scheme that supports the interpretation of algorithm validity ranges. Based on these ranges we discuss groups of similar algorithms in view of their strengths and weaknesses. Particular emphasis is put on the retrieval of optical quantities within the algorithms. We conclude that substantial progress has been made in understanding and improving retrieval of constituents in optically deep and complex waters. Validation practices range from singular vicarious calibration experiments to comparisons using extensive in situ time series. The assessed methods indicate a parallel establishment of problem and water type specific algorithms rather than convergence towards universal, physically based solutions. Future intercomparison

efforts and benchmark exercises will further improve the comparability between and combination of algorithms in view of advanced retrieval capacities and uncertainties.

5.1 Introduction

Optically deep and complex waters are referred to as case 2 waters, as opposed to phytoplankton dominated case 1 waters of the open ocean (Morel and Prieur, 1977). The variety within case 2 waters is large, because the concentrations of chlorophyll (*CHL*), total suspended matter (*TSM*) and coloured dissolved organic matter concentrations (*CDOM*) are influenced by terrigenous discharge. Satellite sensors such as SeaWiFS, MODIS, and MERIS are currently being used to deliver ocean color data, attaining the requirements necessary for ocean biogeochemistry and climate research (Dierssen, 2010; McClain, 2009). Alas, universally applicable algorithms for the retrieval of water constituents from case 2 waters are not known (IOCCG, 2006, 2009). Specific algorithms are thus optimized and validated for commonly understood but ill-defined water types, e.g. turbid (Gitelson et al., 2007) or clear water (Belzile et al., 2004). Other authors address trophic classes (Cheng Feng et al., 2009; Dekker and Peters, 1993; Iluz et al., 2003), for which several diverging definitions exist (Bukata et al., 1995; Carlson and Simpson, 1996; Chapra and Dobson, 1981; Nürnberg, 1996; Wetzel, 1983). Trophic thresholds vary however with ecosystem specific limitations to primary productivity, while the validity of remote sensing algorithms is determined only by the variability in optical properties.

Carder et al. (1999) and Morel and Gordon (1980) distinguish empirical and analytical methods for water constituent retrieval, and in-betweens with the epithet “semi-“. Empirical algorithms are derived by statistical regression (Kabbara et al., 2008; Mahasandana et al., 2009) or endmember selection (Tyler et al., 2006), which implies effective data optimization but limited transferability (Austin and Petzold, 1981). Analytical algorithms apply quantitative physical relationships. This usually requires approximations or calibration with empirical coefficients (Carder et al., 1999), while statistical regression often leads to solutions that coincide with properties known from physical models (e.g. normalizing band ratios (Gitelson, 1992)), explaining the epithet “semi-” from either side. Either type of algorithm is usually applied as a band arithme-

tic solution for one constituent at a time, although empirical solutions can also be found by other approaches (Gonzalez Vilas et al., 2011; Tyler et al., 2006).

In contrast, spectral inversion procedures match spectral measurements with bio-optical forward models by means of inversion techniques. The spectral inherent optical properties (IOPs, (Preisendorfer, 1961)) of all three constituents are thereby retrieved at once from one spectral apparent property (AOP). Several inversion techniques are applied for this procedure, whereby the investigated AOP is matched with simulated AOPs from bio-optical forward models, i.e. either analytical relationships (Albert and Mobley, 2003; Gordon et al., 1975; Lee et al., 2002; Maritorena et al., 2002; Park and Ruddick, 2005) or numerical radiative transfer models (Bulgarelli et al., 1999; Jin and Stamnes, 1994; Mobley, 1989; Zhai et al., 2010).

We discuss in this paper recent studies reporting water constituent retrieval in case 2 waters from satellite imagery using band ratio or spectral inversion algorithms as well as matchup validation campaigns, using an approach by comprehensively reviewing the literature from 2006 to May 2011. Hence accuracy assessments for band ratio or spectral inversion algorithms based only on in situ measurements, e.g. Kostadinov et al. (2007)), Moore et al. (2009) or Shanmugam (2010) or simulated datasets, e.g. Qin et al. (2007), will not be discussed.

We group the paper in 7 sections, where the relevance of IOPs and AOPs in models and algorithms are discussed first, followed by a description of band arithmetic and spectral inversion algorithms. Recent validation experiments for either approach are then summarized and quantitatively analyzed for their range of applicability.

5.2 Relevance of IOPs in models and algorithms

Regarding IOPs, the volume scattering function $\beta(\psi)$ is the elementary property for the integration of the scattering and backscattering coefficients b and b_b, respectively, over scattering angle ψ. Measurements of $\beta(\psi)$ (Chami et al., 2006; Freda et al., 2007; Freda and Piskozub, 2007; Lee and Lewis, 2003; Petzold, 1972; Sokolov et al., 2010; Sullivan and Twardowski, 2009) are normalized to the scattering phase function $\tilde{\beta}(\psi)$. Several models of $\tilde{\beta}(\psi)$ have been proposed to approximate these measurements (Fournier and Forand, 1994; Fournier and Jonasz, 1999; Haltrin, 2002; Mobley et al., 1993). Their ef-

fect on calculated reflectance quantities is up to 20% (Chami et al., 2006; Gordon, 1993; Mobley et al., 2002; Morel et al., 2002; Morel and Gentili, 1996). The ratio of molecular to total scattering, η, is a major proxy for the shape of $\beta(\psi)$, since molecular $\tilde{\beta}_W$ is less anisotropic than particulate $\tilde{\beta}_{TSM}$ (Morel, 1974; Smith and Baker, 1981).

The absorption coefficient a in contrast is omnidirectional, but influences the intensity and anisotropy of reflectance through the single scattering albedo ω_0 (Gordon and Brown, 1973; Gordon et al., 1975; Morel and Prieur, 1977) and the number of subsequent scattering events of a photon before reaching the interface, N (Loisel and Morel, 2001; Morel et al., 2002), respectively. An alternative term for the former is the single backscattering albedo ω_b. The latter indicates the blurring of $\beta(\psi)$ in turbid water (Pfeiffer and Chapman, 2008; Piskozub and McKee, 2011; Sydor, 2007).

The ability to account for variations in these IOPs is limited for band arithmetic algorithms, while increasingly addressed by spectral inversion algorithms for radiative transfer simulations (Doerffer and Schiller, 2007; Schroeder et al., 2007b; Van Der Woerd and Pasterkamp, 2008) or specific semi-analytical models (Albert and Mobley, 2003; Park and Ruddick, 2005).

5.3 Relevance of AOPs in models and algorithms

The first widely used AOP is the bihemispherical irradiance reflectance R^-, which is related to ω_b in the earliest semi-analytical models for case 2 water by means of the linear coefficient f (Gordon et al., 1975; Morel and Prieur, 1977), which again varies with illumination zenith angle θ_s^+ (Gordon, 1989; Kirk, 1991; Sathyendranath and Platt, 1997).

Subsequent experiments for case 1 (Morel and Gentili, 1991, 1993) and case 2 (Loisel and Morel, 2001) waters focus on anisotropy of the underwater light field, described by η, N and the anisotropy factor Q that relates diffuse upwelling irradiance E_u^- to directional upwelling radiance L_u^-. It is found that the directional variations in f and Q partly compensate each other, leaving the subsurface remote sensing reflectance R_{rs}^- less sensitive to anisotropy effects than R^- (Morel and Gentili, 1993). Accordingly, semi-analytical models that relate ω_b directly to R_{rs}^- by means of quadratic coefficients became more popular (Gordon et al., 1988; Lee et al., 1998).

Correction for air-water interface and normalization of the resulting R_{rs}^{+} to zenith illumination and viewing geometry will then result in the normalized water-leaving reflectance $[R_w]_N$ (Gordon et al., 1988; Gordon and Clark, 1981). The calculation of $[R_w]_N$ from at-sensor radiances as well as estimation of the coefficients in semi-analytical models require knowledge of atmospheric and aquatic parameters, which have to be retrieved through iterative procedures (Gordon and Franz, 2008; Morel and Gentili, 1996). Since such procedures are more computationally expensive for case 2 than for case 1 waters (Kuchinke et al., 2009a), approximations find wide use in both cases, compromising the potential improvement due to such normalizations.

5.4 Band arithmetic algorithms

CHL retrieval band arithmetic algorithms make use of the pigment's primary and secondary absorption maxima at 442 nm and 665 nm, respectively (Bricaud et al., 1995), a reflectance peak around 700 nm due to the minimum sum of absorption of phytoplankton and water (Gitelson, 1992; Vasilkov and Kopelevich, 1982; Vos et al., 1986) and its fluorescence emission band at 681 nm (Gower et al., 1999).

The primary feature is superimposed by *CDOM* absorption (Bricaud et al., 1981), and therefore widely used in case 1 waters, where *CDOM* and *CHL* correlate by definition (Morel and Prieur, 1977). Sensor specific standard algorithms for primary *CHL* absorption bands exist for all medium resolution ocean colour spectrometers (Aiken et al., 1995; Clark, 1997; Morel and Antoine, 2007; Murakami et al., 2006; O'Reilly et al., 1998). They are referred to as OC2, OC3 and OC4 depending on the number of bands used.

Using the secondary feature is promoted by weak variations in the spectral properties of all other parameters apart from the increasing absorption by water (Dall'Olmo et al., 2003; Gitelson, 1992; Schalles et al., 1998). Its major limitation is the absence of the feature in oligotrophic and some mesotrophic lakes (Guanter et al., 2010).

Fluorescence line height (FLH) and maximum chlorophyll index (MCI) algorithms are linear baseline algorithms for <30 mg/m^3 and >100 mg/m^3 *CHL* ranges (Gower et al., 2005). They can be applied either with or without atmospheric correction (Binding et al., 2011; Matthews et al., 2010).

TSM and corresponding particle scattering is best quantified outside the *CHL* or *CDOM* features (Binding et al., 2010). Regression with a single band is possible if an accurate, possibly NIR L_w coupled atmospheric correction is applied (Stumpf et al., 2003). Multi band algorithms are however also used on uncorrected at-sensor radiances (Koponen et al., 2007). The choice of spectral bands is in theory a matter of concentrations ranges, whereas appropriate wavelengths increase with turbidity (Wang and Lu, 2010). The increase in absorption of pure water towards the NIR will namely require increasing *TSM* to ensure a sufficient reflectance signal (Ruddick et al., 2006), while less absorbing portions of the spectrum are more suitable for low concentrations. Empirical regression of in situ *TSM* with all eligible bands of a spectroradiometric measurement is a simple way to test this hypothesis (Nechad et al., 2010), and provides the flexibility to derive suitable algorithms even for Landsat TM instruments (Wang et al., 2009; Zhou et al., 2006).

CDOM retrieval methods are restricted to short visible wavelengths, where absorption of *CDOM* and *CHL* coincide (Babin et al., 2003; Ferreira et al., 2009) and inaccuracies due to NIR derived atmospheric correction are largest (Hu et al., 2000). Accordingly, most band arithmetic approaches relate *CDOM* to a ratio of sensitive bands at <600 nm and normalization bands at >600 nm (Kallio et al., 2001). The choice of suitable sensors is smaller than for the estimation of *CHL* and *TSM*, due to insufficient radiometric accuracy of Hyperion (Giardino et al., 2007) and Landsat Thematic Mapper (Kutser et al., 2005b) in the short wave domain of the spectrum.

5.5 Spectral inversion algorithms

The constitution of spectral inversion algorithms is more heterogeneous than band arithmetic algorithms, with differences in water, interface, atmospheric models and inversion techniques. Table 5-1 contains a list of recent studies reporting validation results for spectral inversion algorithms in case 2 waters. NN inversion techniques are dominant, probably due to their improved availability as MERIS level 2 products (Doerffer and Schiller, 2007) and by BEAM plug-ins (Doerffer and Schiller, 2008a; Schroeder et al., 2007b). Other inversion techniques are matrix inversion (Brando and Dekker, 2003), downhill simplex (Heege and Fischer, 2004), least-squares (Santini et al., 2010), spectral optimization (Kuchinke et al., 2009a) and Levenberg-Marquardt optimization (Van Der Woerd and Pasterkamp, 2008). Only one application of the SeaDAS

semi-analytical algorithms (Carder et al., 1999; Lee et al., 2002; Maritorena et al., 2002) is listed in Table 5-1. This is however to a large extent due to their focus on retrieving IOPs rather than constituent concentrations.

Most algorithms are used together with specific atmospheric correction modules. The use of standard level 2 reflectance products is only foreseen for two algorithms (Schuchman et al., 2005; Van Der Woerd and Pasterkamp, 2008). The inversion modules match atmospherically corrected R_{rs}^{+} or R^{-} with Hydrolight simulated data (Brando and Dekker, 2003; Doerffer and Schiller, 2007, 2008a; Santini et al., 2010; Van Der Woerd and Pasterkamp, 2008), other numerical (Jerome et al., 1996; Pozdnyakov et al., 2005) or semi-analytical (Heege and Fischer, 2004; Kuchinke et al., 2009a) simulations. Findings from the validation experiments in Table 5-1 are discussed later.

Table 5-1: List of matchup validation experiments with spectral inversion processed spaceborne data. Concentration thresholds in bold letters indicate successful quantitative validation, italic letters indicate successful quantitative falsification, and regular letters indicate missing validation. Expected minimum R^2 for validation is 0.4 (CHL, CDOM, tripton) and 0.6 (TSM). Asterisks (*) indicate retrieval of tripton instead of TSM; circles (°) indicate retrieval of inorganic suspended matter instead of TSM; plus signs ($^{+}$) indicate "dissolved organics" [mgC/l] instead of CDOM; carets ($\hat{}$) indicate "colored detrital matter" [m^{-1}] instead of CDOM. Concentrations in absorption units are given at 400 nm and, if originally given in another wavelength, converted according to Smith and Baker (1981) with explicitly given spectral exponents (Matthews et al., 2010; Santini et al., 2010) or an approximate 0.017 spectral exponent where not specified (Binding et al., 2011; Giardino et al., 2010; Schroeder et al., 2007b; Van Der Woerd and Pasterkamp, 2008). Algorithm references: [1]Doerffer and Schiller (2007), Moore et al. (1999); [2]Doerffer and Schiller (2008a, b); [3]Schroeder et al. (2007a; 2007b); [4]Pozdnyakov et al. (2005); [5]Brando and Dekker (2003); [6]Heege and Fischer (2004). Strict and relaxed matchups chosen from Cui et al. (2010), Kuchinke et al. (2009b) is omitted due to a lack of absolute in situ concentration values.

Experiment	**Algorithm**	***CHL* [mg/m³]**		***TSM* [g/m³]**		***CDOM* [m⁻¹]**	
		max	**min**	**max**	**min**	**max**	**min**
Binding et al. (2011)	NN algal_2[1]	*70.5*	*1.9*	19.6	0.8	7.1	0.5
Cui et al. (2010)	NN algal_2[1]	**16.1**	**0.7**	*67.8*	*1.5*	2.0	0.7
Minghelli-Roman et al. (2011)	NN algal_2[1]	**9.0**	**0.0**	-	-	-	-
Binding et al. (2011)	NN C2R[2]	*70.5*	*1.9*	19.6	0.8	7.1	0.5
Giardino et al. (2010)	NN C2R[2]	*74.5*	*11.67*	-	-	4.0	1.3
Matthews et al. (2010)	NN C2R[2]	*247.4*	*69.2*	*60.7*	*30.0*	*7.1*	*3.4*
Odermatt et al. (2010)	NN C2R[2]	**9.0**	**0.0**	-	-	-	-
Schroeder et al. (2007b)	NN FUB[3]	**12.6**	**0.1**	**14.3**	**2.7**	**2.0**	**0.8**
Shuchman et al. (2006)	Coupled NN[4]	*2.5*	*0.1*	*2.7°*	*1.3°*	3.5^{+}	0.0^{+}
Giardino et al. (2007)	c-Wombat-c[5]	**2.2**	**1.3**	**2.1***	**0.9***	-	-
Odermatt et al. (2008)	MIP[6]	*4.0*	*0.6*	-	-	-	-
Santini et al. (2010)	2 step inversion	5.0	1.8	13.0*	3.0*	0.8	0.1
Van der Woerd and Pasterkamp (2008)	Hydropt	20.0	0.0	30.0	0.0	1.6	0.0

5.6 Validation experiments

Recent ISI journals (2006-2011) comprise about 50 published papers reporting water constituent retrieval from satellite imagery for optically deep and complex waters, among which about three quarter apply band arithmetic algorithms. Applied selection criteria are the availability of coinciding validation data, concentration ranges and statistical quality measures, namely R^2.

5.6.1 Chlorophyll-a retrieval

All recent band arithmetic *CHL* retrieval applications are depicted in Figure 5-1, with corresponding sensors and concentration ranges. The three previously described major groups are distinguished; green/blue ratios defined for OC algorithms, red-NIR band ratios and further empirical algorithms.

The OC2-OC4 algorithms are successfully applied to retrieve 0-10 mg/m^3 *CHL* in optically complex water, although theoretically configured for Open Ocean. From top to bottom in Figure 5-1, study areas are Lake Erie (OC2 and OC4), the Mississippi Delta (OC2), Lake Tanganyika (OC3) and the Northern Adriatic Sea (OC3 and OC4), and a lagoon in New Caledonia (OC4). Several of these examples indicate that the observed water optical properties resemble those in case 1 water to some extent. Mélin et al. (2007) mention that two thirds of their observations refer to case 1 water, and Horion et al. (2010) assume explicitly that even Lake Tanganyika is case 1. The data by D'Sa et al. (2006) follow a shifted but correlated mixture of constituents as found for case 1 water (Morel and Maritorena, 2001), which can be accounted for by regional adjustment as done by Witter et al. (2009). Dupouy et al. (2010) present a turbidity index for the preselection of applicable data points. Atmospheric correction algorithms provide R_{rs}^{+} and $[R_w]_N$ output for application of the OC algorithms (Gordon and Voss, 2004; Gordon and Wang, 1994; Siegel et al., 2000; Stumpf et al., 2003; Toratani et al., 2007). Further OC applications to optically complex waters lack quantitative matchup validation (Gons et al., 2008; Wang et al., 2011; Werdell et al., 2009).

2 and 3 band NIR-red algorithms are validated using MERIS data for up to 250 mg/m^3 *CHL* in Zeekoevlei (Matthews et al., 2010), and suitable for the 10-100 mg/m^3 interval represented by the Dnieper River, the Sea of Azov, the Gulf of Finland, Lake Dianchi and Kasumigaura, as in vertical order in Figure 5-1. <10

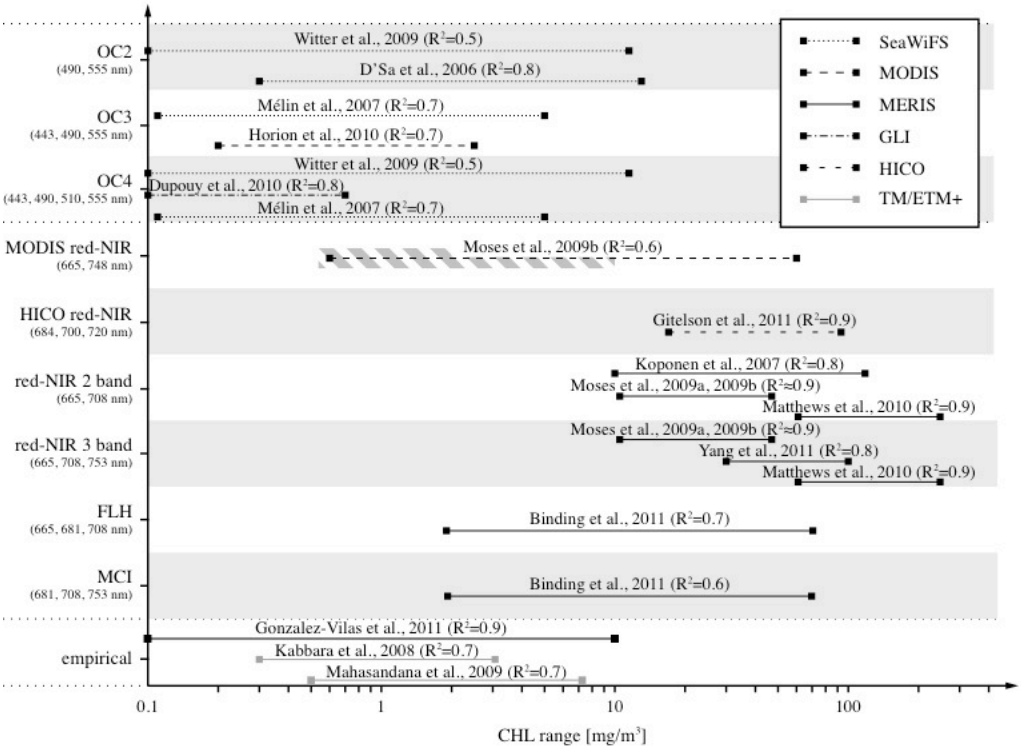

Figure 5-1: Overview of recently (2006-2011) published ISI journal papers on the separate retrieval of chl-a from satellite imagery using matchup-validated semi-analytical and empirical algorithms. Hatched areas indicate disputed application ranges. The red-NIR 3 band application by Chen et al. (2011) is omitted since the variation range retrieved from Hyperion (21-27 mg/m³; R^2=0.6) is too small to display.

mg/m³ *CHL* is only observed in Moses et al. (2009a; 2009b). Their calibration data and RMSEs, as well as previous simulations (Dall'Olmo and Gitelson, 2006) indicate a minimum applicability threshold at 10 mg/m³ *CHL*. Although lower *CHL* is successfully retrieved from field spectroscopy measurements (Gitelson et al., 2009). Enhancement of NIR-red algorithms by *CDOM* and tripton derived coefficients from a look-up-table may even extend the applicable range, but are only validated for waters with high *CHL* (Yang et al., 2011). Advantages in the use of either 2 or 3 bands are inconsistent (Moses et al., 2009a; Moses et al., 2009b). Larger differences in accuracy occur through different atmospheric correction methods. The MERIS bright pixel procedure (Moore et al., 1999) performs considerably better than the C2R atmosphere module (Doerffer and Schiller, 2008b) in Moses et al. (2009b). Other proce-

dures are SCAPE-M (Guanter et al., 2010) for MERIS (Yang et al., 2011) and FLAASH (Cooley et al., 2002) for Hyperion (Chen et al., 2011), which imply the use of either R_{rs}^{+} or R^{-} for *CHL* retrieval. Matthews et al. (2010) demonstrate that NIR-red algorithms can even be used with uncorrected data at the top of atmosphere (TOA). The same applies to MCI, which outperforms FLH, the MERIS Algal_2 and C2R algorithms at the remote measurement of an algae bloom event in the Lake of the Woods (Binding et al., 2011). Accuracy restrictions for low *CHL* are however similar as for the 2 and 3 band NIR-red algorithms as far as RMSE (5.7 and 7.3 mg/m^3 for MCI and FLH, respectively) is concerned. FLH was also found inapplicable to oligotrophic water in the Laurentian Lakes, raising concerns over the fluorescence signal to noise ratio under unfavourable atmospheric conditions (Gons et al., 2008).

The empirical studies by Kabbara et al. (2008) and Mahasandana et al. (2009) consist of regression models for Landsat-7 ETM+ and Landsat-5 TM. They prove the feasibility of *CHL* estimation with high-resolution sensors, but need parameterization for each single image. In contrast, Gonzalez Vilas et al. (2011) train NNs for preclassified MERIS observations and in situ measured concentrations without the application of an explicit bio-optical model. Their approach achieves high accuracy and temporal stability at the expense of regional restriction.

The types of sensors used in the present experiments correlate clearly with the choice of applications; SeaWiFS and MODIS for the OC algorithms and low *CHL* concentrations, MERIS for the retrieval of high *CHL* by means of red-NIR band ratios and Landsat for empirical algorithms. The advantage of MERIS' 681 nm and 708 nm bands over comparable instruments that lack these bands is known (Gitelson et al., 2008; Gower et al., 1999), and demonstrated for MODIS by Moses et al. (2009a). Optimal band positions for a 3 band red-NIR algorithm are spectrometrically derived from limited set of HICO data (Gitelson et al., 2011).The SeaDAS toolbox for SeaWiFS and MODIS is probably an asset regarding the evaluation of different atmospheric corrections (Hu et al., 2000; Ruddick et al., 2000; Stumpf et al., 2003; Vidot and Santer, 2005; Wang, 2007). The feasibility of $[R_w]_N$ normalization may be an additional benefit regarding the removal of directional effects.

5.6.2 Suspended sediment retrieval

Recent *TSM* retrieval validation experiments are listed in Figure 5-2, for increasing central wavelengths of chosen sensors and bands in vertical direction. The convergence in frequently applied methods is not as evident as among the *CHL* algorithms in Figure 5-1. The advantage of semi-analytical over empirical algorithms is a matter of adaptivity and justification rather than accuracy. Application of semi-analytical algorithms implies a physically sound procedure with defined R_{rs}^{+} from atmospheric correction procedures as mentioned for *CHL* (Moore et al., 1999; Ruddick et al., 2000; Stumpf et al., 2003). Their configuration allows adjustment to other sensors or bands (Van der Woerd and Pasterkamp, 2004), and comparison of atmospheric corrections (Matthews et al., 2010) or reflectance models (Nechad et al., 2010). In contrast, empirical algorithms apart from Petus et al. (2010) and Mélin et al. (2007) are applied to uncorrected at-sensor radiances (Koponen et al., 2007) and physically undefined reflectance quantities (Chen et al., 2009; Wang et al., 2009), leaving them unjustified for applications beyond the data they are derived for. However, empirical algorithms are advantageous for evaluation experiments as with the validation of *TSM* from geostationary MSG-SEVIRI data by means of MODIS *TSM* (Neukermans et al., 2009).

An increase in spectral band position with observed *TSM* concentration range is found in Figure 5-2 as well as in several discussions (Fettweis et al., 2011; Wang and Lu, 2010; Zhang et al., 2010). Maximum sensitivity thresholds are estimated at 30 g/m^3 g/m^3 for SeaWiFS' 555 nm band (Eleveld et al., 2008) or around 150-200 g/m^3 for bands at <650 nm (Fettweis et al., 2011; Wang and Lu, 2010). Only one recent quantitative validation experiment investigates such extreme turbidity, accordingly at 860 nm (Wang et al., 2009). In less turbid water, the accuracy variations for 8 MERIS bands between 620 and 885 nm is only R^2=0.89 to 0.93, and lower in absolute values but similar in variation for MODIS (Nechad et al., 2010). Multi band algorithms are recommended for low *TSM* concentrations due to the increasing superimposition by other constituents' optical properties (Nechad et al., 2010). In this regard, Nechad et al. (2010) suggest a 1 g/m^3 minimum threshold for single band algorithms, while Binding et al. (2010) mention that their RMSE increases to 47% of mean concentrations below 5 g/m^3. Matchups of clear, to two thirds case 2 water off the Adriatic coast confirms the challenges in retrieval of low *TSM*, with a relatively low R^2 (Mélin et al., 2007).

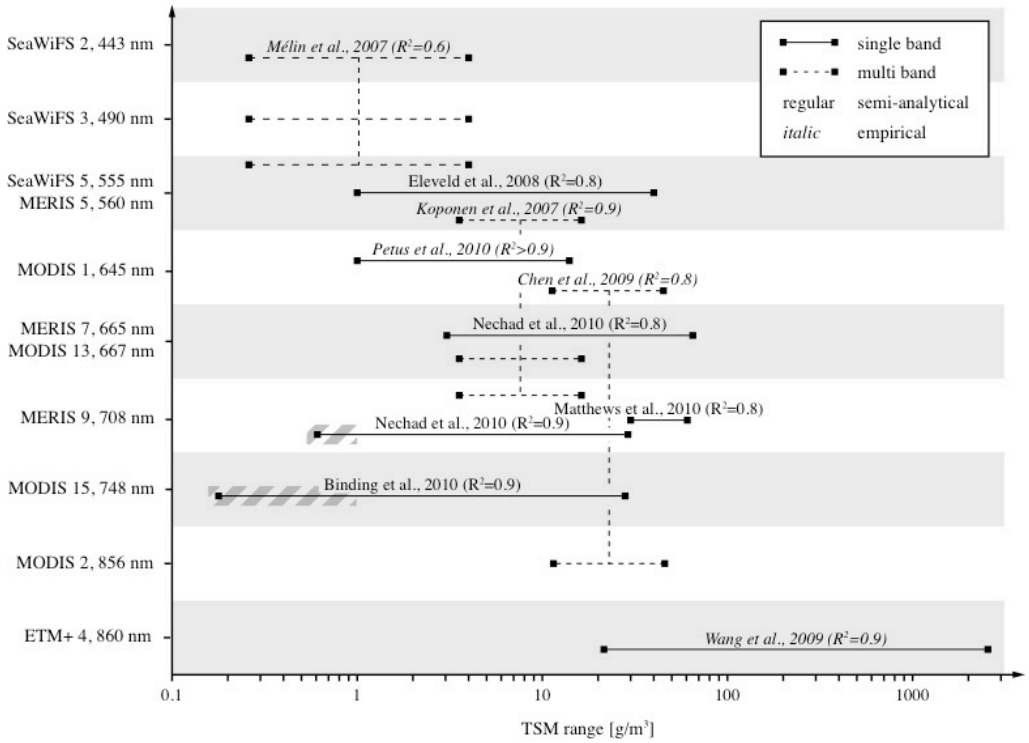

Figure 5-2: Overview of recently (2006-2011) published ISI journal papers on the separate retrieval of TSM from satellite imagery by means of matchup-validated semi-analytical and empirical algorithms. Hatched areas indicate disputed application ranges. The retrieval of tripton from MERIS band 10 (754 nm) at R^2=0.3 was omitted (Yang et al., 2011).

5.6.3 Dissolved organic matter retrieval

All *CDOM* retrieval band arithmetic algorithms in Figure 5-3 are from empirical regression (D'Sa and Miller, 2003; Gitelson et al., 1993; Kallio et al., 2001; Kowalczuk et al., 2005), in the case of Yang et al. (2011) by means of bio-optical simulations (Ammenberg et al., 2002). The examples indicate that single band approaches and bands at less than 490 nm are only applicable to extremely high concentrations and correspondingly strong *CDOM* absorption variations as in Zeekoevlei (Matthews et al., 2010). The two best correlations are calculated for band ratios that apply a 442-490 nm band that is sensitive to both *CHL* and *CDOM* variations, and the *CHL*-sensitive 665 nm band of MERIS for normalization (Koponen et al., 2007; Matthews et al., 2010). In

both cases no atmospheric correction is applied, although *CDOM* in the Gulf of Finland is already much less abundant than in Zeekovlei.

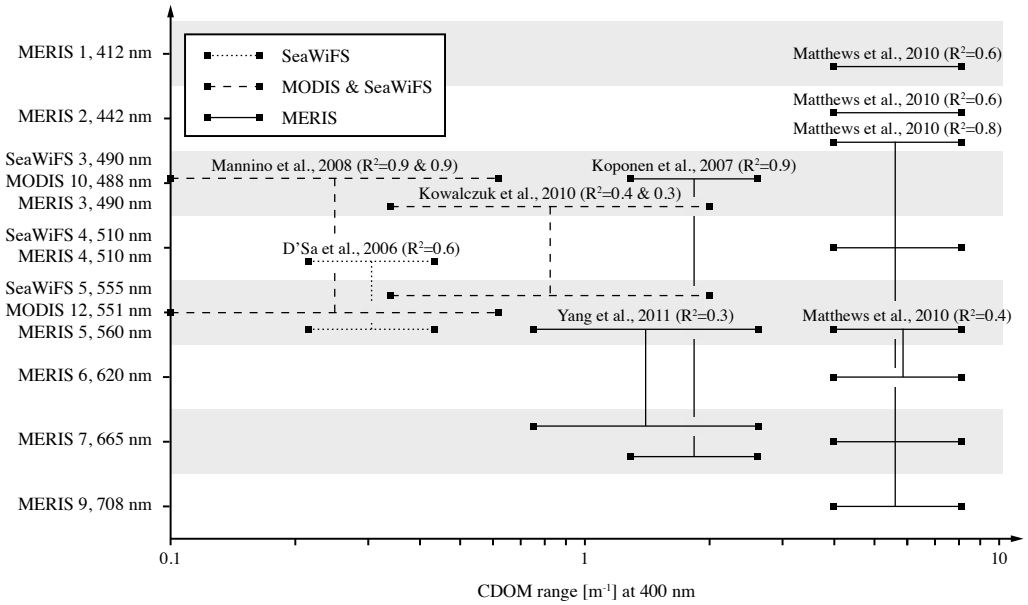

Figure 5-3: Overview of recently (2006-2011) published ISI journal papers on the separate retrieval of CDOM from satellite imagery by means of matchup-validated, arithmetic algorithms. Where necessary, normalization to 400 nm is done with explicitly mentioned spectral exponents (Smith and Baker, 1981), i.e. 0.0157 (Yang et al., 2011), 0.0161 (D'Sa et al., 2006) and 0.0188 (Matthews et al., 2010), or an approximate average of 0.0215 (Mannino et al., 2008).

Ammenberg et al. (2002) uses the 665 nm band to normalize the 560 nm band rather than the 442-490 nm bands, whereas both the interference with *CHL* absorption and the *CDOM* signal are considerably weaker at 560 nm. The correlation of this ratio with intermediate *CDOM* in Lake Dianchi and Lake Kasumigaura remains however relatively low, in spite of the application of a look-up-table retrieved parameterization (Yang et al., 2011). A recent validation exercise with ALI bands 2 and 3 at similar spectral positions is only qualitative and thus not included in Figure 5-3 (Kutser et al., 2009). Earlier studies have however demonstrated the potential of this band combination for mapping *CDOM* in inland waters even at high spatial resolution (Kutser et al., 2005a; Kutser et al., 2005b).

The SeaWiFS and MODIS bands ratios recommended by Kowalczuk et al. (2005) and D'Sa and Miller (2003) omit the red-NIR part of the spectrum as previously found for the band arithmetic retrieval of *CHL* with these two instruments. The former was validated with data of the Baltic Sea from both SeaWiFS and MODIS (the latter not shown in Figure 5-3, R^2=0.3) and outperforms the *CDOM* output from SeaDAS semi-analytical algorithms (Carder et al., 1999; Garver and Siegel, 1997; Maritorena et al., 2002) in all cases (Kowalczuk et al., 2010). A SeaWiFS validation in the Mississippi estuary achieves an even higher correlation at lower concentrations (D'Sa et al., 2006). The two validation exercises are also the seasonally most representative ones given that data matchups from several years and seasons are analyzed.

5.6.4 Spectral inversion applications

13 or a quarter of the selected publications in 2006-2011 ISI journals refer to spectral inversion algorithms (Table 5-1), with several papers on new algorithms where validation is only a subchapter (Santini et al., 2010; Schroeder et al., 2007b; Van Der Woerd and Pasterkamp, 2008). The quantitative content is often less detailed than with band arithmetic algorithms, hindering an estimate of their applicability as shown in Table 5-1.

The MERIS algal_2 product (Doerffer and Schiller, 2007) and *CHL* from C2R and its boreal and eutrophic version (Doerffer and Schiller, 2008a; Koponen et al., 2008) have been applied in several experiments. C2R is successfully validated for low to intermediate concentrations (<16 mg/m^3) (Cui et al., 2010; Minghelli-Roman et al., 2011; Odermatt et al., 2010), while C2R and even its eutrophic water version are found unsuitable for high *CHL* concentrations (Binding et al., 2011; Giardino et al., 2010; Matthews et al., 2010). C2R's *CDOM* is found adequate in a eutrophic lagoon in the Baltic Sea, where concurrent *CHL* is strongly underestimated (Giardino et al., 2010). In contrast, *CDOM* in oligotropic perialpine and Finish lakes is underestimated by both C2R and its boreal version while *CHL* is adequate (Koponen et al., 2008; Odermatt et al., 2010). C2R's atmospheric correction failed at retrieving the red-NIR reflectance peak in several examples, while it outperforms other procedures with its accuracy at blue and green wavelengths (Giardino et al., 2010; Odermatt et al., 2010; Odermatt et al., 2008). *TSM* retrieved by the two NN is inapplicable to turbid water (Cui et al., 2010; Matthews et al., 2010), but accurate at about <15-30 g/m^3 (Koponen et al., 2008).

Validation of the FUB MERIS NN algorithm is successful and thorough at low to intermediate concentrations of all constituents over a wide spatiotemporal range (Schroeder, 2005; Schroeder et al., 2007b). Even lower constituent concentrations are successfully retrieved from a single Hyperion image by means of matrix inversion (Giardino et al., 2007). All other applications do not meet the requirements for quantitative matchup validation. Ground truth comparisons are limited to spectral fits (Van Der Woerd and Pasterkamp, 2008), frequency distribution (Kuchinke et al., 2009b) and transect comparisons (Santini et al., 2010), or display occasional failure that prevent sufficient correlations (Odermatt et al., 2008; Shuchman et al., 2006).

5.7 Discussion

The assessed quantitative validation experiments using band arithmetic algorithms consist of comparisons of several methods where in situ data are acquired for exactly this validation purpose. They are numerous enough to synthesize several general conclusions based on individual findings and validation sites, e.g. the validity range for red-NIR *CHL* algorithms, the suitability of OC algorithms for low and intermediate *CHL*, the choice of *TSM* retrieval wavelengths according to expected concentrations ranges or the *CHL* variation normalization strategies in *CDOM* retrieval algorithms.

A sufficient number of studies with spectral inversion algorithms are only available for the MERIS NN algorithms. Only the algorithm by Schroeder et al. (2007b) has been successfully validated using matchup correlations of all three constituents over several image acquisitions and aquatic regions as given for many band arithmetic algorithms. We presume two main reasons for this difference, namely availability and complexity. The importance of the availability of algorithms is well represented by the frequent use of retrieval algorithms and corresponding atmospheric correction procedures in SeaDAS and BEAM. They lead to the use of OC algorithms, such as the most popular *CHL* retrieval methods based on SeaWiFS and MODIS data, while NN algorithms are evaluated in most experiments using MERIS data. The opposite cases are rare, although not hindered by sensor or data properties. Consequently, the (semi-)operational use of spectral inversion algorithms is mainly limited to their promoters unless other potential users find easier available methods unsuitable, which may again indicate challenging bio-optical conditions, complicating validation.

Crucial sensor and data properties are the red-NIR wavebands as used in MERIS, the spatial resolution of Landsat and ALI instruments and the temporal resolution of MSG-SEVIRI. In the first case, the red-NIR *CHL* retrieval experiments with MERIS outnumber and outperform corresponding experiments for most other sensors, rendering MERIS the preferred instrument for estimating *CHL* in meso- to eutrophic waters. In the case of MSG-SEVIRI, TM, ETM+ and ALI, radiometric accuracy, bandwidths and a lack of appropriate preprocessing tools complicate routine use, as established with dedicated ocean color instruments. However, experimental evidence is given that either of those instruments can be used for case 2 water constituent retrieval under certain circumstances. Simpler methods are however mostly empirical, providing rapid access to data and their correlations, but at the cost of being site specific and not expressing any cause-effect relationship.

On the opposite side, complexity in constitution, application and validation of spectral inversion procedures is clearly highest. They retrieve several aquatic and possibly atmospheric parameters from a larger number of spectral bands. Failure at any point in the procedure, i.e. the assumption of an inappropriate shape in *CDOM* absorption, may propagate errors in the estimates of other parameters, complicating a coherent validation or falsification. Band arithmetic algorithms on the contrary make use of known relationships between one aquatic parameter and 1-3 spectral bands that are sensitive to an optical property of the sought-after parameter or allow the normalization of other variations. The validation or falsification of such relationships is straightforward and reveals a good estimate of an algorithm's validity range.

For a comparison of the known validity ranges for band arithmetic algorithms (Figure 5-1 to Figure 5-3), we apply a scheme that helps to further categorize applications for case 2 waters. Natural variations in each constituent are separated in a low, intermediate and high range. Low *CHL* is referred to as oligotrophic, and ranges up to 3 mg/m^3, the integer average from ecological classification schemes (Bukata et al., 1995; Carlson and Simpson, 1996; Chapra and Dobson, 1981; Nürnberg, 1996; Wetzel, 1983). Previous definitions of the second threshold between mesotrophic and eutrophic waters differ from 5.6 to 20 mg/m^3 and are supplemented with a hypereutrophic water in some schemes (Table 5-2). According to these sources and Figure 5-1 we set the threshold to 10 mg/m^3, which approximately limits the applicability of OC and red-NIR algorithms at the top and bottom of their concentration range, respectively. *TSM* thresholds are set at 3 and 30 g/m^3 due to the experimental ranges in Figure

5-2, corresponding water types are referred to as clear, cloudy or turbid. An analogous portioning is carried out for *CDOM* according to Figure 5-3, allowing the assignment of all collected validation experiments to one or several variation spaces with regard to independent variations in the other two constituents as in Figure 5-4 (e.g. *TSM* retrieval in clear and cloudy water at given *CHL* and *CDOM* (Binding et al., 2010)).

Table 5-2: Trophic levels for coastal and inland waters and corresponding CHL [mg/m^3].

Author	Oligotrophic	Mesotrophic	Eutrophic	Hypereutr.
Chapra and Dobson (1981)	0-2.9	2.9-5.6	>5.6	n.a.
Wetzel (1983)	0.3-4.5	3-11	3-78	n.a.
Bukata (1995)	0.8-2.5	2.5-6	6-18	>18
Carlson and Simpson (1996)	0-2.6	2.6-20	20-56	>56
Nürnberg (1996)	0-3.5	3.5-9	9-25	>25

Published validation experiments as used in Figure 5-1 to Figure 5-3 are depicted in Figure 5-4 if variation ranges of all three constituents are given, even if only individual constituents are retrieved. Only two spectral inversion experiments from Table 5-1 can be positioned. Schroeder et al. (2007b) present proof of the successful simultaneous retrieval of all parameters, while only *CHL* is retrieved accurately in Cui et al. (2010), but variations in *TSM* and *CDOM* are also given. The *CHL* retrieval column in Figure 5-4 shows the suitability of red-NIR algorithms for eutrophic water, and the potential of OC algorithms for oligo- to mesotrophic waters at relatively low *TSM* and *CDOM* variations. Several different algorithms retrieve *TSM* accurately, but the relationship between sensitive wavelength and concentration range (Figure 5-2) is no more visible. Relatively few experiments are assigned to turbid water, probably because measuring in situ *TSM* is much less of an effort than additional *CHL* and *CDOM*. The proof of successful *CDOM* retrieval is however generally scarce, similar as with low *CHL* concentrations.

The directional reflectance properties of water are often neglected. Spectral inversion algorithms that make use of directional radiative transfer simulations are the most adequate solution, as they can account for all influencing parameters assuming a given $\tilde{\beta}(\psi)$ (Doerffer and Schiller, 2008a; Giardino et al., 2007; Van Der Woerd and Pasterkamp, 2008). Regarding classical analytical approaches, directional effects are parameterized using coefficients (e.g. f, Q) that vary with constituent concentrations (Morel and Gentili, 1991, 1993).

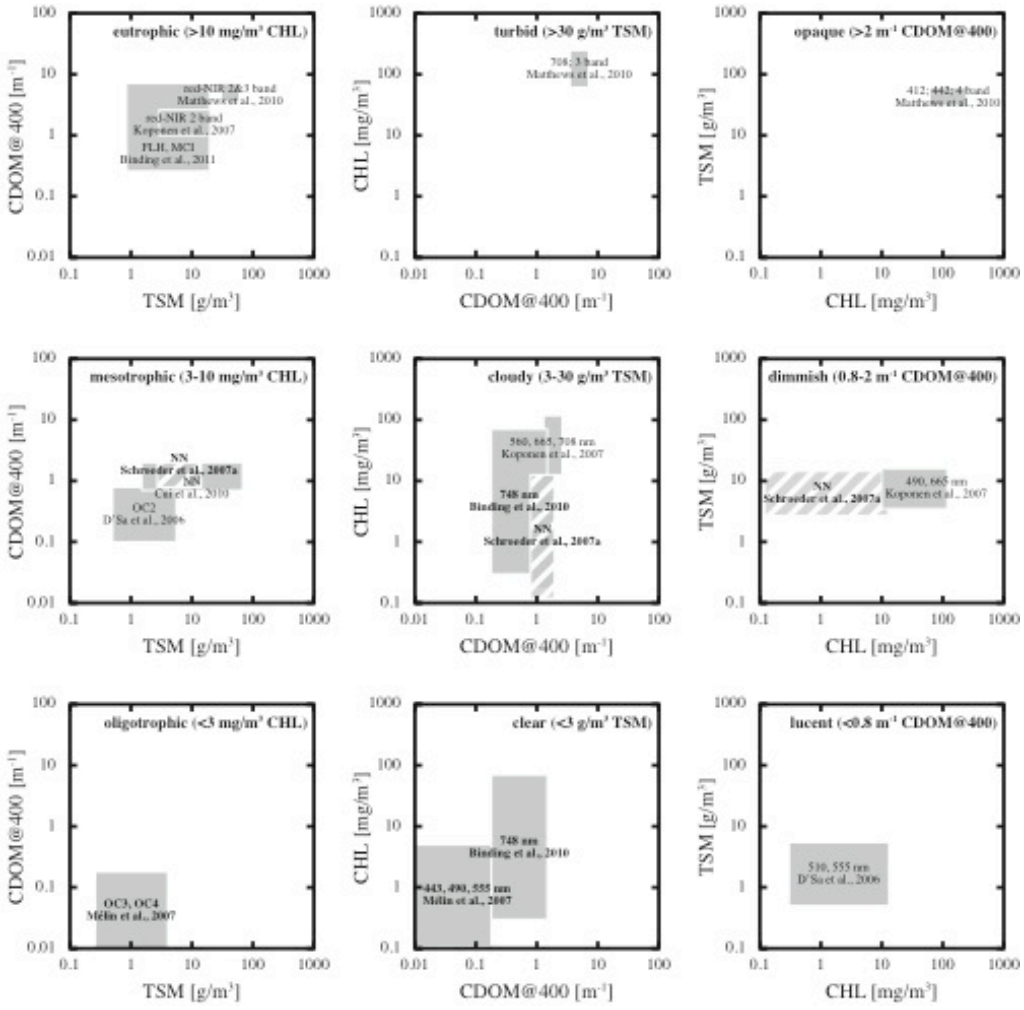

Figure 5-4: Case 2 water classes for CHL (left column), TSM (center) and CDOM (right) concentrations, with high to low concentration classes from top to bottom, and the remaining two constituents varying in x- and y-direction of each box. Class names and concentration ranges are titled in each box. Algorithm validation ranges are indicated as boxes and labeled with corresponding retrieval methods or center wavelengths. Bold labels indicate validation experiments with >10 images, hatched areas indicate simultaneous retrieval of all constituents. Reading example: Binding et al. (2011) validate the FLH and MCI algorithms for CHL in eutrophic waters with 0.85-19.60 g/m^3 TSM and 0.26-7.14 m^{-1} CDOM.

Their estimation requires iterative optimization, which needs an extension for band arithmetic analysis (Yang et al., 2011). More recent analytical models are

even parameterized with a specific geometry (Albert and Mobley, 2003; Park and Ruddick, 2005). A corresponding application example is given in Nechad et al. (2010), where the retrieval of *TSM* from cloudy water using a classical model (Gordon et al., 1988) is surprisingly better than a directional model (Park and Ruddick, 2005). Nonetheless, an improvement is expected especially for water with less particle scattering, i.e. higher η and lower N, and thus with higher anisotropy. Atmospheric correction procedures that provide an accurate $[R_w]_N$ e.g. through iterative procedures are thereby eligible alternatives to more extensively parameterized reflectance models.

The prominence of band-ratio algorithms for the individual retrieval of CHL in case 2 waters reported in this study, warrants however a note of caution. It has been suggested that changes on phytoplankton assemblages, as due to climate change, may shift phytoplankton composition in response to altered environmental forcing (e.g. Montes-Hugo et al., 2008). This process might uncouple *CDOM* and *TSM* concentrations from phytoplankton stocks and lead to further uncertainty in the retrieval of individual constituents, which is usually the case when using empirical algorithms, as opposed to the consolidated retrieval by inversion algorithms (Dierssen, 2010).

Extending from the intercomparison of algorithms performance based on synthetic and in situ data sets (IOCCG, 2006), a series of intercomparison and benchmark exercises including application to satellite imagery and matchup analysis is recommended to shed light on the comparability of water constituent retrieval algorithms and identify their applicability constraints in the near future.

5.8 Acknowledgements

We appreciate early comments and discussions on this work, in particular by Young-Je Park, Arnold Dekker, Els Knaeps, Dries Raymaekers and Viacheslav Kiselev. This work was partly funded by CSIRO's Wealth from Oceans Flagship and by NASA LCLUC program to AAG.

5.9 References

Aiken, J., Moore, G.F., Trees, C.C., Hooker, S.B., & Clark, D.K. (1995). The SeaWiFS CZCS-type pigment algorithm. In: *SeaWiFS Technical Report*

Series, *29* (38 p.), S.B. Hooker & E.R. Firestone (Eds.), Goddard Space Flight Center

Albert, A., & Mobley, C.D. (2003). An analytical model for subsurface irradiance and remote sensing reflectance in deep and shallow case-2 water. *Optics Express,* 11/22, 2873-2890

Ammenberg, P., Flink, P., Lindell, T., Pierson, D.C., & Strombeck, N. (2002). Bio-optical modelling combined with remote sensing to assess water quality. *International Journal of Remote Sensing,* 23/8, 1621

Austin, R.W., & Petzold, T.J. (1981). Water Colour Measurements. In J. Gower (Ed.), *Oceanography from Space* (pp. 239-256). New York: Plenum

Babin, M., Stramski, D., Ferrari, G.M., Claustre, H., Bricaud, A., Obolensky, G., & Hoepffner, N. (2003). Variations in the light absorption coefficients of phytoplankton, nonalgal particles, and dissolved organic matter in coastal waters around Europe. *J. Geophys. Res.,* 108/C7, 3211

Belzile, C., Vincent, W.F., Howard-Williams, C., Hawes, I., James, M.R., Kumagai, M., & Roesler, C.S. (2004). Relationships between spectral optical properties and optically active substances in a clear oligotrophic lake. *Water Resour. Res.,* 40/, W12512

Binding, C.E., Greenberg, T.A., Jerome, J.H., Bukata, R.P., & Letourneau, G. (2011). An assessment of MERIS algal products during an intense bloom in Lake of the Woods. *Journal of Plankton Research,* 33/5, 793-806

Binding, C.E., Jerome, J.H., Bukata, R.P., & Booty, W.G. (2010). Suspended particulate matter in Lake Erie derived from MODIS aquatic colour imagery. *International Journal of Remote Sensing,* 31/19, 5239 - 5255

Brando, V.E., & Dekker, A.G. (2003). Satellite hyperspectral remote sensing for estimating estuarine and coastal water quality. *IEEE Transactions on Geoscience and Remote Sensing,* 41/6, 1378-1387

Bricaud, A., Morel, A., & Prieur, L. (1981). Absorption by dissolved organic matter of the sea (yellow substance) in the UV and visible domains. *Limnology and Oceanography,* 26/1, 43-53

Bricaud, A., Roesler, C., & Zaneveld, J.R.V. (1995). In Situ Methods for Measuring the Inherent Optical Properties of Ocean Waters. *Limnology and Oceanography,* 40/2, 393-410

Bukata, R.P., Jerome, J.H., Kondratyev, K.Y., & Pozdnyakov, D.V. (1995). *Optical Properties and Remote Sensing of Inland and Coastal Waters*: CRS Press, USA

Bulgarelli, B., Kiselev, V., & Roberti, L. (1999). Radiative transfer in the atmosphere-ocean system: The finite-element method. *Appl. Opt.,* 38/9, 1530-1542

Carder, K.L., Chen, F.R., Lee, Z.P., Hawes, S.K., & Kamykowski, D. (1999). Semianalytic Moderate-Resolution Imaging Spectrometer algorithms for chlorophyll a and absorption with bio-optical domains based on nitrate-depletion temperatures. *J. Geophys. Res.,* 104/C3, 5403-5421

Carlson, R.E., & Simpson, J. (1996). A Coordinator's Guide to Volunteer Lake Monitoring Methods. (96 p.), North American Lake Management Society

Chami, M., McKee, D., Leymarie, E., & Khomenko, G. (2006). Influence of the angular shape of the volume-scattering function and multiple scattering on remote sensing reflectance. *Appl. Opt.,* 45/36, 9210-9220

Chapra, S.C., & Dobson, H.F.H. (1981). Quantification of the Lake Trophic Typologies of Naumann (Surface Quality) and Thienemann (Oxygen) with Special Reference to the Great Lakes. *Journal of Great Lakes Research,* 7/2, 182-193

Chen, S., Fang, L., Li, H., Chen, W., & Huang, W. (2011). Evaluation of a three-band model for estimating chlorophyll-a concentration in tidal reaches of

the Pearl River Estuary, China. *ISPRS Journal of Photogrammetry and Remote Sensing,* 66/3, 356-364

Chen, S., Huang, W., Wang, H., & Li, D. (2009). Remote sensing assessment of sediment re-suspension during Hurricane Frances in Apalachicola Bay, USA. *Remote Sensing of Environment,* 113/12, 2670-2681

Cheng Feng, L., Yun Mei, L., Yong, Z., Deyong, S., & Bin, Y. (2009). Validation of a Quasi-Analytical Algorithm for Highly Turbid Eutrophic Water of Meiliang Bay in Taihu Lake, China. *Geoscience and Remote Sensing, IEEE Transactions on,* 47/8, 2492-2500

Clark, D. (1997). Bio-optical algorithms - Case 1 waters. In: *MODIS algorithm theoretical basis document*, *Version 1.2* (50 p.), National Oceanic and Atmospheric Administration

Cooley, T., Anderson, G.P., Felde, G.W., Hoke, M.L., Ratkowski, A.J., Chetwynd, J.H., Gardner, J.A., Adler-Golden, S.M., Matthew, M.W., Berk, A., Bernstein, L.S., Acharya, P.K., Miller, D., & Lewis, P. (2002). FLAASH, a Modtran4-based atmospheric correction algorithm, its application and validation. *Proc. Geoscience and Remote Sensing Symposium, 2002. IGARSS '02. 2002 IEEE International*, 1414-1418 vol.1413

Cui, T., Zhang, J., Groom, S., Sun, L., Smyth, T., & Sathyendranath, S. (2010). Validation of MERIS ocean-color products in the Bohai Sea: A case study for turbid coastal waters. *Remote Sensing of Environment,* 114/10, 2326-2336

D'Sa, E.J., & Miller, R.L. (2003). Bio-optical properties in waters influenced by the Mississippi River during low flow conditions. *Remote Sensing of Environment,* 84/4, 538

D'Sa, E.J., Miller, R.L., & Del Castillo, C. (2006). Bio-optical properties and ocean color algorithms for coastal waters influenced by the Mississippi River during a cold front. *Appl. Opt.,* 45/28, 7410-7428

Dall'Olmo, G., & Gitelson, A.A. (2006). Effect of bio-optical parameter variability and uncertainties in reflectance measurements on the remote estimation of chlorophyll-a concentration in turbid productive waters: modeling results. *Applied Optics,* 45/15, 3577-3593

Dall'Olmo, G., Gitelson, A.A., & Rundquist, D.C. (2003). Towards a unified approach for remote estimation of chlorophyll-a in both terrestrial vegetation and turbid productive waters. *Geophys. Res. Lett.,* 30/18, 1938

Dekker, A.G., & Peters, S.W.M. (1993). Use of the Thematic Mapper for the analysis of eutrophic lakes: A case study in the Netherlands. *International Journal of Remote Sensing,* 14/5, 799-821

Dierssen, H.M. (2010). Perspectives on empirical approaches for ocean color remote sensing of chlorophyll in a changing climate. *Proceedings of the National Academy of Sciences,* 107/40, 17073-17078

Doerffer, R., & Schiller, H. (2007). The MERIS case 2 water algorithm. *International Journal of Remote Sensing,* 28/3, 517-535

Doerffer, R., & Schiller, H. (2008a). MERIS lake water algorithm for BEAM. In: *BEAM Algorithm Technical Basis Document* (17 p.), GKSS Forschungszentrum, Geesthacht, Germany

Doerffer, R., & Schiller, H. (2008b). MERIS regional coastal and lake case 2 water project atmospheric correction. In: *BEAM Algorithm Technical Basis Document* (42 p.), GKSS Forschungszentrum, Geesthacht, Germany

Dupouy, C., Neveux, J., Ouillon, S., Frouin, R., Murakami, H., Hochard, S., & Dirberg, G. (2010). Inherent optical properties and satellite retrieval of chlorophyll concentration in the lagoon and open ocean waters of New Caledonia. *Marine Pollution Bulletin,* 61/7-12, 503-518

Eleveld, M.A., Pasterkamp, R., van der Woerd, H.J., & Pietrzak, J.D. (2008). Remotely sensed seasonality in the spatial distribution of sea-surface

suspended particulate matter in the southern North Sea. *Estuarine, Coastal and Shelf Science,* 80/1, 103-113

Ferreira, A.b., Garcia, V.M.T., & Garcia, C.A.E. (2009). Light absorption by phytoplankton, non-algal particles and dissolved organic matter at the Patagonia shelf-break in spring and summer. *Deep Sea Research Part I: Oceanographic Research Papers,* 56/12, 2162-2174

Fettweis, M., Baeye, M., Francken, F., Lauwaert, B., Van den Eynde, D., Van Lancker, V., Martens, C., & Michielsen, T. (2011). Monitoring the effects of disposal of fine sediments from maintenance dredging on suspended particulate matter concentration in the Belgian nearshore area (southern North Sea). *Marine Pollution Bulletin,* 62/2, 258-269

Fournier, G.R., & Forand, J.L. (1994). *Analytic phase function for ocean water*. Bergen, Norway

Fournier, G.R., & Jonasz, M. (1999). Computer-based underwater imaging analysis, Denver, CO, USA, 62-70

Freda, W., Król, T., Martynov, O.V., Shybanov, E.B., & Hapter, R. (2007). Measurements of Scattering Function of sea water in Southern Baltic. *The European Physical Journal - Special Topics,* 144/1, 147-154

Freda, W., & Piskozub, J. (2007). Improved method of Fournier-Forand marine phase function parameterization. *Opt. Express,* 15/20, 12763-12768

Garver, S.A., & Siegel, D.A. (1997). Inherent optical property inversion of ocean color spectra and its biogeochemical interpretation 1. Time series from the Sargasso Sea. *J. Geophys. Res.,* 102/C8, 18607-18625

Giardino, C., Brando, V.E., Dekker, A.G., Strömbeck, N., & Candiani, G. (2007). Assessment of water quality in Lake Garda (Italy) using Hyperion. *Remote Sensing of Environment,* 109/2, 183-195

Giardino, C., Bresciani, M., Pilkaityte, R., Bartoli, M., & Razinkovas, A. (2010). In situ measurements and satellite remote sensing of case 2 waters: first results from the Curonian Lagoon *Oceanologia,* 52/2, 197-210

Gitelson, A. (1992). The peak near 700 nm on radiance spectra of algae and water: relationships of its magnitude and position with chlorophyll concentration. *International Journal of Remote Sensing,* 13/17, 3367 - 3373

Gitelson, A., Gao, B.-C., Li, R.-R., Berdnikov, S., & Saprygin, V. (2011). Estimation of chlorophyll-a concentration in productive turbid waters using a Hyperspectral Imager for the Coastal Ocean: The Azov Sea case study. *Environmental Research Letters,* 6/024023, 6

Gitelson, A., Garbuzov, G., Szilagyi, F., Mittenzwey, K.H., Karnieli, A., & Kaiser, A. (1993). Quantitative remote sensing methods for real-time monitoring of inland waters quality. *International Journal of Remote Sensing,* 14/7, 1269-1295

Gitelson, A., Gurlin, D., Moses, W.J., & Barrow, T. (2009). A bio-optical algorithm for the remote estimation of the chlorophyll- a concentration in case 2 waters. *Environmental Research Letters,* 4/045003, 5

Gitelson, A.A., Dall'Olmo, G., Moses, W., Rundquist, D.C., Barrow, T., Fisher, T.R., Gurlin, D., & Holz, J. (2008). A simple semi-analytical model for remote estimation of chlorophyll-a in turbid waters: Validation. *Remote Sensing of Environment,* 112/9, 3582-3593

Gitelson, A.A., Schalles, J.F., & Hladik, C.M. (2007). Remote chlorophyll-a retrieval in turbid, productive estuaries: Chesapeake Bay case study. *Remote Sensing of Environment,* 109/4, 464-472

Gons, H.J., Auer, M.T., & Effler, S.W. (2008). MERIS satellite chlorophyll mapping of oligotrophic and eutrophic waters in the Laurentian Great Lakes. *Remote Sensing of Environment,* 112/11, 4098-4106

Gonzalez Vilas, L., Spyrakos, E., & Torres Palenzuela, J.M. (2011). Neural network estimation of chlorophyll a from MERIS full resolution data for the coastal waters of Galician rias (NW Spain). *Remote Sensing of Environment,* 115/2, 524-535

Gordon, H.R. (1989). Dependence of the Diffuse Reflectance of Natural Waters on the Sun Angle. *Limnology and Oceanography,* 34/8, 1484-1489

Gordon, H.R. (1993). Sensitivity of radiative transfer to small-angle scattering in the ocean: Quantitative assessment. *Applied Optics,* 32/36, 7505-7511

Gordon, H.R., & Brown, O.B. (1973). Irradiance Reflectivity of a Flat Ocean as a Function of Its Optical Properties. *Appl. Opt.,* 12/7, 1549-1551

Gordon, H.R., Brown, O.B., Evans, R.H., Brown, J.W., Smith, R.C., Baker, K.S., & Clark, D.K. (1988). A semianalytic radiance model of ocean color. *J. Geophys. Res.,* 93/D9, 10909-10924

Gordon, H.R., Brown, O.B., & Jacobs, M.M. (1975). Computed Relationships Between the Inherent and Apparent Optical Properties of a Flat Homogeneous Ocean. *Appl. Opt.,* 14/2, 417-427

Gordon, H.R., & Clark, D.K. (1981). Clear water radiances for atmospheric correction of coastal zone color scanner imagery. *Appl. Opt.,* 20/24, 4175-4180

Gordon, H.R., & Franz, B.A. (2008). Remote sensing of ocean color: Assessment of the water-leaving radiance bidirectional effects on the atmospheric diffuse transmittance for SeaWiFS and MODIS intercomparisons. *Remote Sensing of Environment,* 112/5, 2677-2685

Gordon, H.R., & Voss, K.J. (2004). MODIS Normalized Water-leaving Radiance. In: *MODIS algorithm theoretical basis documents*, *MOD-18* (125 p.)

Gordon, H.R., & Wang, M. (1994). Retrieval of water-leaving radiance and aerosol optical thickness over the oceans with SeaWiFS: a preliminary algorithm. *Applied Optics,* 33/, 443-452

Gower, J., King, S., Borstad, G., & Brown, L. (2005). Detection of intense plankton blooms using the 709 nm band of the MERIS imaging spectrometer. *International Journal of Remote Sensing,* 26/9, 2005

Gower, J.F.R., Doerffer, R., & Borstad, G.A. (1999). Interpretation of the 685nm peak in water-leaving radiance spectra in terms of fluorescence, absorption and scattering, and its observation by MERIS. *International Journal of Remote Sensing,* 20/9, 1771-1786

Guanter, L., Ruiz-Verdu, A., Odermatt, D., Giardino, C., Simis, S., Estelles, V., Heege, T., Dominguez-Gomez, J.A., & Moreno, J. (2010). Atmospheric correction of ENVISAT/MERIS data over inland waters: Validation for European lakes. *Remote Sensing of Environment,* 114/3, 467-480

Haltrin, V.I. (2002). One-Parameter Two-Term Henyey-Greenstein Phase Function for Light Scattering in Seawater. *Appl. Opt.,* 41/6, 1022-1028

Heege, T., & Fischer, J. (2004). Mapping of water constituents in Lake Constance using multispectral airborne scanner data and a physically based processing scheme. *Canadian Journal of Remote Sensing,* 30/1, 77-86

Horion, S., Bergamino, N., Stenuite, S., Descy, J.P., Plisnier, P.D., Loiselle, S.A., & Cornet, Y. (2010). Optimized extraction of daily bio-optical time series derived from MODIS/Aqua imagery for Lake Tanganyika, Africa. *Remote Sensing of Environment,* 114/4, 781-791

Hu, C., Carder, K.L., & Muller-Karger, F.E. (2000). Atmospheric correction of SeaWiFS imagery over turbid coastal waters: A practical method. *Remote Sensing of Environment,* 74/2, 195

Iluz, D., Yacobi, Y.Z., & Gitelson, A.A. (2003). Adaptation of an algorithm for chlorophyll-a estimation by optical data in the oligotrophic Gulf of Eilat. *International Journal of Remote Sensing,* 24/5, 1157

IOCCG (2006). Remote Sensing of Inherent Optical Properties: Fundamentals, Tests of Algorithms, and Applications. In: *Reports of the International Ocean-Colour Coordinating Group* (122 p.), Z.P. Lee (Ed.), IOCCG

IOCCG (2009). Partition of the Ocean into Ecological Provinces: Role of Ocean-Colour Radiometry. In: *Reports of the International Ocean-Colour Coordinating Group* (98 p.), M. Dowell & T. Platt (Eds.), IOCCG

Jerome, J.H., Bukata, R.P., & Miller, J.R. (1996). Remote sensing reflectance and its relationship to optical properties of natural waters. *International Journal of Remote Sensing,* 17/16, 3135-3155

Jin, Z., & Stamnes, K. (1994). Radiative transfer in nonuniformly refracting layered media: Atmosphere-ocean system. *Appl. Opt.,* 33/, 431-442

Kabbara, N., Benkhelil, J., Awad, M., & Barale, V. (2008). Monitoring water quality in the coastal area of Tripoli (Lebanon) using high-resolution satellite data. *ISPRS Journal of Photogrammetry and Remote Sensing,* 63/5, 488-495

Kallio, K., Kutser, T., Hannonen, T., Koponen, S., Pulliainen, J., Vepsalainen, J., & Pyhalahti, T. (2001). Retrieval of water quality from airborne imaging spectrometry of various lake types in different seasons. *The Science of The Total Environment,* 268/1-3, 59-77

Kirk, J.T.O. (1991). Volume scattering function, average cosines, and the underwater light field. *Limnology and Oceanography,* 36/3, 455-467

Koponen, S., Attila, J., Pulliainen, J., Kallio, K., Pyh‰lahti, T., Lindfors, A., Rasmus, K., & Hallikainen, M. (2007). A case study of airborne and satellite remote sensing of a spring bloom event in the Gulf of Finland. *Continental Shelf Research,* 27/2, 228-244

Koponen, S., Ruiz-Verdu, A., Heege, T., Heblinski, J., Sorensen, K., Kallio, K., Pyhalahti, T., Doerffer, R., Brockmann, C., & Peters, M. (2008). Development of MERIS lake water algorithms. In: *ESA Validation Report* (65 p.)

Kostadinov, T.S., Siegel, D.A., Maritorena, S., & Guillocheau, N. (2007). Ocean color observations and modeling for an optically complex site: Santa Barbara Channel, California, USA. *J. Geophys. Res.,* 112/C7, C07011

Kowalczuk, P., Darecki, M., Zablocka, M., & Gorecka, I. (2010). Validation of empirical and semi-analytical remote sensing algorithms for estimating absorption by Coloured Dissolved Organic Matter in the Baltic Sea from SeaWiFS and MODIS imagery. *Oceanologia,* 52/2, 171-196

Kowalczuk, P., Olszewski, J., Darecki, M., & Kaczmarek, S. (2005). Empirical relationships between coloured dissolved organic matter (CDOM) absorption and apparent optical properties in Baltic Sea waters. *International Journal of Remote Sensing,* 26/2, 345-370

Kuchinke, C.P., Gordon, H.R., & Franz, B.A. (2009a). Spectral optimization for constituent retrieval in Case 2 waters I: Implementation and performance. *Remote Sensing of Environment,* 113/3, 571-587

Kuchinke, C.P., Gordon, H.R., Harding Jr, L.W., & Voss, K.J. (2009b). Spectral optimization for constituent retrieval in Case 2 waters II: Validation study in the Chesapeake Bay. *Remote Sensing of Environment,* 113/3, 610-621

Kutser, T., Paavel, B., Metsamaa, L., & Vahtm√§e, E. (2009). Mapping coloured dissolved organic matter concentration in coastal waters. *International Journal of Remote Sensing,* 30/22, 5843 - 5849

Kutser, T., Pierson, D.C., Kallio, K.Y., Reinart, A., & Sobek, S. (2005a). Mapping lake CDOM by satellite remote sensing. *Remote Sensing of Environment,* 94/4, 535

Kutser, T., Pierson, D.C., Tranvik, L., Reinart, A., Sobek, S., & Kallio, K.Y. (2005b). Using satellite remote sensing to estimate the colored dissolved organic matter absorption coefficient in lakes. *Ecosystems,* 8/6, 709

Lee, M.E., & Lewis, M.R. (2003). A New Method for the Measurement of the Optical Volume Scattering Function in the Upper Ocean. *Journal of Atmospheric and Oceanic Technology,* 20/4, 563-571

Lee, Z., Carder, K.L., & Arnone, R.A. (2002). Deriving Inherent Optical Properties from Water Color: a Multiband Quasi-Analytical Algorithm for Optically Deep Waters. *Appl. Opt.,* 41/27, 5755-5772

Lee, Z., Carder, K.L., Mobley, C.D., Steward, R.G., & Patch, J.S. (1998). Hyperspectral Remote Sensing for Shallow Waters. I. A Semianalytical Model. *Appl. Opt.,* 37/27, 6329-6338

Loisel, H., & Morel, A. (2001). Non-isotropy of the upward radiance field in typical coastal (Case 2) waters. *International Journal of Remote Sensing,* 22/2, 275 - 295

Mahasandana, S., Tripathi, N.K., & Honda, K. (2009). Sea surface multispectral index model for estimating chlorophyll a concentration of productive coastal waters in Thailand. *Canadian Journal of Remote Sensing,* 35/3, 287-296

Mannino, A., Russ, M.E., & Hooker, S.B. (2008). Algorithm development and validation for satellite-derived distributions of DOC and CDOM in the U.S. Middle Atlantic Bight. *J. Geophys. Res.,* 113/C7, C07051

Maritorena, S., Siegel, D.A., & Peterson, A.R. (2002). Optimization of a semianalytical ocean color model for global-scale applications. *Appl. Opt.,* 41/15, 2705-2714

Matthews, M.W., Bernard, S., & Winter, K. (2010). Remote sensing of cyanobacteria-dominant algal blooms and water quality parameters in

Zeekoevlei, a small hypertrophic lake, using MERIS. *Remote Sensing of Environment,* 114/9, 2070-2087

McClain, C.R. (2009). A Decade of Satellite Ocean Color Observations. *Annual Review of Marine Science,* 1/1, 19-42

Mélin, F., Zibordi, G., & Berthon, J.-F. (2007). Assessment of satellite ocean color products at a coastal site. *Remote Sensing of Environment,* 110/2, 192-215

Minghelli-Roman, A., Laugier, T., Polidori, L., Mathieu, S., Loubersac, L., & Gouton, P. (2011). Satellite survey of seasonal trophic status and occasional anoxic 'malaigue' crises in the Thau lagoon using MERIS images. *International Journal of Remote Sensing,* 32/4, 909-923

Mobley, C.D. (1989). A Numerical Model for the Computation of Radiance Distributions in Natural Waters with Wind-Roughened Surfaces. *Limnology and Oceanography,* 34/8, 1473-1483

Mobley, C.D., Gentili, B., Gordon, H.R., Jin, Z., Kattawar, G.W., Morel, A., Reinersman, P., Stamnes, K., & Stavn, R.H. (1993). Comparison of numerical models for computing underwater light fields. *Appl. Opt.,* 32/36, 7484-7504

Mobley, C.D., Sundman, L.K., & Boss, E. (2002). Phase Function Effects on Oceanic Light Fields. *Appl. Opt.,* 41/6, 1035-1050

Montes-Hugo, M.A., Vernet, M., Smith, R., & Carder, K. (2008). Phytoplankton size-structure on the western shelf of the Antarctic Peninsula: a remote-sensing approach. *Int. J. Remote Sens.,* 29/3, 801-829

Moore, G.F., Aiken, J., & Lavender, S.J. (1999). The atmospheric correction of water colour and the quantitative retrieval of suspended particulate matter in Case II waters: application to MERIS. *International Journal of Remote Sensing,* 20/9, 1713 - 1733

Moore, T.S., Campbell, J.W., & Dowell, M.D. (2009). A class-based approach to characterizing and mapping the uncertainty of the MODIS ocean chlorophyll product. *Remote Sensing of Environment,* 113/11, 2424-2430

Morel, A. (1974). Optical properties of pure water and pure sea water. In N.G. Jerlov & E.S. Nielsen (Eds.), *Optical Aspects of Oceanography* (pp. 1-24). New York: Academic Press

Morel, A. (1980). In-water and remote measurements of ocean color. *Boundary-Layer Meteorology,* 18/2, 177-201

Morel, A., & Antoine, D. (2007). Pigment Index Retrieval in Case 1 Waters. (25 p.), Laboratoire d'Océanographie de Villefranche

Morel, A., Antoine, D., & Gentili, B. (2002). Bidirectional Reflectance of Oceanic Waters: Accounting for Raman Emission and Varying Particle Scattering Phase Function. *Appl. Opt.,* 41/30, 6289-6306

Morel, A., & Gentili, B. (1991). Diffuse reflectance of oceanic waters: Its dependence on Sun angle as influenced by the molecular scattering contribution. *Appl. Opt.,* 30/30, 4427-4438

Morel, A., & Gentili, B. (1993). Diffuse reflectance of oceanic waters. II Bidirectional aspects. *Appl. Opt.,* 32/33, 6864-6879

Morel, A., & Gentili, B. (1996). Diffuse reflectance of oceanic waters. III. Implication of bidirectionality for the remote-sensing problem. *Appl. Opt.,* 35/24, 4850-4862

Morel, A., & Maritorena, S. (2001). Bio-optical properties of oceanic waters: A reappraisal. *J. Geophys. Res.,* 106/C4, 7163-7180

Morel, A., & Prieur, L. (1977). Analysis of Variations in Ocean Color. *Limnology and Oceanography,* 22/4, 709-722

Moses, W.J., Gitelson, A.A., Berdnikov, S., & Povazhnyy, V. (2009a). Estimation of chlorophyll- a concentration in case II waters using MODIS and MERIS data - successes and challenges. *Environmental Research Letters,* 4/4, 045005

Moses, W.J., Gitelson, A.A., Berdnikov, S., & Povazhnyy, V. (2009b). Satellite Estimation of Chlorophyll-a Concentration Using the Red and NIR Bands of MERIS - The Azov Sea Case Study. *Geoscience and Remote Sensing Letters, IEEE,* 6/4, 845-849

Murakami, H., Sasaoka, K., Hosoda, K., Fukushima, H., Toratani, M., Frouin, R., Mitchell, B., Kahru, M., Deschamps, P.-Y., Clark, D., Flora, S., Kishino, M., Saitoh, S.-I., Asanuma, I., Tanaka, A., Sasaki, H., Yokouchi, K., Kiyomoto, Y., Saito, H., Dupouy, C., Siripong, A., Matsumura, S., & Ishizaka, J. (2006). Validation of ADEOS-II GLI ocean color products using in situ observations. *Journal of Oceanography,* 62/3, 373-393

Nechad, B., Ruddick, K.G., & Park, Y. (2010). Calibration and validation of a generic multisensor algorithm for mapping of total suspended matter in turbid waters. *Remote Sensing of Environment,* 114/4, 854-866

Neukermans, G., Ruddick, K., Bernard, E., Ramon, D., Nechad, B., & Deschamps, P.-Y. (2009). Mapping total suspended matter from geostationary satellites: a feasibility study with SEVIRI in the Southern North Sea. *Opt. Express,* 17/16, 14029-14052

Nürnberg, G.K. (1996). Trophic State of Clear and Colored, Soft- and Hardwater Lakes with Special Consideration of Nutrients, Anoxia, Phytoplankton and Fish. *Lake and Reservoir Management,* 12/4, 432 - 447

O'Reilly, J.E., Maritorena, S., Mitchell, B.G., Siegel, D.A., Carder, K.L., Garver, S.A., Kahru, M., & McClain, C. (1998). Ocean color chlorophyll algorithms for SeaWiFS. *Journal of Geophysical Research,* 103/C11, 24937-24953

Odermatt, D., Giardino, C., & Heege, T. (2010). Chlorophyll retrieval with MERIS Case-2-Regional in perialpine lakes. *Remote Sensing of Environment,* 114/3, 607-617

Odermatt, D., Heege, T., Nieke, J., Kneubuehler, M., & Itten, K. (2008). Water quality monitoring for Lake Constance with a physically based algorithm for MERIS data. *Sensors,* 8/8, 4582-4599

Park, Y., & Ruddick, K. (2005). Model of remote-sensing reflectance including bidirectional effects for case 1 and case 2 waters. *Appl. Opt.,* 44/7, 1236-1249

Petus, C., Chust, G., Gohin, F., Doxaran, D., Froidefond, J.-M., & Sagarminaga, Y. (2010). Estimating turbidity and total suspended matter in the Adour River plume (South Bay of Biscay) using MODIS 250-m imagery. *Continental Shelf Research,* 30/5, 379-392

Petzold, T.J. (1972). Volume scattering functions for selected ocean waters. *SIO Ref. 72–78* (79 p.), Scripps Institution of Oceanography, Univ. of Calif., San Diego

Pfeiffer, N., & Chapman, G.H. (2008). Successive order, multiple scattering of two-term Henyey-Greenstein phase functions. *Opt. Express,* 16/18, 13637-13642

Piskozub, J., & McKee, D. (2011). Effective scattering phase functions for the multiple scattering regime. *Opt. Express,* 19/5, 4786-4794

Pozdnyakov, D.V., Shuchman, R., Korosov, A., & Hatt, C. (2005). Operational algorithm for the retrieval of water quality in the Great Lakes. *Remote Sensing of Environment,* 97/3, 352

Preisendorfer, R.W. (1961). Application of Radiative Transfer Theory to Light Measurements in the Sea. *International Union of Geodesy and Geophysics Monograph* (pp. 11-29)

Qin, Y., Brando, V.E., Dekker, A.G., & Blondeau-Patissier, D. (2007). Validity of SeaDAS water constituents retrieval algorithms in Australian tropical coastal waters. *Geophys. Res. Lett.,* 34/21, L21603

Ruddick, K., Ovidio, F., & Rijkeboer, M. (2000). Atmospheric correction of SeaWiFS imagery for turbid coastal and inland waters. *Applied Optics,* 39/6, 897-912

Ruddick, K.G., De Cauwer, V., Park, Y.-J., & Moore, G. (2006). Seaborne measurements of near infrared water-leaving reflectance: The similarity spectrum for turbid waters. *Limnology and Oceanography,* 51/2, 1167-1179

Santini, F., Alberotanza, L., Cavalli, R.M., & Pignatti, S. (2010). A two-step optimization procedure for assessing water constituent concentrations by hyperspectral remote sensing techniques: An application to the highly turbid Venice lagoon waters. *Remote Sensing of Environment,* 114/4, 887-898

Sathyendranath, S., & Platt, T. (1997). Analytic model of ocean color. *Appl. Opt.,* 36/12, 2620-2629

Schalles, J.F., Gitelson, A.A., Yacobi, Y.Z., & Kroenke, A.E. (1998). Estimation of chlorophyll-a from time series measurements of high spectral resolution reflectance in an eutrophic lake. *Journal of Phycology,* 34/2, 383-390

Schroeder, T. (2005). *Fernerkundung von Wasserinhaltsstoffen in Küstengewässern mit MERIS unter Anwendung expliziter und impliziter Atmosphärenkorrekturverfahren*. Freie Universität Berlin: Doctoral thesis (in German)

Schroeder, T., Behnert, I., Schaale, M., Fischer, J., & Doerffer, R. (2007a). Atmospheric correction algorithm for MERIS above case-2 waters. *International Journal of Remote Sensing,* 28/7, 1469-1486

Schroeder, T., Schaale, M., & Fischer, J. (2007b). Retrieval of atmospheric and oceanic properties from MERIS measurements: A new Case-2 water processor for BEAM. *International Journal of Remote Sensing,* 28/24, 5627 - 5632

Schuchman, R.A., Korosov, A.A., Pozdnyakov, D.V., Means, J.C., Savage, S., Hatt, C., & Meadows, G.A. (2005). SeaWiFS and MODIS-observed multi-year seasonal and spatial dynamics in biotic and abiotic processes in Lake Michigan as obtained from a new water quality retrieval algorithm. *Proc. Proc. of 31st Int. Symp. on Remote Sensing of Environment*, St. Petersburg, Russia

Shanmugam, P., Ahn, Y.-H., Ryu, J.-H., & Sundarabalan, B. (2010). An evaluation of inversion models for retrieval of inherent optical properties from ocean color in coastal and open sea waters around Korea. *Journal of Oceanography,* 66/6, 815-830

Shuchman, R., Korosov, A., Hatt, C., Pozdnyakov, D., Means, J., & Meadows, G. (2006). Verification and Application of a Bio-optical Algorithm for Lake Michigan Using SeaWiFS: a 7-year Inter-annual Analysis. *Journal of Great Lakes Research,* 32/2, 258-279

Siegel, D.A., Wang, M., Maritorena, S., & Robinson, W. (2000). Atmospheric correction of satellite ocean color imagery: The black pixel assumption. *Applied Optics,* 39/21, 3582-3591

Smith, R.C., & Baker, K.S. (1981). Optical properties of the clearest natural waters (200-800 nm). *Applied Optics,* 20/, 177-

Sokolov, A., Chami, M., Dmitriev, E., & Khomenko, G. (2010). Parameterization of volume scattering function of coastal waters based on the statistical approach. *Opt. Express,* 18/5, 4615-4636

Stumpf, R.P., Arnone, R.A., Gould, R.W., Martinolich, P.M., & Ransibrahmanakul, V. (2003). A partially coupled ocean-atmosphere model for retrieval of water-leaving radiance from SeaWiFS in coastal waters. In: *SeaWiFS Postlaunch Tech. Rep. Ser.*, *22* (51-59 p.), S.B. Hooker & E.R. Firestone (Eds.), NASA Goddard Space Flight Cent.

Sullivan, J.M., & Twardowski, M.S. (2009). Angular shape of the oceanic particulate volume scattering function in the backward direction. *Appl. Opt.,* 48/35, 6811-6819

Sydor, M. (2007). Statistical Treatment of Remote Sensing Reflectance from Coastal Ocean Water: Proportionality of Reflectance from Multiple Scattering to Source Function b/a. *Journal of Coastal Research*, 1183-1192

Toratani, M., Fukushima, H., Murakami, H., & Tanaka, A. (2007). Atmospheric correction scheme for GLI with absorptive aerosol correction. *Journal of Oceanography,* 63/3, 525-532

Tyler, A.N., Svab, E., Preston, T., Présing, M., & Kovács, A. (2006). Remote sensing of the water quality of shallow lakes: A mixture modelling approach to quantifying phytoplankton in water characterized by high-suspended sediment. *International Journal of Remote Sensing,* 27/8, 1521

Van der Woerd, H., & Pasterkamp, R. (2004). Mapping of the North Sea turbid coastal waters using SeaWiFS data. *Canadian Journal of Remote Sensing,* 30/1, 44-53

Van Der Woerd, H.J., & Pasterkamp, R. (2008). HYDROPT: A fast and flexible method to retrieve chlorophyll-a from multispectral satellite observations of optically complex coastal waters. *Remote Sensing of Environment,* 112/4, 1795-1807

Vasilkov, A., & Kopelevich, O. (1982). The reasons of maximum at about 700 nm on radiance spectra of the sea. *Oceanology,* 22/, 945-950

Vidot, J., & Santer, R. (2005). Atmospheric correction for inland waters - application to SeaWiFS. *International Journal of Remote Sensing,* 26/17, 3663

Vos, W.L., Donze, M., & Buiteveld, H. (1986). On the reflectance spectrum of algae in water: The nature of the peak at 700 nm and its shift with varying

concentration. In: *Communication on Sanitary Engineering and Water Management* (86-122 p.)

Wang, J.-J., Lu, X.X., Liew, S.C., & Zhou, Y. (2009). Retrieval of suspended sediment concentrations in large turbid rivers using Landsat ETM+: an example from the Yangtze River, China. *Earth Surface Processes and Landforms,* 34/8, 1082-1092

Wang, J.J., & Lu, X.X. (2010). Estimation of suspended sediment concentrations using Terra MODIS: An example from the Lower Yangtze River, China. *Science of The Total Environment,* 408/5, 1131-1138

Wang, M. (2007). Remote sensing of the ocean contributions from ultraviolet to near-infrared using the shortwave infrared bands: simulations. *Appl. Opt.,* 46/9, 1535-1547

Wang, M., Shi, W., & Tang, J. (2011). Water property monitoring and assessment for China's inland Lake Taihu from MODIS-Aqua measurements. *Remote Sensing of Environment,* 115/3, 841-854

Werdell, P.J., Bailey, S.W., Franz, B.A., Harding Jr, L.W., Feldman, G.C., & McClain, C.R. (2009). Regional and seasonal variability of chlorophyll-a in Chesapeake Bay as observed by SeaWiFS and MODIS-Aqua. *Remote Sensing of Environment,* 113/6, 1319-1330

Wetzel, R.G. (1983). *Limnology*. Philadelphia: W.B. Saunders Co.

Witter, D.L., Ortiz, J.D., Palm, S., Heath, R.T., & Budd, J.W. (2009). Assessing the Application of SeaWiFS Ocean Color Algorithms to Lake Erie. *Journal of Great Lakes Research,* 35/3, 361-370

Yang, W., Matsushita, B., Chen, J., & Fukushima, T. (2011). Estimating constituent concentrations in case II waters from MERIS satellite data by semi-analytical model optimizing and look-up tables. *Remote Sensing of Environment,* 115/5, 1247-1259

Zhai, P.-W., Hu, Y., Chowdhary, J., Trepte, C.R., Lucker, P.L., & Josset, D.B. (2010). A vector radiative transfer model for coupled atmosphere and ocean systems with a rough interface. *Journal of Quantitative Spectroscopy and Radiative Transfer,* 111/7-8, 1025-1040

Zhang, M., Tang, J., Dong, Q., Song, Q., & Ding, J. (2010). Retrieval of total suspended matter concentration in the Yellow and East China Seas from MODIS imagery. *Remote Sensing of Environment,* 114/2, 392-403

Zhou, W., Wang, S., Zhou, Y., & Troy, A. (2006). Mapping the concentrations of total suspended matter in Lake Taihu, China, using Landsat-5 TM data. *International Journal of Remote Sensing,* 27/6, 1177-1191

6 SYNOPSIS

6.1 Main achievements

The main achievements of the thesis are structured according to the four publications embodied and their respective research questions in Chapter 1.5, but with the two validation experiments merged in one section.

6.1.1 Validation of spaceborne chl-a retrieval for perialpine lakes

Publication 1 (Chapter 2):

Odermatt, D., Heege, T., Nieke, J., Kneubuehler, M., & Itten, K. (2008). Water quality monitoring for Lake Constance with a physically based algorithm for MERIS data. *Sensors,* 8/8, 4582-4599

- Can a simple, physically based algorithm for water constituent retrieval be automatized with lake specifically universal input parameters?

The accomplished experiments confirm the general applicability of a lake specific universal parameterization. Training and validation are designed as a bipartite matchup of in situ and remotely measured time series of *chl-a* in 2003-2006. They represent quantitatively unprecedented temporal evidence as far as remote sensing experiments on European freshwater reservoirs are concerned, which is enabled by the simplified parameterization and automatic processing. The correlation of in situ and remotely measured data is altogether satisfactory, two constraints and corresponding error sources are however described.

The two constraints are on one hand the empirical recalibration of several MERIS bands, indicating that the algorithm's underlying model does not account for all relevant variations in the remotely sensed data. On the other hand, the autumn algae bloom in 2006 is not identified by the remote *chl-a* measurements, indicating a shortcoming of the bio-optical model. Error sources for the former are mainly the simplified modeling and parameterization of the at-

mosphere, e.g. the neglected adjacency effects as described in Chapter 1.4.4 (Odermatt et al., 2008). The latter in contrast is due to the simplified parameterization of the water reflectance model, including invariable IOPs and aquatic NIR backscattering contribution.

All in all, it was found that the applied algorithms are able to provide accurate *chl-a* products at an instructive physical clarity, but technically limited with regard to representing the full dynamics of the water-atmosphere system.

Publication 2 (Chapter 3):

Odermatt, D., Giardino, C., & Heege, T. (2010). Chlorophyll retrieval with MERIS Case-2-Regional in perialpine lakes. *Remote Sensing of Environment,* 114/3, 607-617

- Are the C2R neural networks appropriate for the routine processing of *chl-a* products for perialpine lakes?

The C2R algorithms are found to be adequate for *chl-a* retrieval from most larger perialpine lakes. C2R products from more than 200 MERIS images are validated with official water quality monitoring time series in nine lakes. Eligible temporal differences between acquisitions of in situ and satellite data are up to 5 days. This indicates that their exact concurrence is desirable but not necessary if reference sites are chosen accordingly.

The quality in the linear correlations varies primarily with the methods applied for in situ measurements, which include laboratory and fluorescence probe measurements of *chl-a* at various vertical representations. Vertically resolved HPLC estimates from the top 5 m layer of the water column in Lake Zurich suit best with the C2R estimates. 0-5 m fluorescence probe measurements as used for Lake Zug and Lake Zurich are second. Lowest correlations are found between satellite estimates and HPLC measurements from vertically mixed samples of the top 15-20 m layers of Lake Biel and Lake Constance. Only observations from Lake Geneva in 2006-2007 break these ranks.

In 2003-2005, *chl-a* variations in Lake Geneva are comparable to other lakes and well matched by the satellite measurements. In 2006 and 2007 however, both frequency and magnitude of variations increase significantly for in situ data, while remaining the same in satellite estimates. This sudden divergence might be a consequence of modifications to the phytoplankton communities

and accordingly optical properties caused by changing temperature and Phosporous concentrations. Such effects in Lake Geneva are reported for 1972-2005 (Tadonleke, 2010; Tadonleke et al., 2009), more recent interpretation is however not available.

- What are the effects of the adjacency effect correction, and how does their removal propagate to the results of the neural network algorithms?

Comparison with 35 spectroradiometric measurements from 5 lakes shows that the removal of adjacency effect with ICOL significantly improves atmospheric correction and retrieved reflectance spectra. These findings are also confirmed for another atmospheric correction procedure (Guanter et al., 2010). However, water constituent concentrations retrieved by C2R are not consistently enhanced by this improvement. Instead, two other significant modifications are observed. On one hand, a general underestimation of *chl-a* is turned into a weak overestimation, at similar linear correlations. On the other hand, the application of ICOL increases *cdom* concentrations to the expected level, although correlation with field reference data is known to be very low in either case (Koponen et al., 2008). Both modifications represent increases of absorption, but further interpretation is complicated by the black box architecture of the C2R algorithm.

In summary, C2R has demonstrated the technical and physical requirements for automatic processing of *chl-a* and *tsm* products. Interpretation of failure such as in parts of the Lake Geneva *chl-a* data or the *cdom* concentrations are difficult due to the algorithms black box constitution, but could be intercepted by an improved combination of C2R and ICOL or retrieval quality flags.

6.1.2 WFD compliant chl-a products for perialpine lakes

Publication 3 (Chapter 4):

Bresciani, M., Stroppiana, D., Odermatt, D., Morabito, G., & Giardino, C. (2011). Assessing remotely sensed chlorophyll-a for the implementation of the Water Framework Directive in European perialpine lakes. *Science of The Total Environment,* 409/17, 3083-3091

- What variations in *chl-a* concentrations occur in perialpine lakes?

Chl-a variations in Lakes Brienz, Lucerne and Thun on the Northern side of the Alps are low and continuously oligotrophic at less than 5 mg/m^3. The largest lakes (Constance, Garda, Como, Maggiore and Geneva) feature higher average and more variable, oligo- to mesotrophic concentrations, with occasional bloom events. Smaller lakes South of the Alps, i.e. Lake Iseo, Pusiano and Varese, contain most *chl-a* with maxima that frequently exceed 10 mg/m^3. A perennial trend for the period 2003-2009 is only found in the decreasing concentrations of Lake Como.

Generally highest concentrations occur during winter and the autumn-winter and winter spring-transitions. The magnitude of these maxima is however strongly related to the lake's trophic status, whereas variations are smaller in oligotrophic waters and larger in eutrophic waters.

- What is the spatial variability of *chl-a*, and how does it change at several temporal scales?

Significant differences in both spatial and temporal variability of *chl-a* are observed for different lakes. They can be related to the hydrographic and topographic conditions and corresponding wind mixing effects, to the influence of tributary rivers or residence times. The spatio-temporal resolution inherent to remote measurements provides thus a means to estimate the representativity of in situ monitoring protocols, and to validate their compliance with WFD requirements.

Considerable variations in *chl-a* at small scales are observed in the smaller, meso- to eutrophic lakes South of the Alps. Larger lakes with narrow, branched basins such as Lake Como and Lake Maggiore feature similar characteristics, whereas the sub-basins vary individually. The statistical predictability of *chl-a* is low for most of these lakes.

In the larger, wider basins on the contrary, the predictability is higher since hydrographic conditions cause spatial variations that however remain relatively consistent in time. In Lake Garda and Lake Constance for instance, the Sarca and Rhine tributary, respectively, significantly dominate spatial variations. In Lake Garda, the transition from a narrow, shallow sub-basin around the Sarca's estuary in the mountainous North, to the densely populated Southern part further enhances this spatial pattern.

- Can the WFD be applied to remote observations of lakes in the perialpine region?

The demonstrated results proof the suitability of remote observations for integration in WFD-compliant water quality monitoring. The applied data and methods provide reliable and in many cases validated measurements of *chl-a* in perialpine lakes for the past almost 10 years since ENVISAT's launch.

Comparing satellite-measured *chl-a* of variable locations and dates of the six relevant seasonal and transitional periods allows an estimation of their spatio-temporal representativity. It is shown that limitations in this representativity may cause erroneous classifications in the WFD scheme (Wolfram et al., 2009) if measurements are only aquired bi-monthly. With regard to spatial variations, sub-basins for individual observation and methods that indicate variability in smaller lakes are proposed.

In summary, satellite measured *chl-a* reveals a great potential to efficiently provide and even enhance the *chl-a* indications currently acquired by in situ monitoring, lacking however its vertical dimension. Therefore, most comprehensive understanding of *chl-a* variations and related limnic processes is expected from an optimized combination of the two.

6.1.3 Constituent retrieval for other optically complex waters

Publication 4 (Chapter 5):

Odermatt, D., Gitelson, A., Brando, V., Schaepman, M. (2011). Review of constituent retrieval in optically deep and complex waters from satellite imagery. *Submitted to Remote Sensing of Environment*, September 2011

- Which recent spaceborne remote sensing sensors and according algorithms have been validated for case 2 waters since 2005?

About 50 recent matchup validation experiments are reviewed; whereas three quarters refer to band ratio and one quarter to spectral inversion algorithms. Implementation of the latter is more demanding with regard to model simulations and inversion methods, and their validation is more extensive since it usually comprises the comparison of all *chl-a*, *tsm* and *cdom* at once.

Most band ratio retrieval experiments are found for *chl-a*. They use either the blue-green portion of the spectrum as in OC algorithms or the red-NIR spectrum for meso- to eutrophic waters. Band ratios for *tsm* retrieval apply the largest variety in number and position of bands. Experiments on the retrieval of *cdom* finally reveal the lowest correlations. Recommended retrieval bands depend apparently on variations in the other two constituents.

The range of spectral inversion algorithms validated in recent years has strongly converged towards NN. Although only one case is known where sufficient quantitative validation of all concurrent constituents is available. However, separate application of *chl-a* is validated manifold, and needed especially in waters whose variations exceed the validity range of band ratio algorithms.

Medium resolution, oceanographic imaging spectrometers (e.g. MERIS, MODIS, SeaWiFS) are chosen for most experiments. Atmospheric correction methods distributed through corresponding processing software (SeaDAS, BEAM) are clearly preferred. Multispectral instruments of finer spatial resolutions are only applied for empirical case studies.

- For what typical constituent concentration ranges are these methods valid?

Red-NIR band ratios are found valid for meso- to eutrophic waters, while OC algorithms apply to oligotrophic waters with *tsm* and *cdom* close to the relations in case 1 water. For *tsm*, practice confirms the theoretical proposition that increasing ranges require increasing wavelength bands. The accuracy of *cdom* retrieval finally is inconsistent at all concentrations.

Spectral inversion algorithms lack the abundance of band ratio validation experiments as far as high concentrations and variations are concerned. On the contrary, successful constituent retrieval in clear waters is more frequent than with band ratios.

- What typology can be applied to further classify case 2 waters with regard to applicable remote sensing methods?

A 3-by-3 scheme for the characterization of case 2 waters is proposed. It displays 9 charts for the retrieval of high, medium and low *chl-a*, *tsm* and *cdom* in 3 rows and columns, respectively. Each chart features minimum to maximum concentrations of the two remaining constituents on the x and y axis. The

scheme enables a precise assignment of the water types specific algorithm validation experiments address, if reference concentrations of all constituents are known.

Thresholds for classes of low, medium and high concentrations are defined according to typical application ranges found in the reviewed papers. *chl-a* concentration classes refer to the known scheme of trophic states, namely oligo-, meso- and eutrophic waters (Carlson and Simpson, 1996; Chapra and Dobson, 1981; Wetzel, 1983). Corresponding terms for *tsm* and *cdom* classes are clear, cloudy and turbid, and lucent, dimmish and opaque, respectively.

6.2 Conclusions

This thesis has demonstrated the feasibility of operational remote water constituent concentration retrieval for water quality monitoring purposes in optically complex waters. Appropriate methods have been validated, the WFD-compliance of remotely sensed products has been investigated and alternative algorithms for distinct case 2 water types have been reviewed.

The validation experiments apply automatic processing routines for the use of the MIP, C2R and ICOL algorithms. These routines allow for the efficient exploitation of a collection of more than 200 MERIS images. Quantitative validation of remotely measured *chl-a* is achieved through comparison with in situ measured monitoring data acquired by environmental agencies and research institutes in Switzerland and neighboring countries. Spectroradiometric field measurements complement the validation with regard to the adequacy of forward optical models and inversion methods. Results demonstrate that the observation conditions and relatively low range of constituent variations of perialpine lakes require accurate optical models and autonomic algorithms. The C2R NN is found highly suitable for this purpose, achieving a good agreement with reference data of 7 of the largest perialpine basins.

WFD compliant water quality products are compiled through temporal integration of discrete remote measurements. Specific concentration ranges and seasonal variations are described for 12 perialpine lakes, which all achieve maximum concentrations between the autumn-winter and winter-spring transitions. A significant recent trend towards reoligotrophication is only observed for Lake Garda. Other than this, similarly oligotrophic and meso- to eutrophic states are estimated for small lakes North and South of the Alps, respectively,

while larger lakes on either side reveal more variable, oligo- to mesotrophic conditions. Satellite mapped *chl-a* concentrations also enable an investigation of the spatial representativeness of single in situ measurements. It is thereby found that variations in large basins are relatively well predictable since they come with large tributary rivers that constitute stable hydrographic sub-basins. On the contrary, spatial variations in smaller basins are statistically much less predictable. Altogether, remotely measured *chl-a* has proven beneficial for WFD compliant monitoring programs, and synoptic application with in situ measurements will allow for a representative, integral description of water quality in both horizontal and vertical dimension.

A comprehensive review of case 2 validation experiments published in 2005-2011 reveals applicable concentration ranges for band ratio and spectral inversion algorithms. The diverging *chl-a* thresholds in previous classifications of trophic level are revised to match typical algorithm application ranges. Similar ranges are defined for *tsm* and *cdom* retrieval, representing an enhancement to the widely employed separation of case 1 and case 2 waters. A graphic scheme is presented that helps to assign algorithm validation experiments to specific water types. It displays the variability of water bodies that have been investigated in recent years, experimental clusters such as *tsm* retrieval from clear to cloudy waters, and *chl-a* retrieval from eutrophic waters, along with less exploited fields such as *chl-a* in oligotrophic waters or *cdom* in general. Furthermore, a significant convergence towards the use of data from ocean color spectrometers is observed.

This thesis demonstrates the feasibility of spaceborne chlorophyll-a concentration monitoring in perialpine lakes, and gives an overview of other sufficiently validated applications. Most of these methods achieve accuracies in the range of probe measurements by means of entirely automatic image processing. They therefore indicate an essential progress towards operational use.

6.3 Outlook

Imaging spectrometry has a proven potential to support inland water quality monitoring protocols, although no universally valid algorithms are known. This fosters the existence of a variety of relatively simple, water type specific methods and improved numerical model inversion algorithms at the same time. Predominantly the former are experimentally validated to a point where operational application to specific regions or water types is mainly a matter of de-

mand, while the enhancement of model accuracies and inversion algorithms is an ongoing effort.

Initiatives such as the GEO inland water quality group address both threads. On one hand, joint end-to-end demonstration projects are planned for the improved dissemination of validated remote sensing products. The approach described in Chapter 3 and Chapter 4 is under discussion for this purpose, and monthly averaged maps are therefore developed. An extension of the Chlorophyll Globally Integrated Network (ChloroGIN) to large lakes is considered as a suitable platform. On the other hand, further improvement of models and algorithms is sought particularly by individuals and teams, e.g. ongoing training of the C2R NN with further input data. This enhancement is expected to improve the algorithm's range of applicability, but will also require confirmation of previous validations for the new version of C2R.

Synoptic assimilation of different in situ and remotely sensed data can support both the dissemination and enhancement of remote sensing products, in terms of added value and (cross-)calibration/validation, respectively. The GEMS (Global Environmental Monitoring System) archive of in situ measurements and hydrologic transport models bears a large synergetic potential for integration with optical remote measurements. Corresponding coastal ocean monitoring and forecasting services in the frame of the European GMES program are already being assessed within the framework of the MyOcean project (Bahurel et al., 2010). Moreover, the joint use of optical and thermal remote observations has still not been fully exploited. Such coupling could for example enable a more differentiated investigation of concurrent warming and reoligotrophication processes reported for Lake Geneva (Tadonleke, 2010; Tadonleke et al., 2009).

6.4 References

Bahurel, P., Adragna, F., Bell, M.J., Jacq, F., Johannessen, J.A., Le Traon, P.-Y., Pinardi, M., & She, J. (2010). Ocean Monitoring and Forecasting Core Services, the European MyOcean Example. *Proc. OceanObs'09*, Venice, Italy

Carlson, R.E., & Simpson, J. (1996). A Coordinator's Guide to Volunteer Lake Monitoring Methods. (96 p.), North American Lake Management Society

Chapra, S.C., & Dobson, H.F.H. (1981). Quantification of the Lake Trophic Typologies of Naumann (Surface Quality) and Thienemann (Oxygen) with Special Reference to the Great Lakes. *Journal of Great Lakes Research,* 7/2, 182-193

Guanter, L., Ruiz-Verdu, A., Odermatt, D., Giardino, C., Simis, S., Estelles, V., Heege, T., Dominguez-Gomez, J.A., & Moreno, J. (2010). Atmospheric correction of ENVISAT/MERIS data over inland waters: Validation for European lakes. *Remote Sensing of Environment,* 114/3, 467-480

Koponen, S., Ruiz-Verdu, A., Heege, T., Heblinski, J., Sorensen, K., Kallio, K., Pyhalahti, T., Doerffer, R., Brockmann, C., & Peters, M. (2008). Development of MERIS lake water algorithms. In: *ESA Validation Report* (65 p.)

Odermatt, D., Kiselev, V., Heege, T., Kneubühler, M., & Itten, K.I. (2008). Adjacency effect considerations and air/water constituent retrieval for Lake Constance. *Proc. 2nd MERIS/AATSR workshop*, Frascati, Italy

Tadonleke, R. (2010). *Evidence of warming effects on phytoplankton productivity rates and their dependence on eutrophication status*. Waco, TX, ETATS-UNIS: American Society of Limnology and Oceanography

Tadonleke, R., Lazzarotto, J., Anneville, O., & Druart, J.-C. (2009). Phytoplankton productivity increased in Lake Geneva despite phosphorus loading reduction. *Journal of Plankton Research,* 31/10, 1179-1194

Wetzel, R.G. (1983). *Limnology*. Philadelphia: W.B. Saunders Co.

Wolfram, G., Argillier, C., de Bortoli, J., Buzzi, F., Dalmiglio, A., Dokulil, M., Hoehn, E., Marchetto, A., Martinez, P.-J., Morabito, G., Reichmann, M., Remec-Rekar, Š., Riedmüller, U., Rioury, C., Schaumburg, J., Schulz, L., & Urbanič, G. (2009). Reference conditions and WFD compliant class boundaries for phytoplankton biomass and chlorophyll-a in Alpine lakes. *Hydrobiologia,* 633/1, 45-58

7 GLOSSARY

Abbreviations

Acronym	Meaning
(A)ATSR	(Advanced) Along Track Scanning Radiometer
AfU	Office of Environmental Protection of the Canton of Zug
ALI	Advanced Land Imager
AOP	Apparent Optical Properties
AOT	Atmospheric Optical Thickness
APPA	Environmental Protection Agency of Trento
ASD	Analytical Spectral Device
BAFU	Swiss federal Office for the Environment
BAG	Swiss federal Office of Public Health
BEAM	Basic ERS & Envisat (A)ATSR and MERIS toolbox
BIL	Band Interleaved by Line
BWG	Swiss federal Office for Water and Geology
C2R	Case 2 Regional
CARRTEL	Alpine Research Center on Trophic Food Webs in Limnic Ecosystems
CASI	Compact Airborne Spectrographic Imager
CDOM	Coloured Dissolved Organic Matter
CHL	Chlorophyll(-a)
ChloroGIN	Chlorophyll Globally Integrated Network
CIPAIS	International Commission for the Protection of Italo-Swiss Waters
CIPEL	International Commission for the Protection of Lake Geneva
CNR	Italian National Research Council
CRA	Center for Environmental Monitoring
CTD	Conductivity Temperature Density probe
CV	Coefficient of Variation
CZCS	Coastal Zone Color Scanner
DIMAP	Digital Image Map
DLR	German Aerospace Center
EC	European Commission

Acronym	Meaning
EEA	European Economic Area
ENVISAT	ESA Environmental Satellite
ERS	European Remote Sensing Satellite
ESA	European Space Agency
ETM	Enhanced Thematic Mapper
EU	European Union
EULAKES	European Lakes under Environmental Stressors
FLAASH	Fast Line-of-sight Atmospheric Analysis of Spectral Hypercubes
FLH	Fluorescence Line Height
FR	Full Resolution
FU	Fischbach-Uttwil testsite
FUB	Free University of Berlin
GBL	Water and Soil Protection Laboratory of the Canton of Berne
GEMS	Global Environmental Monitoring System
GLI	Global Land Imager
GMES	Global Environment Monitoring System
GEO	Group on Earth Observation
HICO	Hyperspectral Imager for the Coastal Ocean
HPLC	High Performance Liquid Chromatography
HRV	High Resolution Visible
ICOL	Improved Contrast between Ocean and Land
IDL	Interactive Data Language
IGKB	International Commission for the protection of Lake Constance
INRA	French National Institute Agricultural Research
IOCCG	International Ocean Colour Coordinating Group
IOP	Inherent Optical Properties
IREA	Institute for Remote Sensing of Environment
ISE	Institute of Ecosystem Study
ISF	Institute for Lake Research
ISI	Institute for Scientific Information
LUBW	State Institute for Environment, Measurements and Nature Conservation Baden-Wuerttemberg
LUT	Look-Up-Table
MCI	Maximum Chlorophyll Index
MELINOS	Monitoring European Lakes by means of an Integrated Earth Observation System
MERIS	Medium Resolution Imaging Spectrometer
MIP	Modular Inversion and Processing System

Acronym	Meaning
MODIS	Moderate Resolution Imaging Spectrometers
MOS	Modular Optoelectronic Scanner MOS
MSG	Meteosat Second Generation
NIR	Near Infrared
NN	Neural Network
OC	Ocean Color
OCTS	Ocean Color and Temperature Scanner
POLDER	POLarization and Directionality of the Earth's Reflectances
RMSE	Root Mean Square Error
ROI	Region Of Interest
RR	Reduced Resolution
SCAPE-M	Self-Contained Atmospheric Parameters estimated by MERIS
SCUFA	Self-Contained Underwater Fluorescence Apparatus
SeaDAS	SeaWiFS Data Analysis System
SeaWiFS	Sea-viewing Wide Field-Of-View Sensor
SEVIRI	Spinning Enhanced Visible and Infrared Imager
SNR	Signal-to-Noise Ratio
SIOP	Specific Inherent Optical Properties
SM	Suspended Matter
SOS	Successive Order of Scattering
SPOT	Probational Earth Observation Satellite System
TM	Thematic Mapper
TOA	Top-of-atmosphere
TSM	Total Suspended Matter
UMR	Joint Research Unit
UN	United Nations
UNEP	United Nations Environmental Programme
UNICEF	United Nations Children's Fund
UTC	Coordinated Universal Time
VITO	Flemish Institute for Technological Research
WFD	Water Framework Directive
WHO	World Health Organization
Y	Yellow substance

Symbols

Symbol	Definition	Unit
A	Surface area	m^2
a	Absorption coefficient	m^{-1}
b	Scattering coefficient	m^{-1}
b_b	Backscattering coefficient	m^{-1}
CHL, chl-a	Chlorophyll-a concentration	mg/m^3
cdom	Coloured dissolved organic matter concentration	m^{-1}
E_u, E_d	Up- and downwelling Irradiance	$W\ m^{-2}$
f	Gordon model coefficient ()	-
h	Park & Ruddick model coefficient	-
L_u, L_d	Up- and downwelling radiance	$W\ m^{-2}\ sr^{-1}$
L_w	Water-leaving radiance	$W\ m^{-2}\ sr^{-1}$
l	Gordon et al. model coefficient	-
M	Kirk model coefficient	-
n_w	Refraction index of water	-
p	Albert & Mobley model coefficients	-
Q	Anisotropy factor	sr^{-1}
R^-, R^+	Irradiance reflectance above and below surface	-
R_{rs}	Remote sensing reflectance	sr^{-1}
r	Fresnel interface reflectance	-
sm	Suspended matter concentration	g/m^3
T	Diffuse atmospheric transmittance	-
t	Fresnel interface transmittance	-
TSM, tsm	Total suspended matter concentration	g/m^3
Y, y	Yellow substance concentration	m^{-1}
z	Depth in water	m
z_{90}	Euphotic depth	m
β	Volume scattering function	$m^{-1}\ sr^{-1}$
$\tilde{\beta}$	Scattering phase function	sr^{-1}
Φ	Radiant flux	W
ϕ_s, ϕ_v	Illumination and viewing azimuth angle	°
γ_b	Particle fraction of total backscattering	-
λ	Wavelength	nm
θ_s, θ_v	Illumination and viewing zenith angle	°
ω_0	Single scattering albedo	-
ω_b	Single backscattering albedo	-
ψ	Scattering angle	°

8 CURRICULUM VITAE

Education

2006-2011 **Ph.D.** University of Zurich, Department of Geography, Remote Sensing Laboratories. Thesis: *Spaceborne inland water quality monitoring*. Advisors: M. E. Schaepman, K. I. Itten, M. Kneubühler, J. Nieke, T. Heege.

1999-2005 **Dipl. Geogr.** University of Zurich, Department of Geography, Remote Sensing Laboratories. Thesis: *Analysis of the directional reflectance properties of snow*. Advisors: K. I. Itten, D. Schläpfer, M. Lehning. Minor subjects: Glaciology, Environmental Sciences.

Teaching

2009 **B.Sc. mentoring:** Stephan Müller, *Korallen, Makrophyten, Sedimente – Fernerkundung des Benthal* (unpublished)

2008 **M.Sc. co-supervision**: Mona Stockhecke, *The annual particle cycle of Lake Van*. Co-supervision with the Swiss Federal Institute of Aquatic Science and Technology (EAWAG)

2008 **B.Sc. mentoring:** Isabel Plana, *Methoden zur Bestimmung von Wasserinhaltsstoffen in Case 2 Gewässern* (unpublished)

2008 **Lecture assistance**: Remote Sensing 4: *Spectroradiometry and imaging spectrometry* (lecture), subtopic application examples

2006 **Lecture assistance**: Remote Sensing 1: *Basics* (lecture and exercises), subtopic stereoscopy

2003 **Tutorage:** Remote Sensing 4: *Spectroradiometry and imaging spectrometry* (lecture and exercises)

Professional experience

2006-2011	**Research Assistant,** University of Zurich, Department of Geography, Remote Sensing Laboratories, Zurich
2004	**Software testing and documentation**, ReSe Remote Sensing Application Schläpfer, Wil
2002-2003	**Internship**, Swiss avalanche warning team, Swiss Federal Institute for Snow and Avalanche Research (SLF), Davos
1999-2001	**Documentation associate**, Telegyr Systems, Zug

Peer reviewed journal papers

Bresciani, M., Stroppiana, D., Odermatt, D., Morabito, G. & Giardino, C. (2011). Assessing remotely sensed chlorophyll-a for the implementation of the Water Framework Directive in European perialpine lakes. *Science of The Total Environment,* 409/17, 3083-3091

Guanter, L., Ruiz-Verdu, A., Odermatt, D., Giardino, C., Simis, S., Estelles, V., Heege, T., Dominguez-Gomez, J.A. & Moreno, J. (2010). Atmospheric correction of ENVISAT/MERIS data over inland waters: Validation for European lakes. *Remote Sensing of Environment,* 114/3, 467-480

Hueni, A., Biesemans, J., Meuleman, K., Dell'Endice, F., Schlapfer, D., Odermatt, D., Kneubuehler, M., Adriaensen, S., Kempenaers, S., Nieke, J. & Itten, K.I. (2009). Structure, Components, and Interfaces of the Airborne Prism Experiment (APEX) Processing and Archiving Facility. *IEEE Transactions on Geoscience and Remote Sensing,* 47/1, 29-43

Itten, K., Dell Endice, F., Hueni, A., Kneubuehler, M., Schlaepfer, D., Odermatt, D., Seidel, F., Huber, S., Schopfer, J., Kellenberger, T., Buehler, Y., D Odorico, P., Nieke, J., Alberti, E. & Meuleman, K. (2008). APEX - the Hyperspectral ESA Airborne Prism Experiment. *Sensors,* 8/10, 6235-6259

Odermatt, D., Gitelson, A., Brando, V. E. & Schaepman, M. (2011). Review of constituent retrieval in optically deep and complex waters from satellite imagery. *Submitted to Remote Sensing of Environment*, September 2011

Odermatt, D., Giardino, C. & Heege, T. (2010a). Chlorophyll retrieval with MERIS Case-2-Regional in perialpine lakes. *Remote Sensing of Environment,* 114/3, 607-617

Odermatt, D., Heege, T., Nieke, J., Kneubuehler, M. & Itten, K. (2008a). Water quality monitoring for Lake Constance with a physically based algorithm for MERIS data. *Sensors,* 8/8, 4582-4599

Odermatt, D., Schläpfer, D., Lehning, M., Schwikowski, M., Kneubühler, M. & Itten, K.I. (2005). Seasonal study of directional reflectance properties of snow. *EARSeL eProceedings,* 4/2, 203-214

Stockhecke, M., Anselmetti, F.S., Meydan, A.F., Odermatt, D. & Sturm, M. (2011). The annual particle cycle of Lake Van (Turkey). *Submitted to Palaeogeography, Palaeoclimatology, Palaeoecology*, September 2011

Other scientific publications

Heege, T., Kiselev, V., Odermatt, D., Heblinski, J., Schmieder, K., Tri Vo, K. & Trinh Thi, L. (2009). Retrieval of water constituents from multiple earth observation sensors in lakes, rivers and coastal zones. *Proc. IEEE International Geoscience & Remote Sensing Symposium IGARSS*, Cape Town, SA

Knaeps, E., Raymaekers, D., Sterckx, S., Bertels, L. & Odermatt, D. (2010a). Monitoring inland waters with the APEX sensor, a wavelet approach. *Proc. WHISPERS*, Reykjavik, Iceland

Knaeps, E., Raymaekers, D., Sterckx, S. & Odermatt, D. (2010b). An intercomparison of analytical inversion approaches to retrieve water quality for two distinct inland waters. *Proc. ESA Hyperspectral Workshop*, Frascati, Italy

Kötz, B., Morsdorf, F., Curt, T., Van der Linden, S., Borgniet, L., Odermatt, D., Alleaume, S., Lampin, C., Jappiot, M. & Allgöwer, B. (2007). Fusion of Imaging Spectrometer and LIDAR Data using Support Vector Machines for Land Cover Classification on the Context of Forest Fire Management. *Proc. Intl. Symposium on Physical Measurements and Signatures in Remote Sensing ISPMSRS'07*, Davos, Switzerland

Nieke, J., Odermatt, D., Itten, K.I., Mauser, W., Oppelt, N., Ruhtz, T., Preusker, R., Fischer, J., Vohland, M. & Hill, J. (2007). EO-HALO, an earth observation mission for regional studies in Europe. *Proc. EARSeL Workshop on Imaging Spectroscopy*, Bruges, Belgium

Odermatt, D., Heege, T., Nieke, J., Kneubühler, M. & Itten, K.I. (2007a). Constitution of an Automized Processing Chain to Analyse a MERIS Time Series of Swiss Lakes. *Proc. Intl. Symposium on Physical Measurements and Signatures in Remote Sensing ISPMSRS'07*, Davos, Switzerland

Odermatt, D., Heege, T., Nieke, J., Kneubühler, M. & Itten, K.I. (2007b). Evaluation of a physically based Inland Water Processor for MERIS Data. *Proc. EARSeL Special Interest Group Workshop Remote Sensing of the Coastal Zone*, Bolzano, Italy

Odermatt, D., Heege, T., Nieke, J., Kneubühler, M. & Itten, K.I. (2007c). Parameterisation of an automized processing Chain for MERIS Data of Swiss Lakes, at the Example of Lake Constance. *Proc. ENVISAT Symposium 2007*, Montreux, Switzerland

Odermatt, D., Heege, T., Nieke, J., Kneubühler, M. & Itten, K.I. (2008b). MERIS chl-a timeseries of Lake Constance 2003-2006. *Proc. IEEE International Geoscience & Remote Sensing Symposium IGARSS*, Boston, Massachusetts

Odermatt, D., Kiselev, V., Heege, T., Giardino, C., Bresciani, M., Kneubühler, M., Nieke, J. & Itten, K.I. (2009). Calibration, parameterization and application of MERIS water constituent algorithms for perialpine lakes. *Proc.*

IEEE International Geoscience & Remote Sensing Symposium IGARSS, Cape Town, SA

Odermatt, D., Kiselev, V., Heege, T., Kneubühler, M. & Itten, K.I. (2008c). Adjacency effect considerations and air/water constituent retrieval for Lake Constance. *Proc. 2nd MERIS/AATSR workshop*, Frascati, Italy

Odermatt, D., Knaeps, E., Raymaekers, D., Sterckx, S., Kneubuehler, M. & Schaepmann, M.E. (2010b). Towards the simulation and inverstion of user-defined inland water imaging spectrometer data. *Proc. ESA Hyperspectral Workshop*, Frascati, Italy

Ruiz-Verdu, R., Koponen, S., Heege, T., Doerffer, R., Brockmann, C., Kallio, K., Pyhälahti, T., Pena, R., Polvorinos, A., Heblinski, J., Ylöstalo, P., Conde, L., Odermatt, D., Estelles, V. & Pulliainen, J. (2008). Development of MERIS lake water algorithms: Validation results from Europe. *Proc. 2nd MERIS/AATSR workshop*, Frascati, Italy

Schopfer, J., Huber, S., Schneider, T., Dorigo, W., Oppelt, N., Odermatt, D., Koetz, B., Kneubühler, M. & Itten, K.I. (2007). Towards a comparison of spaceborne and ground-based spectrodirectional reflectance data. *Proc. ENVISAT Symposium 2007*, Montreux, Switzerland

9 ACKNOWLEDGEMENTS

I thank my parents and my brother, who not only raised me to independence and confidence, but also gave me the ability to accept failure without losing optimism. I owe them my ability to tackle an adventure such as this thesis.

My gratitude also extends to all teachers who supported me attain new heights, as well as to those who taught me justified criticism. New opportunities presented themselves to me as an employee at the fuel station of Mrs Kocher and as a volunteer for UHC Rainbow Cham, both of which strengthened my initiative, sense of responsibility and patience.

Peers, supporters, rivals, role models, team- and roommates, fellow combatants, companions in misfortune, favorite waste of time – I am grateful to all my friends for how well they do their job. My five best school friends forever, Michi, Ralph, Silvan, Stefan and Stephan, will bear with pleasure if I happen to occasionally show off a PhD title in the future. Felix, Michi and Othmar are the best at showing me that life as an "egghead" can be as ordinary as a flag capture on the Harvest Day. Still, none of those people are around when I need a coffee to get out of bed in the morning, Livia. Folks, you keep me smiling!

Several scientists have greatly contributed to this thesis as supervisors and collaborators. Jacques, Thomi and Wisi (SLF) helped to arouse my initial interest in research. I thank Klaus, Dani, Mathias, Jürg (RSL), Michi, Andy (SLF) and Margit (PSI) for supporting my Diploma Thesis, which turned out to be more inspiring and motivating than I thought it could ever be. Klaus, Michi, Mathias and Jens (RSL) steered my academic further by challenging and intriguing me with a tailor-made PhD thesis. This opportunity enabled enriching collaborations with commendable colleagues from around the world, namely Thomas and Viacheslav (EOMAP), Claudia and Mariano (CNR-IREA), Luis (GFZ), Els and Dries (VITO), Anatoly (Univ. of Nebraska) and Vittorio (CSIRO), whom I all sincerely thank for sharing their knowledge and experience.

Last but not least, I thank all my colleagues at RSL and GIUZ, as well as my fellow sportsmen from the Wednesday lunch-hour football sessions.